1991

Magnetic Resonance Spectroscopy Of Probe Labelled Glycolipids In Model Membranes, And Development Of Lipid Probes For Magnetic Resonance Imaging

Eugene Florio

MAGNETIC RESONANCE SPECTROSCOPY OF PROBE LABELLED GLYCOLIPIDS IN MODEL MEMBRANES, AND DEVELOPMENT OF LIPID PROBES FOR MAGNETIC RESONANCE IMAGING

by

Eugene Florio

Department of Biochemistry

Submitted in partial fulfillment of the requirement
for the degree of
Doctor of Philosophy

Faculty of Graduate Studies
The University of Western Ontario
London, Ontario
October, 1990

ISBN 0-315-64266-1

ABSTRACT

Glycosphingolipids are the carbohydrate-bearing lipids of animal cells. These usually minor constituents of the plasma membrane have been proposed to have major roles in structure and recognition. Glycosphingolipids are distinctly different from phospholipids in that: i) they possess donor H-bonding groups, ii) they often have disproportionately long, single fatty acid chains and iii) they can be α-hydroxylated on the fatty acid chain.

As part of a research program to investigate the behaviour and interaction of glycosphingolipids in biological membranes we have developed spin labelled and deuterium labelled derivatives. These included novel 24-carbon (lignoceric acid) spin labelled at C-12 or C-16, and also perdeuterated lignoceric, stearic and α-hydroxy-stearic acid. Spin labelled fatty acids were linked to simple neutral glycosphingolipids such as galactosyl ceramide and lactosyl ceramide (dihydro) as well as to the complex neutral glycosphingolipid globoside and to the charged ganglioside, G_{M1}. Probe-labelled glycosphingolipids were assembled at low concentrations in bilayer model membranes to mimic the situation in cell membranes. EPR and ^2H NMR spectra generated with these labelled glycosphingolipids provided data for quantitation of dynamic properties.

For a glycosphingolipid bearing spin-labelled lignoceric acid (24-carbon) (in all of the phospholipid matrices, DMPC (14 carbon), DPPC (16 carbon), DSPC (18 carbon) and DPPC/cholesterol, the order parameter S was always greater than for a glycosphingolipid bearing a stearic acid (18 carbon) acyl chain. We interpreted this as indicating that interdigitation was occurring in the fluid state.

The technology of probe-labelled lipids for assembly into liposomes was extended to Magnetic Resonance Imaging - a recent diagnostic modality employed to visualize body organs and any related pathology, which may accompany it. By employing paramagnetic species such as Gd^{3+}, one can alter the relaxation rate of free water, hence augmenting visual definition of organs via contrast enhancement. We have developed liposome-associated contrast agents for *in vivo* use: a spin labelled phosphatidylcholine and a metal chelator, phosphatidylethanolamine-diethylenetriaminepentaacetic acid. Both of these non-toxic, liposome preparations target the reticuloendothelial system when injected intravenously and were effectively used to highlight liver and spleen of experimental animals.

Acknowledgments

I wish to thank my family and my friends who have helped and supported me, in more ways than one, throughout this interminable and perilous journey.

I would like to extend my thanks to my supervisor and friend Dr. C.W.M. Grant for making this work enjoyable as well as a learning experience. I would also like to thank Kathryn R. Barber for her help in the laboratory as well as for the proofreading of this thesis. To Barbara L. Green go my thanks and my money for typing this manuscript.

Finally, I am grateful to Dr. S.J. Karlik, Department of Radiology, University Hospital, Dr. J.R. Bolton, Department of Chemistry, Dr. R.R. Shivers, Department of Zoology, and Dr. H. Jarrell, Division of Biological Science (NRC) Ottawa, for the use of their facilities.

This work was supported by the Medical Research Council of Canada.

TABLE OF CONTENTS

LIST OF TABLES

LIST OF FIGURES

PAGE

ABBREVIATIONS

GSL	glycosphingolipid
gal cer	galactosyl ceramide
lac cer	lactosyl ceramide
DTPA	diethylenetriaminepentaacetic acid
PE	phosphatidylethanolamine
PC	phosphatidylcholine
SLPC	spin labelled phosphatidylcholine
PE-DTPA	phosphatidylethanolamine-diethylenetriamine-pentaacetic acid complex
DMPC	dimyristoyl phosphatidylcholine
DPPC	dipalmitoyl phosphatidylcholine
DSPC	distearoyl phosphatidylcholine
TEMPO	2,2,6,6-tetramethylpiperidine-N-oxyl
DCC	N,N′-dicyclohexylcarbodiimide
EPR	electron paramagnetic resonance
NMR	nuclear magnetic resonance
MRI	magnetic resonance imaging
μ	magnetic dipole moment
B_o	strong, stationary, external magnetic field
M	magnetization vector
γ	gyromagnetic ratio
T	tesla

MHz	mega hertz
RF	radio frequency
FID	fourier induction decay
TR	repetition time
TE	echo time
T_1	spin-lattice relaxation time
T_2	spin-echo relaxation time
T_m	phase transition temperature
TLC	thin layer chromatography
LD_{50}	dose lethal to 50%
TIBS	2,4,6-triisopropylbenzene sulfonyl chloride
DSC	differential scanning calorimetry
CI	chemical ionization

CHAPTER 1. INTRODUCTION

1.1 General Introduction to Glycosphingolipids

Glycosphingolipids (GSL) are the carbohydrate-bearing lipids of animal cells. Generally they are minor constituents, although their concentration ranges as high as 30 percent of the total membrane lipid in several tissues and their restriction to the outer leaflet effectively doubles their local concentration. Thus this family of sphingolipids is considered to have the potential to contribute to membrane physical properties (Curatolo, W. 1987a), in addition to having an established role as recognition sites that may mediate the interaction of the cell with its surroundings (Curatolo, W. 1987b). Subtle details of GSL physical behaviour and arrangement in membranes have been demonstrated to be involved with both their structural and receptor roles (Curatolo, W., 1987a; Curatolo, W., 1987b; Thompson, T.E. and Tillack, T.W., 1985; Grant, C.W.M. et al., 1987b).

Glycosphingolipids have features that set them distinctly apart from phospholipids and have the potential to influence their physical behaviour and arrangement: donor H-bonding groups in a potentially complex carbohydrate headgroup and sphingosine backbone, a disproportionately long (single) fatty acid, and often α-hydroxylation of the fatty acid (Fig. 1). The significance of these features has been subject to considerable speculation with regard to GSL function. It has been pointed out that in addressing questions related to glycosphingolipid arrangement and dynamics it will be important to examine membrane systems which mimic the low

Figure 1

Structure depicting a simple neutral glycosphingolipid galactosyl ceramide A) along with a common phospholipid phosphatidylcholine B). Both have 18-carbon long fatty acid chains. Notice that the glycosphingolipid has the potential to influence the physical behaviour and arrangement of its environment by way of donor H-bonding groups.

A

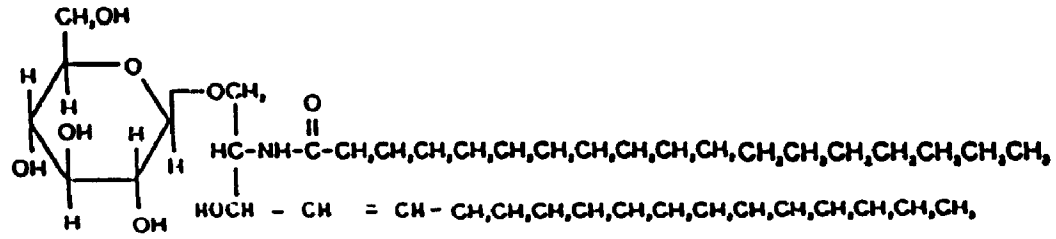

B

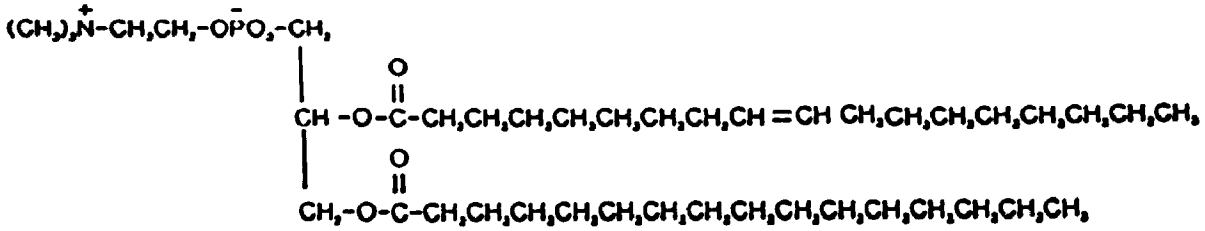

overall GSL concentrations and non-cooperative, semi-fluid nature of cell plasma membranes. In addition, the question has arisen in a variety of contexts as to whether different families of GSL may behave differently within cell membranes. Certainly there is reason to anticipate some differences since headgroup oligosaccharides vary considerably in H-bonding potential, size, charge, and configuration.

The major technique we have used to examine this question is magnetic resonance spectroscopy. The sensitivity of this technique permits answers to some questions through simple spectral inspection. However, quantitation is also desirable. We first tried comparison with a set of standards of known composition. Another method of quantitation is use of order parameters. There are various methods of quantitating EPR spectroscopic data obtained from spin labelled lipid systems in terms of dynamic properties. One such method utilizes the "order parameter" S and has been described in extensive detail by other workers (Seelig, J., 1970; Hubbell, W.L. and McConnell, H.M., 1971; Griffith, O.H. and Jost, P.C., 1976; Gaffney, B.J., 1976; and Marsh, D., 1981). Its measurement relies on spin label sensitivity to orientation in the magnetic field and the reflection of this sensitivity in the EPR spectrum. An S value approaching 1 for a fatty acid spin label derivative indicates that the fatty acid backbone region to which the label is covalently attached is in general oriented so that its long axis has a time average orientation perpendicular to the plane of the membrane. S values approaching 0 indicate that the backbone region to which the label is attached has a time-averaged random orientation. The degree of fatty acid chain orientation decreases toward the center of the bilayer. Since the spin labelled lipids (in our hands) were at very low concentrations in the membrane

and should not be subjected to marked clustering, the S values should reflect the behaviour of an isolated probe molecule surrounded by unmodified phospholipids from a natural source. Qualitatively the two sets of data are very similar between phospholipid and glycosphingolipid. Quantitatively the order parameter for the GSL was always higher than that of the corresponding phospholipid in the same membrane. Thus far, in the limited number of systems studied, this has proven to be a general observation (Mehlhorn, I.E. et al., 1989; Esmann, M. et al., 1988).

1.2 Structure and Nomenclature of Glycosphingolipids

Glycosphingolipids are molecules composed of a hydrophobic ceramide portion and a hydrophilic carbohydrate headgroup. These amphipathic molecules have their ceramide portions embedded in the lipid bilayer whilst the hydrophilic sugar groups are exposed to the aqueous environment which surrounds it. Unlike phospholipids which generally have a glyceride backbone, the glycosphingolipid can be based on either glyceride (i.e. bacteria and plants) or ceramide (i.e. mammalian cells) backbones. Glycosphingolipids have several features which are important to their function namely, they have the ability to form H-bonding via the -OH groups found in the sugar headgroup, and through the -OH, -NH and C=O groups on the sphingosine portion. The ceramide portion of mammalian glycosphingolipids typically contains sphingosine, but one can also find dihydrosphingosine. Glycosphingolipids have a great range of fatty acid chain lengths. The single fatty acid is linked via an amide bond to the amino function of sphingosine. Glycosphingolipid fatty acids have typical chain lengths from 16-24 carbons and it is not uncommon to have an α-

hydroxy group present on the fatty acid chain.

Glycosphingolipids are classified according to the chemical structure of the carbohydrate headgroup which includes the type of glycosyl residues, the positional and anomeric linkages of the sugar moieties, the sequence of these sugars and the presence of charged groups if any. Based on the oligosaccharide portion, glycosphingolipids can be grouped as: neutral (i.e. galactosyl ceramide), complex neutral (i.e. globoside), gangliosides (i.e. G_{M1}) and sulfated glycosphingolipids (i.e. galactosyl ceramide sulfate). Table 1 shows the common name, structure and IUPAC-IUB Notation (1977) from the Nomenclature Commission, of the glycosphingolipids commonly used in this study.

1.3 Interdigitation of Glycosphingolipids

The hydrophobic midplane of the cell (bilayer) membrane is frequently presented as a well-defined region at which two planar surfaces comprised of acyl chain methyl termini contact one another. However, it is well known that there is considerable disparity in acyl chain length of membrane lipids: chains as short as 14 carbons and as long as 24 carbons being widely observed. The concept of "interdigitation" has been put forward to describe the phenomenon whereby a chain longer than half the membrane thickness might cross the midplane to protrude amongst acyl chains of the opposing monolayer (Keough, K.M.W. and Davis, P.J., 1979; Davis, P.J. and Keough, K.M.W., 1985; Huang, C. and Mason, J.T., 1986; Mattai, J. et al., 1987; Boggs, J.M. and Mason, J.T., 1986). This concept has been addressed most systematically for bilayer model membranes comprised of single pure

TABLE 1 Common names, structure and IUPAC-IUB notation for the glycosphingolipids typically used in this study.

TABLE 1

Common Name	Structure	IUPAC-IUB Notation
Galactosyl Ceramide	Gal(ß1→1)cer	Gal Cer
Lactosyl Ceramide	Gal(ß1→4)Glc(ß1→1)cer	Lac Cer
Globoside	GalNac(ß1→3)Gal(α1→4)-Gal(ß1→4)Glc(ß1→1)Cer	GB_4 Cer
G_{M1}	Gal(ß1→4)GalNAc(ß1→4)-11-(NeuAcα1→3)Gal(ß1→4)-Glc(ß1→1)Cer	11 ^{3}NeuAcGgOSe$_4$ Cer

phospholipids with one long and one short fatty acid chain (i.e. phosphatidylcholines exhibiting intramolecular fatty acid chain length disparity). Pure sphingomyelins with fatty acids of selected lengths (Maulik, P.R. et al., 1986; Levin, I.W. et al., 1985) and pure galactosyl glycosphingolipids (Bunow, M.R. and Levin, I.W., 1980; Boggs, J.M. et al., 1988) have also been studied. In these situations the longer chains are seen as matching up stoichiometrically with the shorter chains of the opposing monolayer when chain length differences are not extreme.

Our interest has been to extend this concept to glycosphingolipids in cell membranes. The glycosphingolipid molecule possesses one fatty acid, typically 16-26 carbons in length. The sphingosine portion, which contributes the equivalent of a second acyl chain, extends to a membrane depth of only 13-15 carbons. Hence glycosphingolipids may be expected to behave as mixed-chain lipids. However glycosphingolipids are a small fraction of the total lipids in most eucaryote membranes, and are restricted to the outer surface. Furthermore, since the single fatty acid is commonly up to 24-26 carbons long, acyl chain length mismatch within a given glycosphingolipid is greater than that in surrounding phospholipids - most of which will have 16- or 18-carbon fatty acids. Thus the situation for glycosphingolipids in cell membranes is different from that of the pure single-component systems so far studied (Harwood, J.L., 1989).

We have proposed that GSL long chain fatty acids exhibit a type of interdigitation in phospholipid membranes. This was based on the results of our experiments with Gal Cer, Lac Cer globoside and G_{M1} bearing the long chain (24-carbon) spin labelled fatty acid (Grant, C.W.M. et al., 1987b; Mehlhorn, I.E. et al.,

1988). If the glycosphingolipid acyl chain length were roughly compatible with that of surrounding phospholipids, one might anticipate that it would simply behave much like another phospholipid with regard to chain organization. Such a view is compatible with our findings and those of others. However, a very long fatty acid attached to sphingosine would be faced with extending into and across the plane defined by the host matrix methyl termini or collapsing via *trans* → *gauche* isomerization.

1.4 Deuterium NMR of Glycosphingolipids

^2H NMR has proven to be a very effective technique for probing the highly anisotropic membrane structure (Seelig, J. and Browning, J.L., 1978; Smith, I.C.P. and Mantsch, H.H., 1982; Smith, I.C.P. et al., 1977; Seelig, J., 1977; Davis, J.H., 1983). An advantage ^2H NMR has over the spin label approach is its virtual lack of potential for system perturbation. Although ^2H lacks the spin label's inherent sensitivity to lateral distribution, its spectrum does reflect very directly the motional characteristics of the molecule to which it is attached. Thus by measuring the quadrupole splittings one can infact calculate an order parameter.

1.5 Basic Principles of NMR

Hydrogen or any other element which possesses an odd number of protons and/or neutrons (i.e., sodium ^{23}Na and phosphorus ^{31}P), has an inherent spin and a magnetic dipole moment defined by (μ). The individual moments are oriented in random fashion within a tissue (Fig. 2). When a strong stationary external magnetic

Figure 2

The inherent spin and magnetic dipole moments (μ) of hydrogen atoms oriented in random fashion as indicated along side the Cartesian coordinate system.

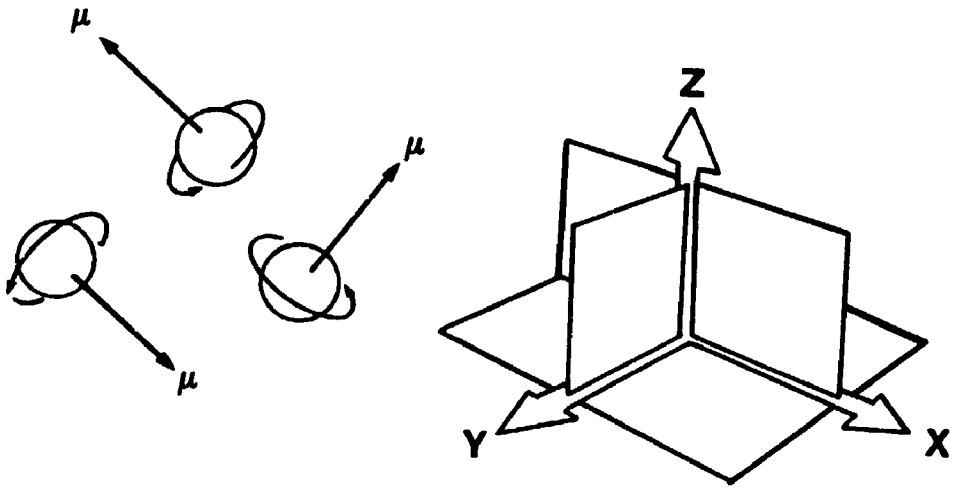
μ
μ
μ
Z
Y
X

field, designated B_o is applied to a tissue two events occur. Firstly, the protons tend to align themselves with the magnetic field, and secondly, the protons begin to precess around the axis of B_o (by definition in the z axis) (Fig. 3).

At the onset of B_o each proton can exist in two energy states. In the low-energy state the protons' moment is oriented nearly parallel with the stationary magnetic field (B_o). In the high-energy state the protons' moment is oriented in the anti-parallel direction relative to B_o. In the equilibrium condition, a population difference occurs such that there is a slightly greater number of protons in the low-energy state than exist in the high energy state. It is this population difference (1 proton per million) which produces a net magnetization vector (M), which is oriented in the direction of B_o.

The rate at which protons precess is called the Larmor frequency. This is governed by two factors: the gyromagnetic ratio (γ) which is a constant for the nuclear species involved, and the strength of the applied magnetic field (B). Field strengths in the area between 0.15 and 1.5 tesla (T) will cause the proton to precess at frequencies of 6.4 and 64 MHz, respectively. These frequencies are in the range of radiowaves, thus are referred to as RF frequencies.

By applying an RF pulse to the system (B_{RF}), the equilibrium state can be altered. The frequency with which the B_{RF} pulse alternates is made equal to the Larmor frequency. This causes two things to happen. Firstly, the protons are brought into phase with each other, such that they precess at the same frequency and also precess in phase. Secondly, some of the protons located in the low-energy state become excited and enter the high-energy state. These two events cause the vector

Figure 3

A strong stationary external magnetic field (B_o) applied to the hydrogen atoms, causing them to align themselves with the magnetic field as well as to begin to precess around the axis of B_o.

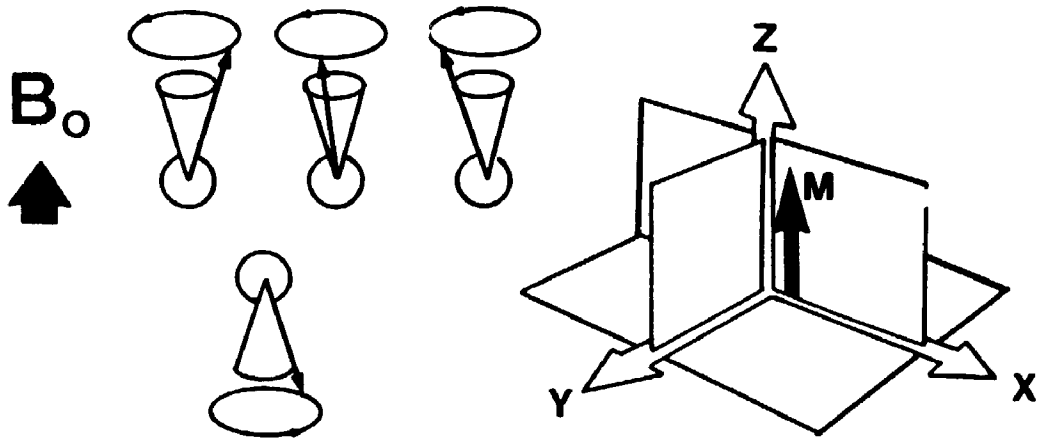
B_o
Z
M
Y
X

M to precess away from its alignment with B_o, and the longer the B_{RF} is applied the more M tips towards the XY plane (Fig. 4). If the B_{RF} is not of the frequency which matches the inherent frequency of the system (Larmor frequency) the protons will not resonate. It is this principle which forms the basis of slice selection in cross-sectional imaging. On the other hand, if the B_{RF} is the appropriate frequency and is applied long enough, the protons will absorb energy and go from the low-energy state into the high-energy state. There comes a time when the population of protons is equal in both the low- and high-energy states. Consequently the magnetization vectors that are parallel and anti-parallel to B_o will cancel each other out, and no longitudinal magnetization will be present. However, each proton's moment is precessing at a slight angle to B_o and because they are now precessing in phase, the magnetization vectors perpendicular to B_o summate. This gives rise to a net vector M which has now undergone a 90° pulse because it has been tipped into the transverse (XY) plane (Fig. 5).

When the B_{RF} is turned off the system returns to equilibrium via two relaxation phenomena. Firstly, a measure of the time it takes for dephasing to occur is called T_2, or the transverse relaxation time, (Fig. 6). Secondly, a measure of the time it takes for the protons to reestablish their equilibrium population in the two different energy states is called T_1, or the longitudinal relaxation time (Fig. 7). These relaxation times are important aspects of MR imaging because different tissues have different relaxation times, and it is these differences which give us the contrast between tissue types (Berquist, T.H. ed, 1987).

Figure 4

The application of an external RF pulse, when made equal to the inherent frequency of the system brings the hydrogen atoms into phase with each other. Consequently they all precess in phase and some of the hydrogens located in the low-energy state become excited and enter the high-energy state. These events will cause the magnetization vector M to precess away from its alignment with B_o.

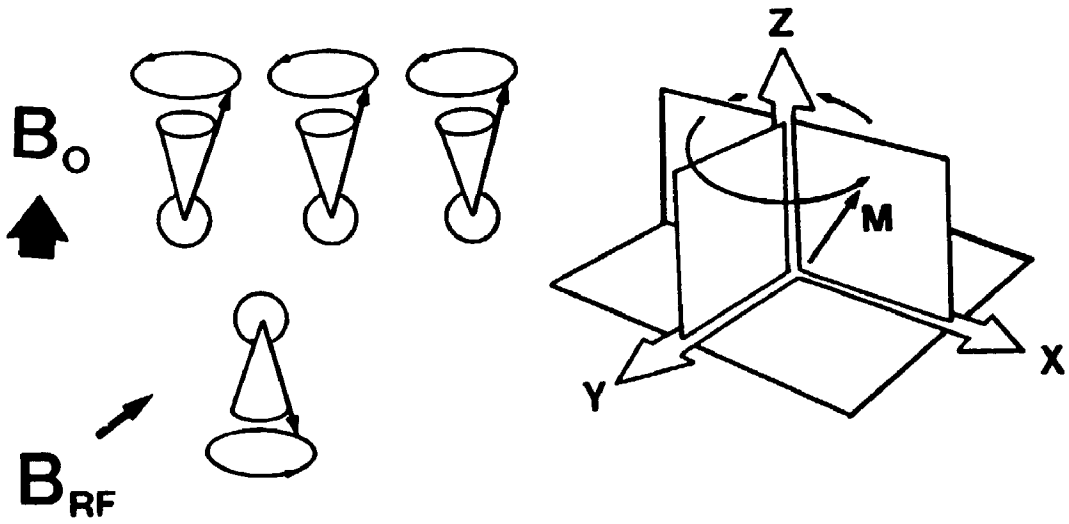
B_O
B_{RF}
Z
M
Y
X

Figure 5

When the external RF pulse is the appropriate frequency and is applied long enough, the protons absorb energy and go from the low-energy state into the high energy state. When the population of protons in the two energy states is equal (the magnetization vectors that are parallel and anti-parallel to B_o will cancel each other out) there will be no longitudinal magnetization. However, due to the protons' moments precessing at a slight angle to B_o the magnetization vectors perpendicular to B_o summate. This gives rise to a vector M which has undergone a 90° pulse.

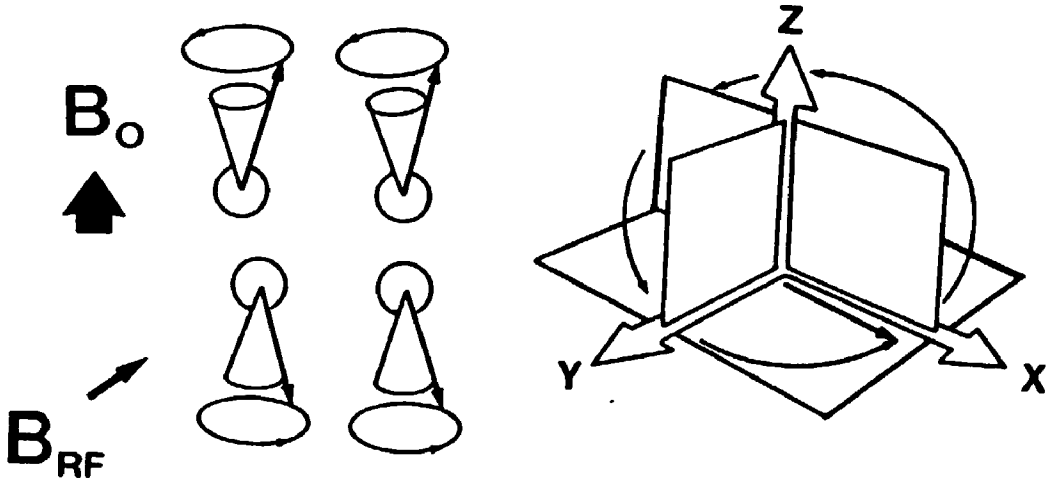
B_o
B_{RF}
Z
Y
X

Figure 6

Transverse Relaxation Time (T_2). T_2 reflects the characteristic time constant for loss of phase coherence among spins, due to interactions between the spins, (spin-spin) resulting in loss of transverse magnetization and MR signal. Starting from a non-zero value of the magnetization in the XY plane, the XY magnetization will decay so that it decays to 37% of its final value in a time T_2.

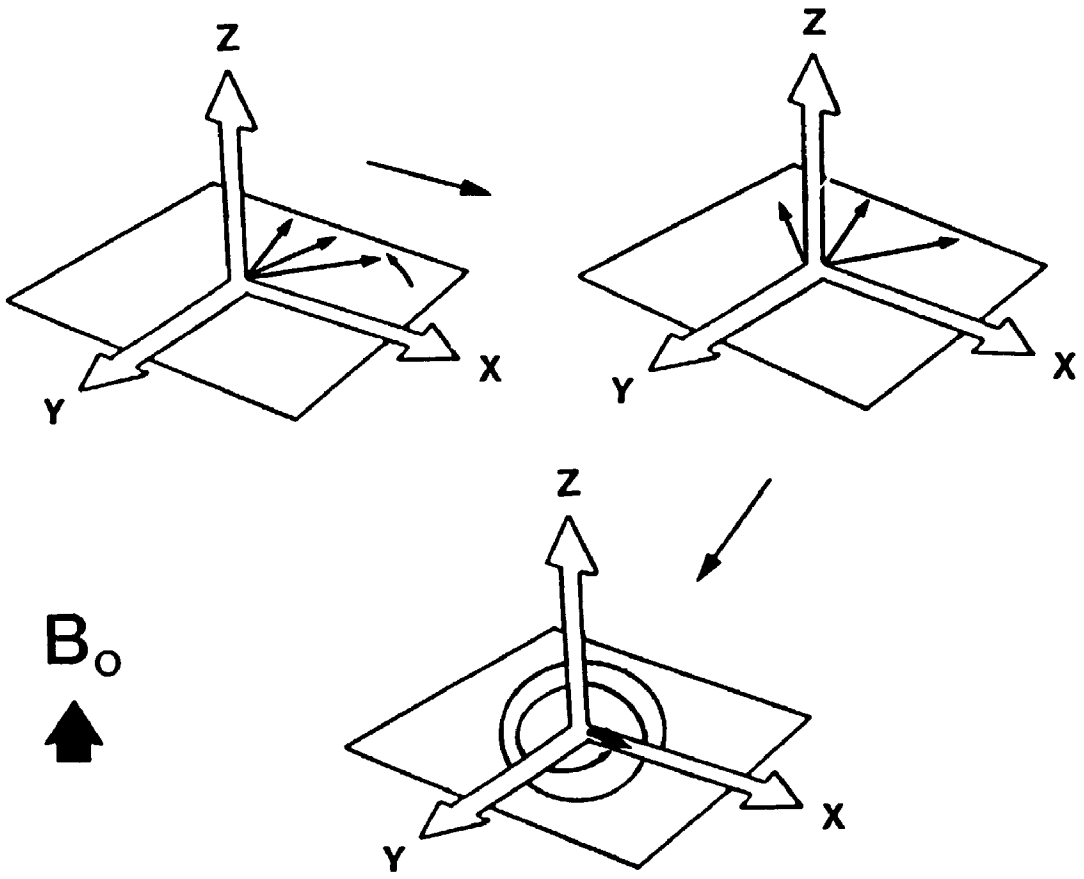
Z
X
Y
Z
X
Y
Z
X
Y
B_o

Figure 7

Longitudinal Relaxation Time (T_1). T_1 reflects the characteristic time constant for spins to align themselves with the external magnetic field. Starting from zero magnetization in the Z direction, the Z magnetization will grow to 63% of its final maximum value in a time T_1.

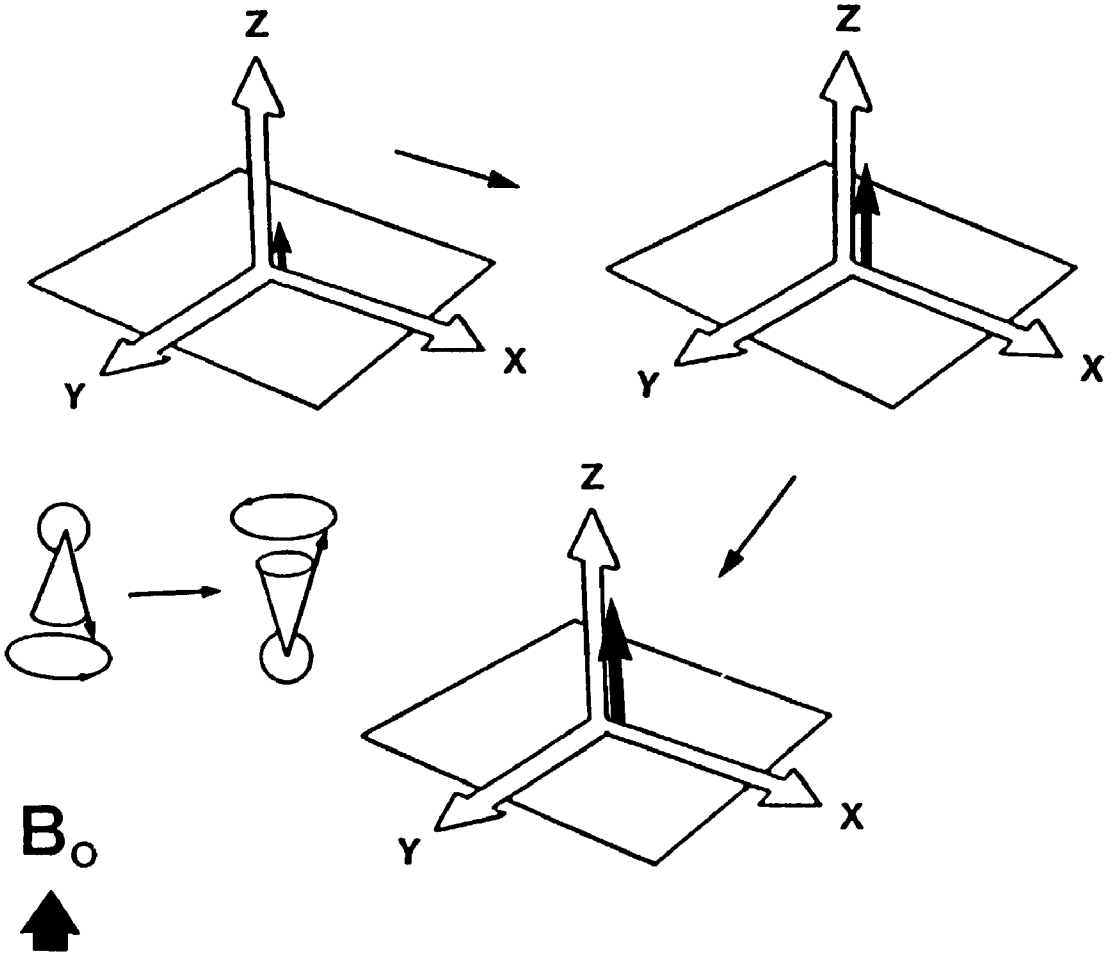
Z
Y
X
Z
Y
X
Z
Y
X
B_o

1.6 Basic Principles of MR Imaging

In 1972 Paul Lauterbur first showed that by superimposing linear field gradients on the main field, projections of an object can be generated from which an image can be reconstructed (Kumar, A. et al., 1975). The term "gradient" designates that the magnetic field is altered along a selected direction. For example, when the field is varied linearly along the X coordinate of a cartesian coordinate system:

$$\partial B_o / \partial x = G_x = \text{constant}$$

the resonance frequency becomes dependent on the location of the volume element of interest with respect to X. Envisage having two cylindrical objects (non magnetic) in the magnet with the holes aligned in the Z axis (by convention, in the direction of the applied field B_o), but the two objects have different locations with respect to X. In the absence of a gradient (when $G_x=0$) the two cylinders are indistinguishable because they resonate at the same frequency because they experience the same field. Thus the free induction decay curve (FID) for this example will contain only one frequency. However, when you turn on the gradient, the two cylinders will no longer experience the same magnetic field strength, and the resulting free induction decay will be the superposition of two different frequency components.

In a typical situation, signals are collected from a multitude of spacial locations and the FID is a composite consisting of many different frequencies. To arrive at individual frequencies, the time domain of the FID is converted into a frequency domain by way of a mathematical analysis called Fourier Transformation. This transformstion enables one to pick out the individual frequencies with their associated amplitudes which are proportional to the magnetization or spin density at the

particular spatial locations. By rotating the gradient in small angular increments, this generates a series of projections of the object to be imaged. Typically, this can be achieved by mixing gradients (Gx and Gy for a transverse image). In todays scanners the image is reconstructed using a two-dimensional Fourier transformation (Johnson, G.A. et al., 1986).

1.7 MRI Contrast Agents

The recent introduction of Magnetic Resonance Imaging into clinical settings has been accompanied by efforts to develop contrast-enhancing agents for the technique. There is a need today for injectable drugs that will sharpen visual definition of the body's organs and any related pathology that may accompany it. Agents that will do this are paramagnetic species - i.e., species such as nitroxide radicals (spin labels) and certain ions (Gd^{3+}). A major subset of this work is the involvement of liposome-associated contrast agents. The reasoning behind this is that these non-toxic intravenous liposomes target to the reticuloendothelial system and this enables us to enhance the liver and spleen or the lymphatics if injected interstitially (Poznansky, M.J. and Juliano, R.L., 1984). As part of this research program, which has also involved liposomal drug delivery, we require that the markers remain liposome-associated in the body allowing them to then be localized by non-invasive techniques. One approach used by other researchers to 'mark' liposomes that are to be injected has been to trap substances within their aqueous interiors. This technique relies upon the bilayer membrane to act as a barrier that prevents escape of some water-soluble and lipid-insoluble substances. A variety of such substances,

including radioisotopes, x-ray opaque species and paramagnetic agents have been considered (Caride, V.J. and Sostman, H.D., 1984; Barratt, G.M. et al., 1984; Brasch, R.G., 1985; Seltzer, S.E. et al., 1984; Bacic, G. et al., 1988). It would be preferred that the marker substance not depend upon entrapment since bilayer membrane leakiness is greatly enhanced in tissue fluids (Scherphof, G.L. et al., 1984; Allen, T.M. et al., 1985). The best method is to associate the marker with the bilayer itself. The most attractive approach would be to use a marker which is itself a lipid. This type of agent would be very tightly bound, yet minimally perturb the structure and properties of liposomes. With this in mind, two species were prepared and tested: one a phospholipid with spin label in the choline headgroup, previously synthesized for membrane spectroscopy (Grant, C.W.M. et al., 1987a) and the other a novel derivative of phosphatidylethanolamine which we developed that has a powerful chelating agent (DTPA) on its headgroup (Grant, C.W.M. et al., 1988).

CHAPTER 2. DEVELOPMENT OF TWO MEMBRANE-BASED LIPOSOMAL MRI CONTRAST AGENTS

2.1 Introduction

The rapid introduction of MRI into clinical settings has been accompanied by efforts to develop contrast-enhancing agents for the technique. Amongst the compounds proposed, stable nitroxide radicals ("spin labels") show special promise (Brasch, R.C., 1985) as well as divalent cation metal chelators such as DTPA. Our involvement in liposomal drug delivery has led us to consider agents that may be firmly associated with bilayer membranes so that their relaxation effects will be most pronounced in regions of liposome biodistribution. Ideally such an agent should minimally perturb the structure and properties of liposomes. In many cases one would prefer that the contrast material not depend upon entrapment within the aqueous interior of liposomes, (there have been several recent articles which have described entrapment of water soluble DTPA and bound cations by lipid bilayer structures (Bacic, G., et al., 1988; Turski, P. et al., 1988)) since bilayer leakiness is greatly enhanced in the presence of tissue fluids. Phospholipids are of course the basic structural feature of the liposome itself. Hence we describe here an investigation of phosphatidylcholine with a nitroxide spin label replacing one methyl group of the choline headgroup - a species originally designed for studies of membrane architecture, and thought to behave like natural phospholipids (Kornberg, R.D. and McConnell, H.M., 1971). One should be able to simply mix such a contrast agent with

other phospholipids in generating liposomes by any of the conventional techniques. The result would be bilayer membranes whose surfaces bore free radicals in direct contact with their aqueous surroundings. We wished to know whether such structures would adequately influence the relaxation time of sample water, and whether they had appropriate morphology to warrant animal trials.

A few reports have already appeared of liposome-borne MRI contrast agents. Caride et al. described the use of the water-soluble agent Mn^{2+}-DTPA entrapped within the aqueous interior of liposomes (Caride, V.J. et al., 1984). Hnatowich et al developed a lipidic chelating agent by attaching DTPA to the lipid stearylamine (octadecylamine) (Hnatowich, D.J. et al., 1981). The same species was more recently studied by Kabalka et al (Kabalka, G. et al., 1987). Buonocore et al. covalently linked stearylamine to DTPA so that it became non-polar enough to associate with liposomes, which would then carry Gd^{3+} to the liver and spleen after intravenous injection (Bunonocore E., et al., 1985). We used instead a phospholipid, phosphatidylethanolamine (PE) for covalent attachment to DTPA, since stearylamine has been employed in the past to confer a (+) charge upon liposomes for injections, and was found to be neurotoxic (Adams, D.J. et al., 1977). Chan et al. studied the *in vitro* interaction of macrophages with liposomes which had a small water-soluble spin label trapped within their aqueous interiors (Chan, H.C. et al., 1985). Without experiments, it is difficult to predict which approach may have advantages -especially given that route of administration, target organ, toxicity, cost, and *in vivo* degradation will influence utility. Since phospholipids are a natural body component they possess an extremely high LD_{50} (Poznansky, M.J., and Juliano, R.L., 1984; Szoka, F.C. et al.,

1987). DTPA alone and attached to various other molecules represents an important class of such agents since paramagnetic ions like Gd^{3+} when bound to DTPA induce dramatic alterations in the relaxation times of surrounding nuclei (H_2O). This chapter emphasizes this aspect of the PE-DTPA-Gd^{3+}, which could provide a contrast agent for regions of liposome biodistribution. Also we reported the use of a nixtroxide spin label attached to PC as a liposome-associated contrast agent for MRI (Grant, C.W.M. et al., 1987a). However chelating agents already have achieved wide usage both clinically and experimentally as carriers of radioisotopes, and we have taken advantage of this sensitive technique in an initial assessment of the intravenous fate of our PE-DTPA-Gd^{3+} contrast agent as well as the SLPC contrast agent.

There are several reasons for investigating liposome-associated contrast agents. Firstly, liposomes injected into experimental animals are known to be largely taken up by the reticuloendothelial system (Mayhew, E., 1983; Weinstein, J.N. and Leserman, L.D., 1984; Poznansky, M.J. and Juliano, R.L., 1984), so that they may be valuable for imaging related organs. The reticuloendothelial (RE) system is an organ axis consisting of liver, spleen, bone marrow and lungs. These tissues contain phagocytic cells that are able to rapidly clear the circulatory system of particulate matter such as liposomes. There is a very real need for diagnostic drug delivery systems aimed at the RE system and the region of its anatomical distribution. Thus, injected intravenously, liposomes 'target' to the liver and spleen if they are small enough to escape entrapment in the lung capillary bed. Injected subcutaneously, intramuscularly, or intraperitoneally they tend to follow the lymphatic routes (Mayhew, E., 1983; Mauk, M.R. et al., 1980; Khato, J. et al., 1983). Secondly

liposomes are of interest as drug delivery vehicles (Mayhew, E., 1983; Weinstein, J.N. and Leserman, L.D., 1984; Poznansky, M.J. and Juliano, R.L., 1984; Gregoriadis, G. (ed)., 1984) and have been shown in clinical trials in several parts of the world to be well tolerated by patients.

2.2 Materials and Methods

2.2.1 Source of Materials

L-α-phosphatidylcholine Type III-E isolated from egg yolk was purchased from Sigma, St. Louis, MO, and further purified on a column of silicic acid (Bio-Sil A 200-400 mesh from Bio-Rad, Richmond, CA) eluted with 30% $CH_3OH/CHCl_3$. Dipalmitoyl phosphatidylethanolamine (PE) and diethylenetriaminepentaacetic (DTPA) anhydride were also obtained from Sigma. Gadolinium chloride hexahydrate 99.999% was from Aldrich Chemical Co., Milwaukee, WI. Phosphatidic acid from an egg yolk source was from Avanti Polar Lipids Inc., Birmingham, AL. 4-(N,N-dimethyl-N-(2-hydroxyethyl))ammonium-2,2,6,6-tetramethyl-piperidine-1-oxyl(Tempocholine) was from Molecular Probes Inc., Eugene, OR. 2,4,6-Tri isopropyl-benzenesulfonyl chloride (TIBS) was from Aldrich Chemical Company., Milwaukee, WI.

Solvents used were reagent grade or "spectral" grade. All lipids used ran as single spots on thin layer plates (Merck Silica Gel 60) eluted with 65:25:4 $CHCl_3/CH_3OH/H_2O$, or 65:25:4:1 $CHCl_3/CH_3OH/H_2O/HCOOH$ (by volume) and developed with sulfuric acid/ethanol spray (1:2.75) prior to charring.

2.2.2 Synthesis of Spin Labelled Phosphatidylcholine (SLPC)

In a 500 ml spinner culture flask, 2.0 g of phosphatidic acid, 0.375 g of Tempocholine, 2.0 g of TIBS, 45 g of glass beads, along with 10 ml of $CHCl_3$ and 5 ml of pyridine (CaH_2 dried) were mixed for 24 hrs. Water was added (10 ml) and the mixture was allowed to stir for an additional 3 hrs. The suspension was extracted with $CHCl_3$ (250 ml) and washed with 0.5 N H_2SO_4 (2 x 150 ml), H_2O (150 ml) CH_3OH-$NaHCO_3$ (3%) 1:2 v/v (225 ml) and finally with CH_3OH-H_2O 1:2 v/v (225 ml). The organic phase was dried over Na_2SO_4 and applied onto a silica gel column. The SLPC was isolated using a CH_3OH gradient. Yield was 60% based on the Tempocholine. It was stored at -20°C in $CHCl_3/CH_3OH$.

2.2.3 Synthesis of Phosphatidylethanolamine-diethylenetriaminepentaacetic acid (PE-DTPA)

Covalent attachment of DTPA to the -NH_2 group of dipalmitoyl PE was performed by mixing a 10-fold molar excess (a 20-fold equivalent excess) of DTPA anhydride with the phospholipid in anhydrous pyridine. Several variants of this approach were tried, all of which produced satisfactory results, however the best overall yield was obtained as follows. 1 g of PE was added to anhydrous pyridine (100 ml dried over CaH_2) in a 500 ml round bottom flask fitted with a reflux condenser and drying tube. The mixture was heated until the lipid dissolved to give a clear solution. In a separate flask, 5 g of DTPA anhydride was warmed with 100 ml of anhydrous pyridine until it dissolved. The DTPA anhydride solution was added from a dropping funnel via a sidearm to the stirred lipid solution over a period of 10 min.

Following the addition, the solution was heated to reflux for 70 min, during which time an orange tint appeared but the solution remained clear. To the reaction mixture was then added 50 ml of H_2O, and refluxing was continued for 70 min to hydrolyse remaining anhydride linkages. The mixture was cooled to room temperature and rotary evaporated to dryness. In our TLC system of silicic acid plates eluted with 65:25:4:1 $CHCl_3/CH_3OH/H_2O$/Formic Acid, DTPA remained at the origin (R_F value 0) and PE ran at the solvent front (R_F value 1). The reaction mixture showed a new spot which ran as a broad band with an R_F value of 0.4. The reaction mixture was dissolved in 150 ml of the 65:25:4:1 solvent system (leaving a small solid residue), and the soluble portion chromatographed on a silica gel column (3 cm x 50 cm; Bio-Sil A Silicic Acid 200-400 mesh from Bio-Rad, Richmond, CA) eluted with the 65:25:4:1 solvent system. The final yield was 1.022 g PE-DTPA (65% yield based on PE starting material). In the acid form this material is soluble in organic solvents such as CH_3CH_2OH and $CHCl_3$. Proton NMR showed the combined features of DTPA and PE. The material was stored as a stock solution in 1:1 $CHCl_3/CH_3OH$.

2.2.4 Liposome Preparation

For preparation of liposomes, appropriate aliquots of stock lipid solutions were mixed in 1:1 $CHCl_3/CH_3OH$ in disposable 3 ml glass test tubes 12 mm in diameter. The clear solutions (total volume about 300 µl) were taken to dryness under a stream of N_2 gas, and subsequently pumped on *in vacuo* for several hours to remove solvent traces. The resultant dry films (SLPC) were hydrated at 4°C with 1.0 or 2.0 ml phosphate buffered saline (pH 7.4) whereas the PE-DTPA dried films were

hydrated at 20°C with 1.0 ml of 0.15 N saline. The liposomes were then sonicated in the same tubes using a Heat Systems Ultrasonics model W-375 sonifier equipped with a Branson 1/8" microtip probe, in a stirred ice bath for 30 min at power setting 2. The lipid concentration was 40 mg/ml. Samples were then centrifuged at 120 x g for 10-15 min at 4°C to remove residual large liposomes and titanium fragments generated by the probe tip. Lipid lost in this step was less than 1-2% as determined by spectral analysis of the resulting pellet. Gadolinium hydrochloride (in 0.15 N saline) could be added to liposomes prior to or after sonication, with much the same result since the percentage volume trapped is small. For work presented here, trivalent ions were added in 10 µl aliquots to sonicated vesicles while vortexing vigorously (eg. total volume of 100 µl of gadolinium stock solution to 1 ml of vesicles). This approach minimized vesicle aggregation.

2.2.5 Freeze-Fracture Electron Microscopy

Samples of lipid vesicles for freeze-fracture electron microscopy were removed from the test specimens and rapidly frozen on gold discs in a Freon slush cooled in liquid nitrogen. Platinum/carbon replicas of these specimens were prepared at -105°C in a Balzers BAF 300 high vacuum coating unit equipped with electron beam guns (Balzers, Liechtenstein). Replicas were cleaned in $NaClO_4$, rinsed with distilled water, and further cleaned with 1:1 acetone/ethanol prior to viewing in a Philips EM 300.

2.2.6 EPR Spectroscopy

EPR spectra of samples were run on a Varian E12 spectrometer equipped

with a TM_{110} cavity and variable temperature accessory (Varian Assoc., Palo Alto, CA). For this purpose vesicle suspensions typically containing 2 mg total lipid in *ca.* 25 µl total buffer volume were held in 50 µl Dade^R disposable glass micro-sampling pipettes sealed at one end and supported in a plastic sleeve which permitted gas flow.

2.2.7 NMR Relaxation Times

Relaxation times were determined at 20°C on samples in 10 mm glass tubes using a Praxis II proton NMR spectrometer operating at 10.7 MHz (Praxis Corporation, San Antonio, TX). T_1 values were obtained by the saturation recovery technique using a total of 32 time spacings between sequential 90° pulses. Repetition time was greater than three times T_1 of the sample involved and relaxation time of distilled water was 3 sec. T_2 values were measured by the spin echo technique. Each decay curve contained 32 points and was fitted to a monoexponential decay yielding a correlation coefficient in excess of 0.99.

2.3 Results and Discussion

2.3.1 Aspects Regarding Spin Labelled Phosphatidylcholine

In Figure 8 the basic structural features of the contrast agent (SLPC) employed is depicted: a nitroxide-containing ring replacing one methyl group of phosphatidylcholine. The resultant spin labelled phosphatidylcholine has a molecular weight of 1024 based on a value of 760 for the native egg phosphatidylcholine. The structure of this new contrast agent is such that it would be expected to behave like a phospholipid, with the spin label as part of the polar headgroup region. Earlier

work by Kornberg and McConnell (1971) concluded that this spin labelled phospholipid was assembled into the lipid bilayer like normal phospholipids. Our data is in agreement with this statement. As indicated in Figure 8, at low concentrations of SLPC (before or after sonication) the EPR spectrum consists of three lines. The obvious lack of spin-exchange broadening (Devaux, P.D. et al., 1973), is an indication that the SLPC is dispersed amongst the unlabelled phospholipids. Spin exchange broadening occurs in solutions of monoradicals at high concentration. At the moment of collision, a biradical state is formed. The greater the frequency of collision, the greater the contribution biradical states can make to the EPR lineshape. As the rates of collision between monoradicals become very high this then leads to line broadening to a point where a single resonance line appears. This is known as the so-called exchange-narrowing limit. Exchange broadening can occur in lipid films, where the spin probes are excluded to form aggregates which are insoluble in water or highly localized due to preferential solubility in one lipid component, so-called patching. Increasing the SLPC/native phospholipid ratio leads to a measurable increase in spectral line width (eg. Fig. 8, 12.5 wt% vs 25 wt% samples) and the presence of only 3 very broad and obviously spin-exchange broadened lines at 50 wt% collapse to a single broadline at 100%.

Vigorously sonicated unilamellar vesicles are typically reported to have diameters in the range of 20-40 nm (Andrews, S.B. et al., 1975). Structures of this size are too small to be visualized by light microscopy, and a suspension of such species is optically clear since particles >100 nm give a cloudy suspension. Sonicated unilamellar vesicle suspensions used in the experiments were clear but yellow due to

Figure 8

Chemical structure of phosphatidylcholine with a spin label ring replacing one methyl group of the choline headgroup (SLPC), and its EPR spectra in bilayers of egg phosphatidylcholine. Total lipid concentration 40 mg/ml, of which 1, 12.5, 25 and 50 wt% was SLPC. Lipids were mixed in appropriate ratios in 1:1 $CHCl_3/CH_3OH$ prior to drying as thin films. EPR samples consisted of lipid bilayer structures produced by hydration of these films in physiological saline buffered at pH 7.4 with 20 mM phosphate. Spectra were run at 20°C.

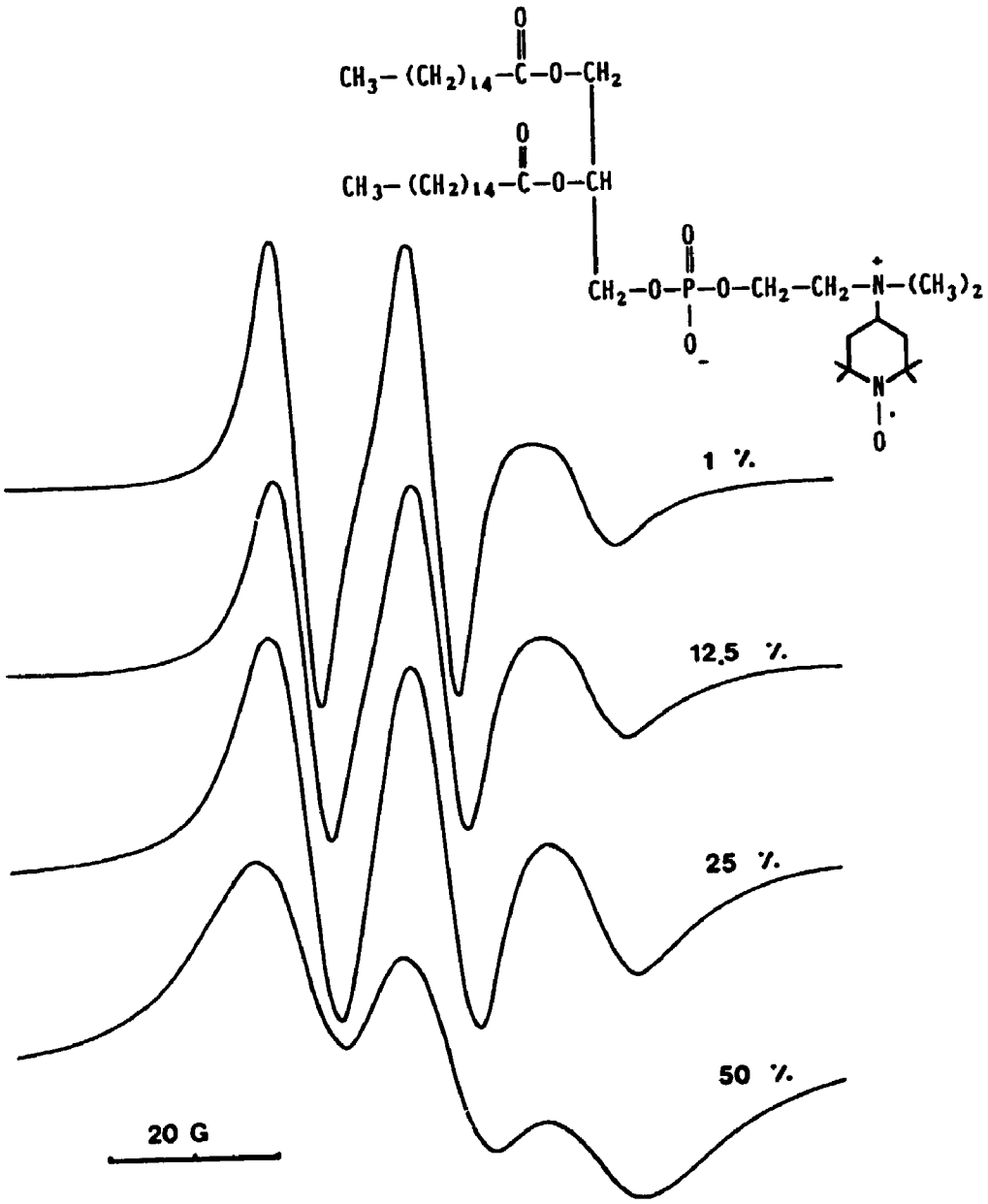
1 %.
12.5 %.
25 %.
50 %.
20 G

the presence of the nitroxide radical. Samples of these vesicles were examined via electron microscopy. We chose the freeze-fracture method because it employs cryogenic fixation rather than depending upon chemical fixatives. The results are found in Figure 9, in which sonicated unilamellar vesicles of egg phosphatidylcholine are shown along with those bearing a 1:1 weight ratio of SLPC. Only sealed vesicular structures were seen in each case. No amorphous or crystalline masses were apparent in any of the samples. The appearance is typical of sonicated unilamellar vesicles.

MRI contrast-enhancing properties of paramagnetic species are related to their effect on water proton relaxation times. Any substance that has an unpaired electron (spin labels) will have paramagnetic properties and thus can be used as an MRI contrast agent. One drawback of this is that most organic substances that can assume an electronic configuration with an unpaired electron are unstable. Nitroxide stable free radicals have been investigated primarily by Brash et al (Brash, R.C. et al., 1983), early in the evolution of MR contrast media. There are two major classes of nitroxide stable free radicals; pyrrolidine-N-oxyl and piperidine-N-oxyl. In this study the latter species was used. These agents have paramagnetic properties caused by the presence of an unpaired electron which is delocalized between the nitrogen and oxygen atoms. The delocalized electron and the steric hindrance supplied by the adjacent bulky methyl groups, stabilize the free radical *in vitro*, however, their paramagnetic properties are weak as compared to many paramagnetic metal ions such as Gd^{3+}. This type of compound appears to be relatively unstable *in vivo* (see Grifeth, L.K. et al., 1984 for pharmacokinetic properties) (Grifeth, L.K., et al., 1984) and may undergo reduction to the corresponding hydroxylamine which is not

Figure 9

Freeze-etch electron micrographs of the sonicated unilamellar vesicles used in this work.

A) Natural egg phosphatidylcholine alone.

B) 50:50 (wt. ratio) mixture of natural phosphatidylcholine with spin labelled phosphatidylcholine (SLPC).

In each case the sample in phosphate buffered normal saline pH 7.4 was quenched from 22°C in Freon cooled to a slush in liquid nitrogen.

Magnification x 100,000

Bar = 100 nm. Platinum shadow is from bottom to top of page.

paramagentic.

In vivo results will be influenced in a complex way by drug (liposome in this case) biodistribution and rate of destruction. In this chapter we study the effects seen in the absence of biological tissue as a point of departure for future animal studies (see Chapter 3). Each sample consisted of 1 cc of physiological saline containing 40 mg total phospholipid (egg phosphatidylcholine plus SLPC). T_1 values for such a sample containing 40 mg/ml total lipid of which 50 wt% was SLPC were in the range of 300 msec, which corresponds to a relaxivity of 0.27 $mM^{-1}sec^{-1}$ (Fig. 10). In a sample of pure SLPC the T_1 value was reduced to 85 msec. In the latter case though sonication was much less effective in producing small lipid vesicles, and the micellar nature of the suspended matter in the total absence of native phosphatidylcholine has not been studied. The results of a typical experiment are illustrated in Figure 10. Note that a linear relationship exists between spin label concentration and T_1 for sample water when other factors are held constant. The effect was noted to be stable for at least 18 hrs.

2.3.2 Aspects Regarding Phosphatidylethanolamine-diethylenetriaminepentaacetic acid

Figure 11 illustrates the probable structure of the adduct formed when the -NH_2 group of PE was covalently attached to a -COOH group of DTPA. The basic features of a phospholipid are retained: hydrophobic fatty acid chains and polar headgroup on a glycerol backbone. The -COOH groups on the headgroup make it an acidic phospholipid, and influence the solubility and chromatographic properties.

Figure 10

Solvent proton T_1 values for aqueous suspensions of sonicated unilamellar vesicles bearing the contrast agent, TEMPO phosphatidylcholine (SLPC). The quantity of spin label in each 1 ml sample is shown on the x-axis (total lipid 40 mg/ml in phosphate buffered saline pH 7.4). $1/T_1$ values in sec^{-1} are displayed on the y-axis (measured at 20°C on a Praxis II instrument operating at 10.7 MHz by the saturation recovery technique). Instrument repeatability was 2% while intrasample reproducibility was 5%.

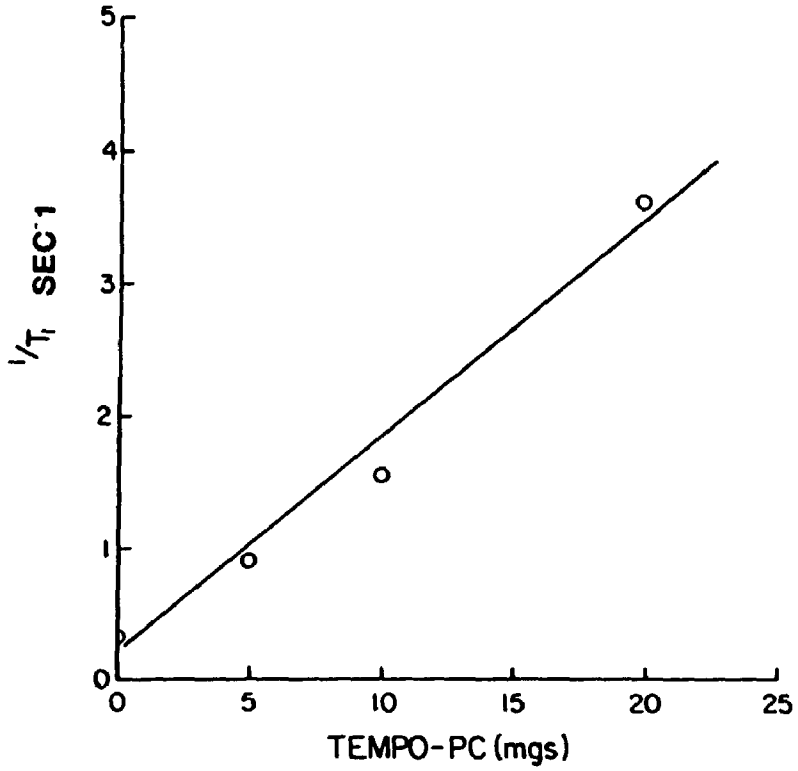
5
4
3
2
1
0
$^1/T_1$ SEC^{-1}
0
5
10
15
20
25
TEMPO-PC (mgs)

Figure 11

Proposed structure of phosphatidylethanolamine-diethylenetriaminepentaacetic acid (PE-DTPA).

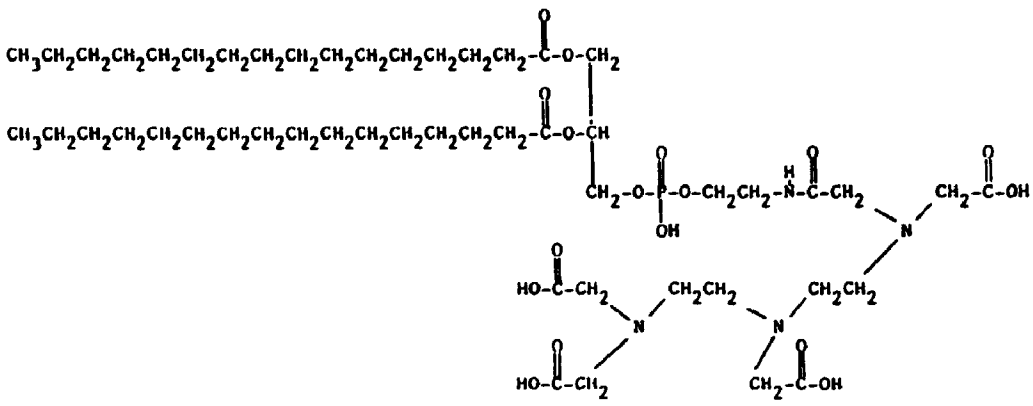

In the protonated form PE-DTPA dissolved in organic solvents such as chloroform and ethanol. In the salt form it was sparingly soluble in organic solvents. Both forms were water-insoluble.

Figure 12 illustrates at high magnification the appearance of the structures generated when dry films of PC with up to 50 wt% of PE-DTPA are hydrated and sonicated. "Liposome" is a term that refers to the structure formed when a lipid bilayer folds back upon itself and seals at the edges to produce a closed capsule trapping an aqueous compartment. Extensive sonication of liposomes caused them to fragment into smaller, single bilayer "vesicles" that also trap an aqueous compartment but approach a limiting minimum size of 20-50 nm (Szoka, F. and Papahadjopoulos, D., 1980). A suspension of liposomes (vesicles) whose sizes have been reduced by sonication to less than about 200 nm becomes clear or opalescent due to reduced light scattering. This behaviour was seen in liposomes of egg PC bearing up to 50 wt% PE-DTPA. In the presence of Gd^{3+}, sonicated liposomes were very sensitive to aggregation. Thus rapid addition of $GdCl_3 \cdot 6H_2O$ in 0.15N saline to a clear suspension of PE-DTPA-containing liposomes caused aggregation as manifest by immediate clouding of the suspension, and subsequent slower clearing. Slow addition with rapid mixing minimized this problem. Nevertheless vesicle clusters were a common feature of the preparations, and these are apparent in the electron micrographs. It was found to be technically easier to sonicate liposomes bearing lower ratios of PE-DTPA to egg PC (i.e., 12.5 wt% or 25 wt% vs 50 wt%). They also gave fewer problems of aggregation upon Gd^{3+} addition.

Figure 12A illustrates the electron microscopic appearance of sonicated egg

Figure 12

Freeze-etch electron micrographs of the lipid bilayer structures used in this work. Pure lipids or lipid mixtures were dissolved in organic solvent and dried in glass vessels. Resultant films were hydrated with 0.15 N saline and sonicated extensively using a probe sonicator. Measured quantities of the trivalent cation, Gd^{3+}, were added subsequently with rapid mixing (details in Materials and Methods).

A) Pure egg phosphatidylcholine

B) 12.5 wt% PE-DTPA-Gd^{3+} in egg PC

C) 25 wt% PE-DTPA-Gd^{3+} in egg PC

D) 50 wt% PE-DTPA-Gd^{3+} in egg PC.

Samples were "quenched" (frozen) from 22°C in a Freon slush cooled in liquid nitrogen. Specimens shown in B - D were etched for 2 min at -103°C prior to shadowing with platinum. Magnification x 78,000. Shadow direction is from bottom to top.

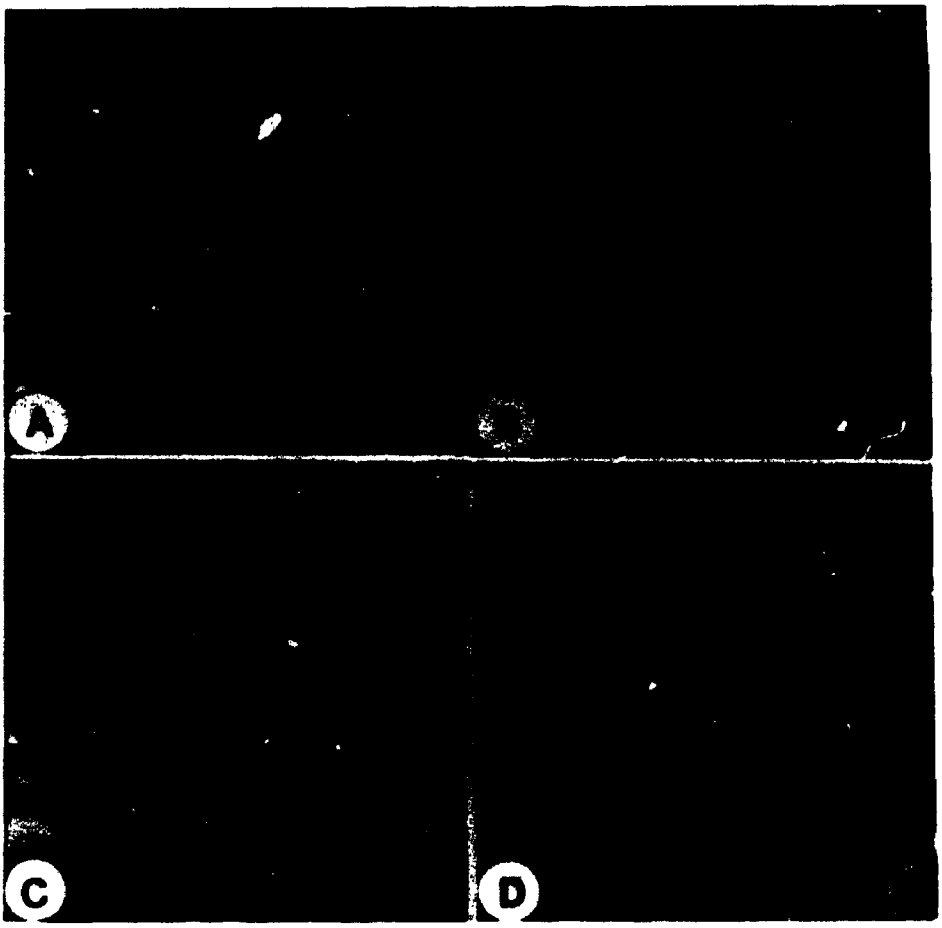
A
C
D

PC vesicles suspended in 0.15N saline. Note that the basic feature is spherical structures between 20-50 nm in diameter, which can also occur in clusters or loose aggregates. Figures 12B-D are typical of specimens produced when the chelating agent, PE-DTPA, was mixed with egg PC in organic solvents prior to solvent evaporation, hydration, and sonication.

Paramagnetic metal ions in the form of metal chelates are very important in MR imaging. It is known that chelates can maintain ions in solution under physiological conditions, at concentrations which would normally be insoluble in blood. A major problem with the direct use of paramagnetic ions as contrast agents arises from their comparative toxicity. Highly stable complexes could be used (metal chelates) to reduce the toxic effect of the metal, whereas weaker complexes could transport the ions to sites of higher affinity. The use of ion chelators can confer other advantages to the contrast agent. For example, the rotational correlation time is increased, rendering the relaxation process more efficient and enabling lower doses to be used. Also, complexes which contain hydrophobic regions can bind to serum proteins, which can enhance their own relaxivity. Many metal ions are presently being studied but the most interesting ones are Mn^{2+}, Fe^{3+} and of course Gd^{3+} (Morris, P.G., 1986).

Samples containing chelating agent were etched prior to shadowing with platinum and carbon. That is, some ice was allowed to sublime away after the frozen specimen was fractured in the freeze-etch preparation process. Thus vesicle outer surfaces and cleaved hydrophobic interiors are visible in places. There is no significant difference in features amongst the various preparations: features seen are

those expected of sonicated unilamellar vesicles.

Liposomes bearing Gd^{3+} bound to PE-DTPA have strong paramagnetic relaxation effects upon surrounding water protons. Adding a paramagnetic material to biological fluids will cause proton relaxation to occur in the fluid. The total relaxation process can be written as follows:

$$R_{OBS} = R_{H\,O} + R_{TIS} + R_{CA}$$

(Kressel, H.Y., 1985) where R_{OBS} is the observed T_1 or T_2 relaxation rate, and $R_{H\,O}$ is the relaxation rate of bulk water, R_{TIS} are the relaxation sites contributed by the tissue and R_{CA} is the relaxation enhancement due to the paramagnetic contrast agent. $R_{H\,O}$ is not field-dependent but R_{TIS} and R_{CA} are. Typically one measures R_{OBS} with and without contrast agent at a particular imaging field strength to determine the actual amount of relaxation enhancement which is due to R_{CA}.

For example, in Figures 13 and 14, sonicated liposomes of egg PC bearing 12.5, 25 or 50 wt% PE-DTPA were suspended at a total lipid concentration of 40 mg/ml, and from these samples the relaxation times of sample water protons were recorded. T_1 and T_2 were sensitive, inverse functions of both the quantity of contrast agent in the liposomes and the concentration of liposomes in the samples.

Unlike most imaging modalities which depend on a single static parameter, such as electron density for image contrast, MRI is determined mainly by the differences in the dynamic properties of the tissue protons which determine the relative intensity of the neighbouring pixels (the smallest discrete part of a digital image display (Kressel, H.Y., 1987). It is not the concentration of tissue protons, but their relaxation rate $1/T_1$ and $1/T_2$ that dominate considerations of contrast in MRI.

Figure 13

Solvent proton $1/T_1$ values for aqueous suspensions of sonicated unilamellar vesicles bearing the chelating contrast agent, PE-DTPA-Gd^{3+}. Inverse relaxation times are displayed as a function of Gd^{3+} concentration for samples having 12.5 (●), 25 (■) and 50(▲) wt% chelating agent in egg PC liposomes prepared as in caption to Figure 12. T_1 values were recorded at 20°C on 1 cc samples in 10 mm diameter glass tubes using a Praxis II pulsed NMR instrument operating at 10.7 MHz via the saturation recovery technique. In each case a straight line has been drawn through the data points to a least squares fit with correlation coefficient > 0.99.

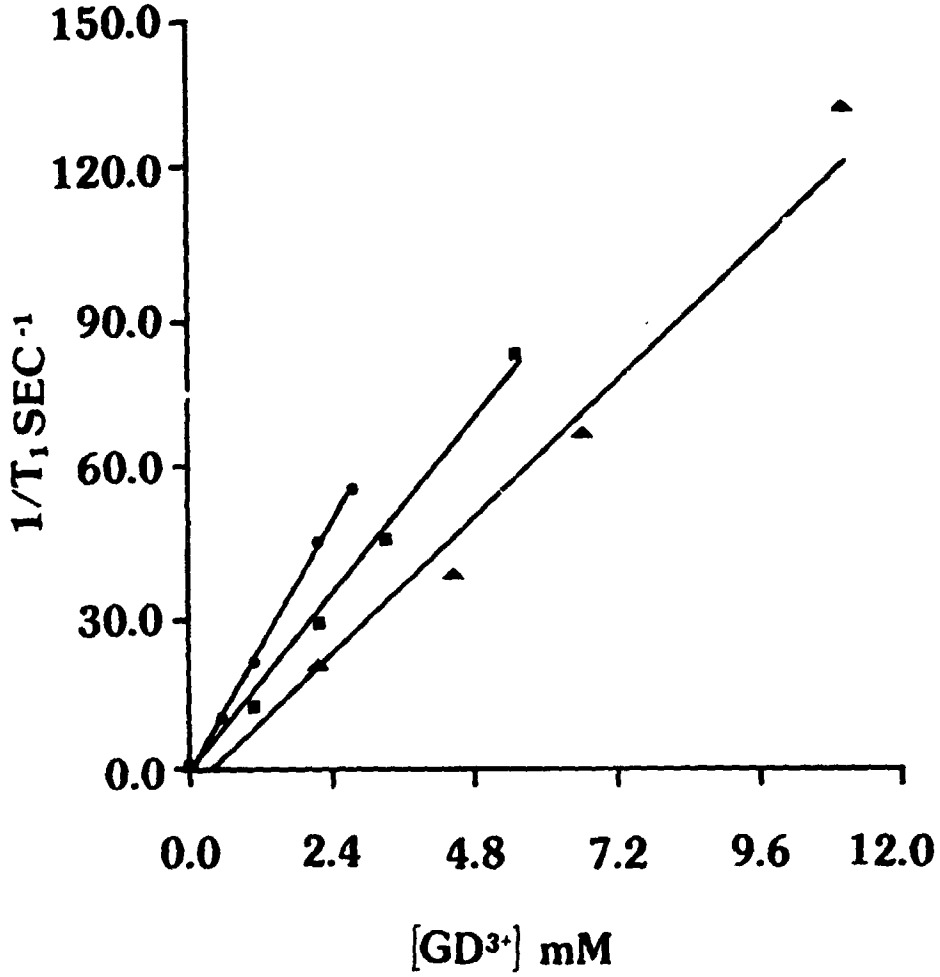
150.0
120.0
90.0
60.0
30.0
0.0
1/T1 SEC-1
0.0
2.4
4.8
7.2
9.6
12.0
[GD3+] mM

Figure 14

Solvent proton $1/T_2$ values for aqueous suspensions of sonicated unilamellar vesicles bearing the chelating contrast agent, PE-DTPA-Gd^{3+}. Inverse relaxation times are displayed as a function of Gd^{3+} concentration for samples having 12.5 (●), 25 (■) and 50 (▲) wt% chelating agent in egg PC liposomes prepared as in caption to Figure 12. Values were recorded at 20°C on 1 cc samples in 10 mm diameter glass tubes using a Praxis II pulsed NMR instrument operating at 10.7 MHz via the spin echo technique. In each case a straight line has been drawn through the data points to a least squares fit with a correlation coefficient > 0.99.

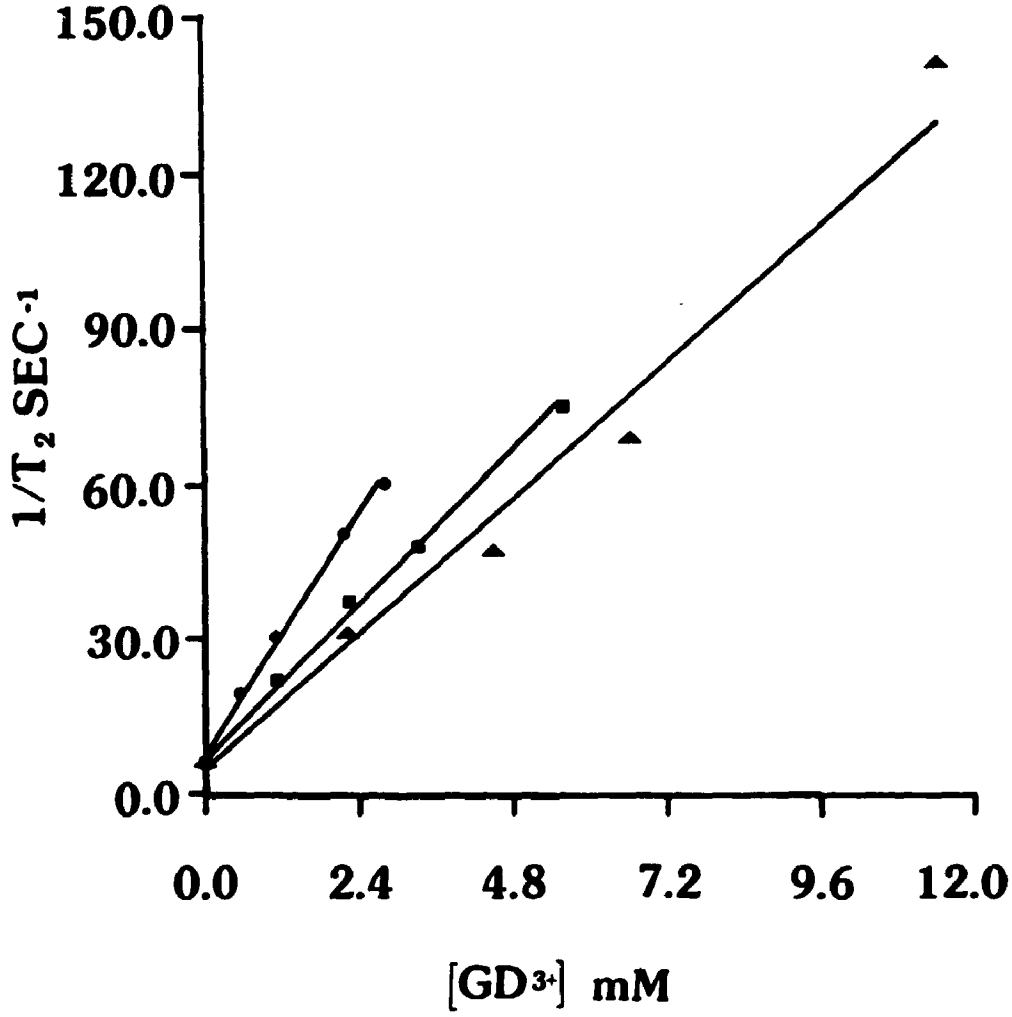
150.0
120.0
90.0
60.0
30.0
0.0
1/T2 SEC-1
0.0
2.4
4.8
7.2
9.6
12.0
[GD3+] mM

It is also known that $1/T_1$ and $1/T_2$ are not fixed parameters of a given tissue, rather their values can vary significantly with Bo, the applied external magnetic field and with temperature. Since MRI contrast images are dominated by $1/T_1$ and $1/T_2$ parameters, this leads us to consider materials which can alter $1/T_1$ and $1/T_2$ so as to be useful as contrast-enhancing agents. As previously stated such agents are nitroxide radicals (spin labels) and paramagnetic metal ions such as Gd^{3+}.

In each case a straight line has been drawn with least squares fit to the data points plotted as a function of concentration of Gd^{3+}. The results for $1/T_1$ and $1/T_2$ are essentially superimposable. Plotted in this way the slopes of the lines correspond to the relaxivity of the contrast agent. As taken from the $1/T_1$ plots, the relaxivities for sonicated liposomes bearing 12.5, 25 and 50 wt% chelating agent are 21, 15 and 12 $mM^{-1}\ S^{-1}$ respectively. Thus the Gd^{3+} complex appears most efficient as a contrast agent when present at low local concentrations in bilayer membranes. This phenomenon is reproducible, and seems likely to result from the extreme proximity of paramagnetic ions to one another in liposomes having a high ratio of chelating agent to egg PC.

Relaxation is presumed to occur only in the hydrated complex with rapid exchange distributing the effect among all solvent protons. The theory of outer sphere relaxation by such small, highly symmetric complexes is rather well developed (Koenig, S.H., 1987). Briefly, the main parameters are the relative diffusion constant of water in the vicinity of the complex and the mean distance of closest approach of the protons to the complex. The same phenomenon has recently been reported for the relaxivity of Mn^{2+} ions bound to phosphatidylserine sonicated vesicles in aqueous

suspension (Koenig, S.H. et al., 1988). Such effects combined with their greater aggregability may account for increased point scatter in the curves corresponding to 50 wt% PE-DTPA. The relaxivity values observed here are similar to values recorded in the literature for Gd^{3+} complexed to DTPA (Koenig, S.H. and Brown, R.D. III, 1987).

Preliminary indications are that the chelating agent, PE-DTPA, survives with bound trivalent cations *in vivo* for long periods, as would be necessary for a marker of liposome biodistribution. For instance the data in Figure 15 records the results of intravenous injections of PE-DTPA liposomes tagged with a gamma-emitting radioisotope $^{111}In^{3+}$. Rats were injected via the right femoral vein with 1.5 cc of saline containing 60 mg of total lipid in the form of sonicated liposomes with bound Gd^{3+} and a trace of $^{111}In^{3+}$. Animals were sacrificed at 5 hrs and 24 hrs, and the organs were removed for gamma counting. Free $^{111}In^{3+}$ and DTPA are cleared rapidly via excretion in the urine (Runge, V.M. et al., 1985; Welch, M.J. and Welch, T.J., 1975). Clearly a very different picture was seen for the fate of $^{111}In^{3+}$ bound to PE-DTPA in sonicated unilamellar vesicles. Circulation in the blood was significant even at 5 hrs, although markedly reduced by 24 hours. Major uptake was by liver and spleen, as anticipated (Poznansky, M.J. and Juliano, R.L., 1984; Mayhew, E., 1983) for liposomes injected intravenously provided they are small enough to escape becoming lodged within the lung capillary bed. At 24 hrs the GI tract had considerable radioisotope-consistent with amphiphilic PE-DTPA-$^{111}In^{3+}$ being excreted into the bile.

Figure 15

Organ distribution of the chelating agent, PE-DTPA, in sonicated unilamellar vesicles after intravenous injection. Vesicles having 12.5 wt% chelating agent in egg PC were prepared as in the caption to Figure 12, but with an added tracer of bound $^{111}In^{3+}$. A total of 60 mg lipid in 1.5 cc of saline was injected as a bolus via the femoral vein of male 500 g Sprague-Dawley rats under Somnotol/Ketamine anesthesia. Rats were sacrificed at 5 hr and 24 hr post injection. Organs were removed, rinsed with saline, blotted dry, and counted in a Beckman Gamma 8000 Gamma-counter. Values are expressed on the vertical axis as fraction of total counts - each point represents 2 animals. "Body" counts refer to carcass with stated organs removed. Open and shaded rectangles show 5 and 24 hr data respectively. The counts were not normalized on a weight basis.

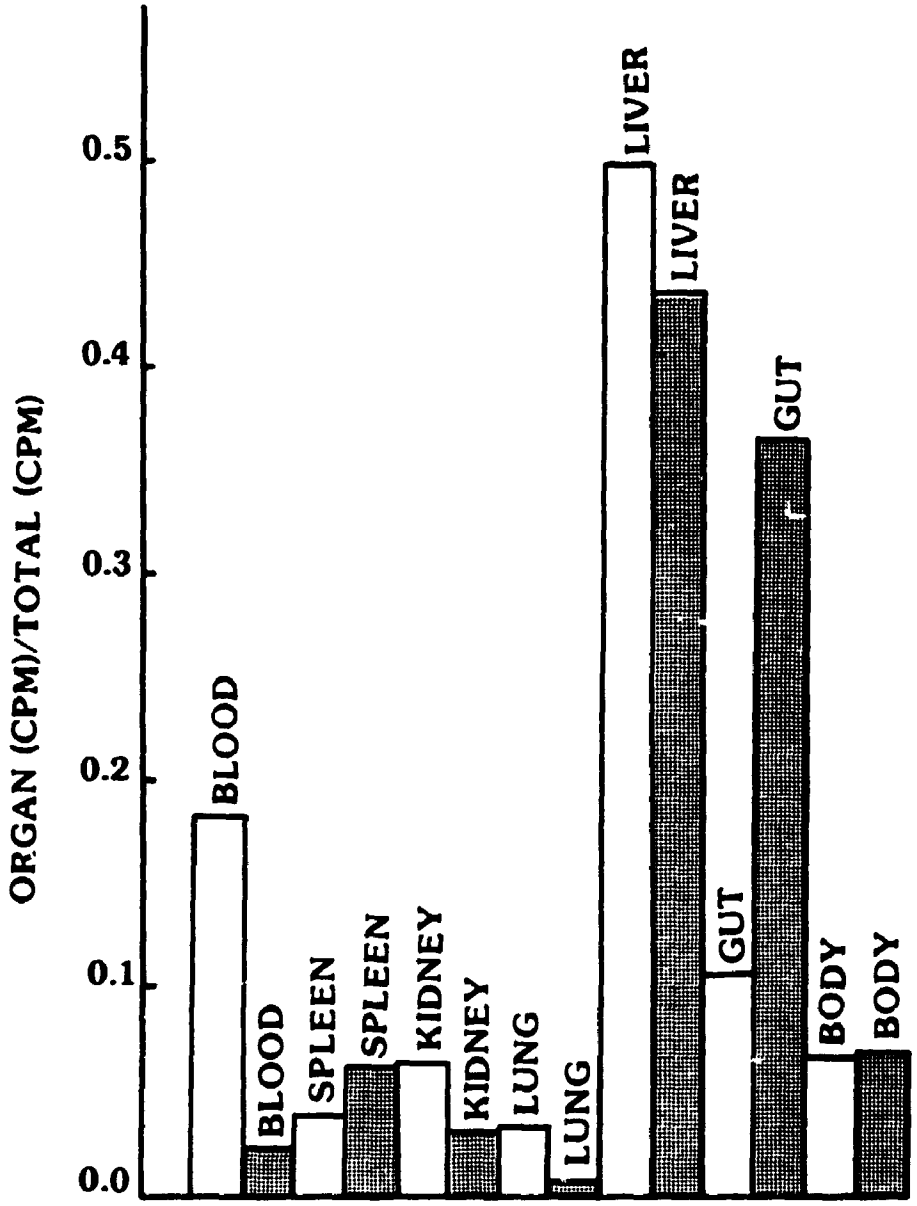
ORGAN (CPM)/TOTAL (CPM)
0.0
0.1
0.2
0.3
0.4
0.5
BLOOD
BLOOD
SPLEEN
SPLEEN
KIDNEY
KIDNEY
LUNG
LUNG
LIVER
LIVER
GUT
GUT
BODY
BODY

2.4 Conclusions

We have demonstrated that phosphatidylcholine with a spin label replacing one methyl group of the choline moiety is an effective agent for reducing the relaxation time of surrounding water protons when assembled in lipid bilayers. The critical micelle concentration of phosphatidylcholine is very low so that virtually all of the material in aqueous samples exists in the form of bilayers (a special form of micelle peculiar to phospholipids). Results of EPR spectroscopy and electron microscopy were consistent with the concept that SLPC contrast agent behaved basically like a normal phospholipid molecule. There was no difficulty in producing uniform populations of sonicated unilamellar vesicles from mixtures that were at least 50 wt% SLPC, with less than 1-2% large particles. The relaxivity found is similar to that quoted by other workers for water-soluble spin labels in aqueous solution.

The chelating agent DTPA, was attached covalently to the amino-headgroup of PE to produce a phospholipid which is also a powerful chelating agent. It readily assembles into the walls of lipid bilayer structures as a liposome-associated carrier of cations for MR contrast or radioisotope studies. Freeze-etch electron microscopy showed that PE-DTPA satisfactorily formed sonicated vesicles when mixed up to 50 wt% with natural phospholipids. The resultant structures with bound gadolinium effectively shortened T_1 and T_2 of surrounding water protons. When sonicated liposomes bearing chelating agent with bound $^{111}In^{3+}$ were injected intravenously into rats, uptake was primarily by liver and spleen. By 24 hours post injection there was biliary excretion of this material. PE-DTPA may have some general utility as an amphiphilic liposomal chelating agent for cations.

CHAPTER 3. AN *IN VIVO* COMPARATIVE EVALUATION OF TWO MEMBRANE-BASED LIPOSOMAL MRI CONTRAST AGENTS

3.1 Introduction

An active subset of MR imaging is the use of liposomes as particulate carriers of contrast material (Seltzer, S.E., 1989). The reason for this type of application is that phospholipid liposomes have an extremely high LD_{50} (Olson, F., 1982; Poznansky, M.J. and Juliano, R.L., 1984; Szoka, F.C. et al., 1987) and they target dependably to liver, spleen and lung when injected intravenously, and to the lymphatics when injected subcutaneously or intraperitoneally (Poznansky, M.J. and Juliano, R.L., 1984; Gregoriadis, G., 1988).

Our interest in the development of membrane based MR probes for spectroscopy has led us to synthesize and test two MR imaging contrast agents that consist of natural phospholipids. Contrast agents based upon a phospholipid backbone incorporate with 100% efficiency into the liposome bilayer with no special manipulations, lead to minimal structural perturbation of the membrane, and are not influenced by liposome leakiness. Furthermore, they may well be excreted in the bile and so temporally image all regions of liver and its duct systems.

Nitroxide free radicals ("spin labels") and Gd^{3+} held by a chelating agent represent two major families of paramagnetic compounds that are being widely studied as potential contrast agents for MR imaging (Brasch, R.C., 1985; Koenig, S.H. and Brown III, R.D., 1984). Both are satisfactorily non-toxic and have demonstrated potential *in vitro* and *in vivo*. In this chapter, we report *in vivo* studies of the two

families of phospholipid-based contrast agents developed by us, and a comparison of their relative utilities.

3.2. Materials and Methods

3.2.1 Source of Materials

Same as in section 2.2.1.

3.2.2 Liposome Preparation

Same as in section 2.2.4.

3.2.3 Freeze-Fracture Electron Microscopy

Same as in section 2.2.5.

3.2.4 NMR Relaxation Times

Same as in section 2.2.7.

3.2.5 MR Imaging

MR imaging data were obtained using a GE Signa clinical scanner. Three or four treated rats were imaged together in the head coil using standard spin echo techniques. Although some T_2-weighted sequences were run, T_1-weighted (TR=500 msec; TE=20 or 25 ms) images were routinely obtained in the coronal plane with 3 mm slice thickness, 1.5 mm gap to cover the abdomen of the animal. Fat-suppressed MR imaging was performed using the chopper fat suppression technique of

Szumowski et al (Szumowski, J. and Plewes, D.B., 1987), which has proved to be effective in contrast applications where fat is present (Simon, J.H. and Szumowski, J., 1989). This fat suppression sequence utilized both a 1:3:3:1 saturating prepulse and the Dixon method of phase subtraction.

3.3 Results and Discussion

The natures of the contrast agents used in this work, and the relative potencies of their *in vitro* effects on the T_1 of surrounding water protons are summarized in Figure 16. They are representative of two major families of paramagnetic species being widely considered for use in MR imaging. Note that in each case the paramagnetic species is part of a natural phospholipid and is held at the membrane/water interface, in direct contact with the aqueous medium. Data are shown for 25 wt % contrast agent in sonicated 20-70 mm vesicles of egg PC as aqueous suspensions in glass tubes 10 mm in diameter. The plots presented produce calculated relaxivities of 0.13 and 15 $mM^{-1}S^{-1}$ for the phosphatidylcholine spin label and phosphatidylethanolamine-DTPA-Gd^{3+} agents, respectively. Thus it will be seen that in this particular *in vitro* situation, with the contrast agent located at a liposome surface, the PE-DTPA-Gd^{3+} is by far the more potent of the 2 major families of contrast agents studied (nitroxide radical vs Gd^{3+}). Our initial studies of both contrast agents involved assembly into sonicated unilamellar vesicles of egg PC. We found that the chelating agent may readily be substituted for up to 25 wt % of the host membrane lipid without adversely affecting the physical nature of the resultant bilayer structures (Grant, C.W.M. et al., 1987a); while the spin label agent could be taken

Figure 16

Solvent proton $1/T_1$ values for aqueous suspensions of sonicated unilamellar vesicles bearing 25 wt % membrane-associated liposomal contrast agent: PC spin label (●) and PE-DTPA-Gd^{3+} (■). Concentration of nitroxide radical or Gd^{3+} is indicated on the x-axis. Liposome suspensions were clear/opalescent and were prepared by hydration and probe sonication of dry films of contrast agent plus egg PC. Samples for study contained 0.17 to 16 mg/ml total lipid in phosphate buffered 0.15 N saline pH 7.4 (in 10 mm glass tubes). T_1 values were measured at 20°C on a Praxis II instrument operating at 10.7 MHz by the saturation recovery method. The plots produce relaxivity values of 0.13 and 15 mM^{-1} S^{-1} for the PC spin label and PE-DTPA-Gd^{3+} respectively. Contrast agent structures and presumed membrane arrangement are indicated.

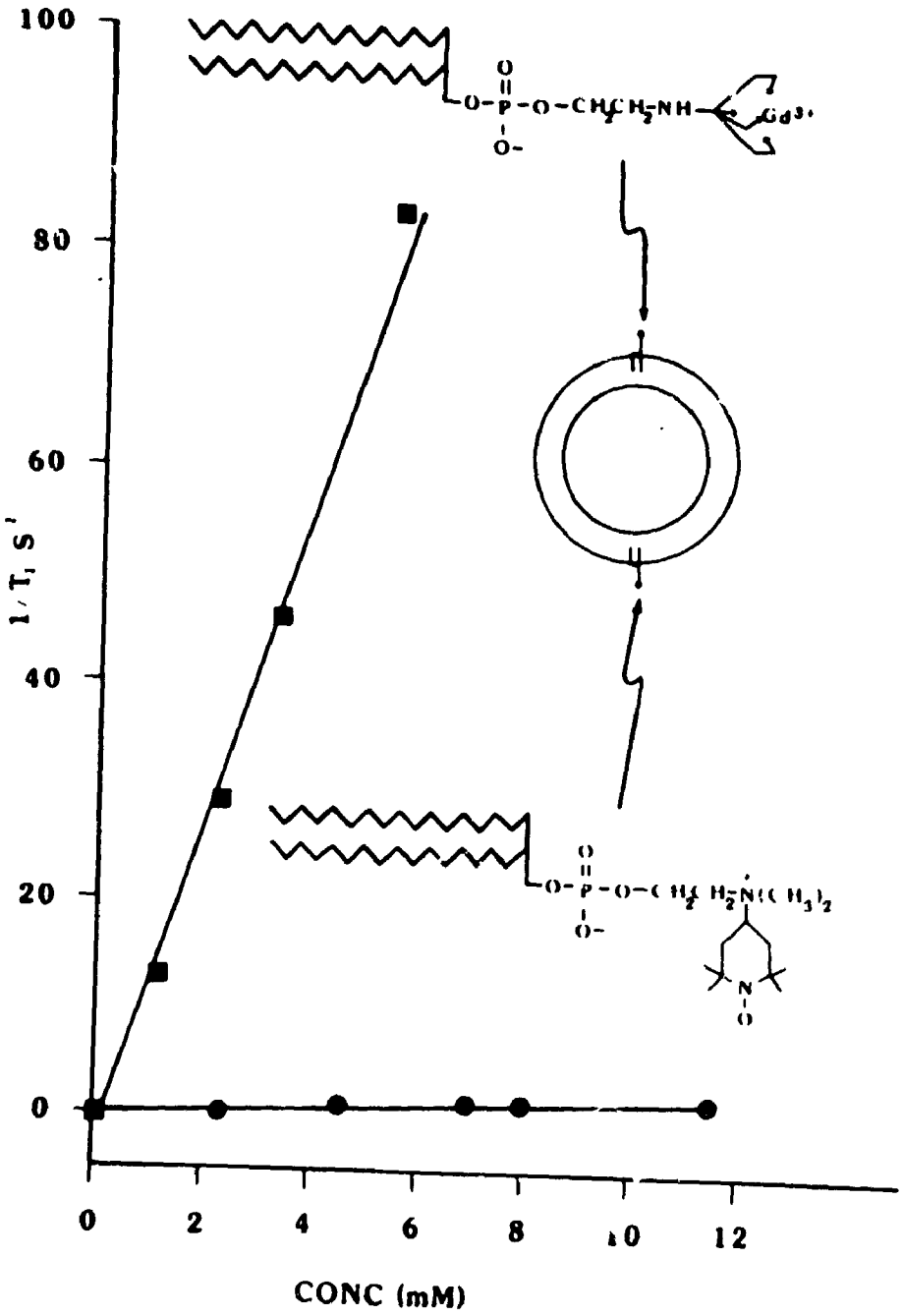
100
80
60
40
20
0
1/T1 S-1
0
2
4
6
8
10
12
CONC (mM)
Gd3+

up to 50 wt % (Kabalka, G.W. et al., 1988). Beyond these concentrations in the bilayer, sonication became less effective at producing the opalescent suspensions characteristic of very small sealed single bilayer vesicles, presumably due to structural differences between contrast agent and natural phospholipid. It is desirable to have a high concentration of contrast agent in the liposome membrane in order to provide a potent effect on relaxation times without having to exceed convenient volumes of liposome suspension and while maintaining a lipid concentration of 40 mg/ml or less. Hence we have chosen 50 wt % phosphatidylcholine spin label and 25 wt % PE-DTPA for the *in vivo* work described here, as reasonable compromises between potency of contrast enhancement and bilayer disruption.

The question arose then as to how spectroscopy experiments such as those summarized in Figure 16 would translate to results with an MR imager. We first addressed this question by imaging aqueous samples in 10 mm diameter glass test tubes held in plastic test tube racks. Pulse sequences were carried out using a constant TE of 20 ms but varying the TR. A typical result is illustrated in Figure 17. In this example 3 rows of tubes were scanned. The image plane is parallel to the base of the test tube rack so that it transects the samples, making each appear as a circle. The column on the left of Figure 17 comprised 5 samples: the lowest one being simply a buffered saline blank, and the next 4 being increasing concentrations of egg PC liposomes bearing PE-DTPA-Gd^{3+} contrast agent. Note that image intensity is a function of contrast agent concentration. Note also that the most concentrated sample of liposomal PE-DTPA-Gd^{3+} is actually 'invisible' since at very short relaxation times (high contrast agent concentration) the sample protons are fully relaxed in a

Figure 17

MR imaging of aqueous contrast agents in 10 mm glass sample tubes supported in plastic test tube racks. Typical image of 3 rows of tubes in a single rack: image plane parallel to base of rack and transecting each tube so that contents appear as a disc (TR=500, TE=20). Left hand (vertical) column consisted of 5 samples which contained, from bottom to top, a blank of phosphate buffered 0.15 N saline pH 7.4, sonicated egg PC liposomes prepared as in caption to Figure 16 with 25 wt % PE-DTPA contrast agent bearing Gd^{3+} at 0.31, 0.61, 3.1 and 6.1 mM respectively (lipid concentration 1.3 -26.6 mg/ml). Note that the tube corresponding to the highest contrast agent concentration (left row top) was not visualized due to its short relaxation time (see text). Middle column comprised four concentrations of sonicated egg PC liposomes with 50 wt % PC spin label at (from bottom to top) 0.72, 1.4, 7.6 and 14.8 mM respectively (lipid concentrations 1.3 to 26.6 mg/ml). Right hand column comprised 5 tubes containing from bottom to top commercial water-soluble DTPA-Gd^{3+} (Magnevist^{R} 0.4 M in a 12 mm tube), egg PC liposomes without contrast agents at 1.3, 2.6, 13.6 and 26.6 mg/ml respectively. All liposome samples were 1 ml in volume and were in 0.15 N phosphate buffered saline pH 7.4

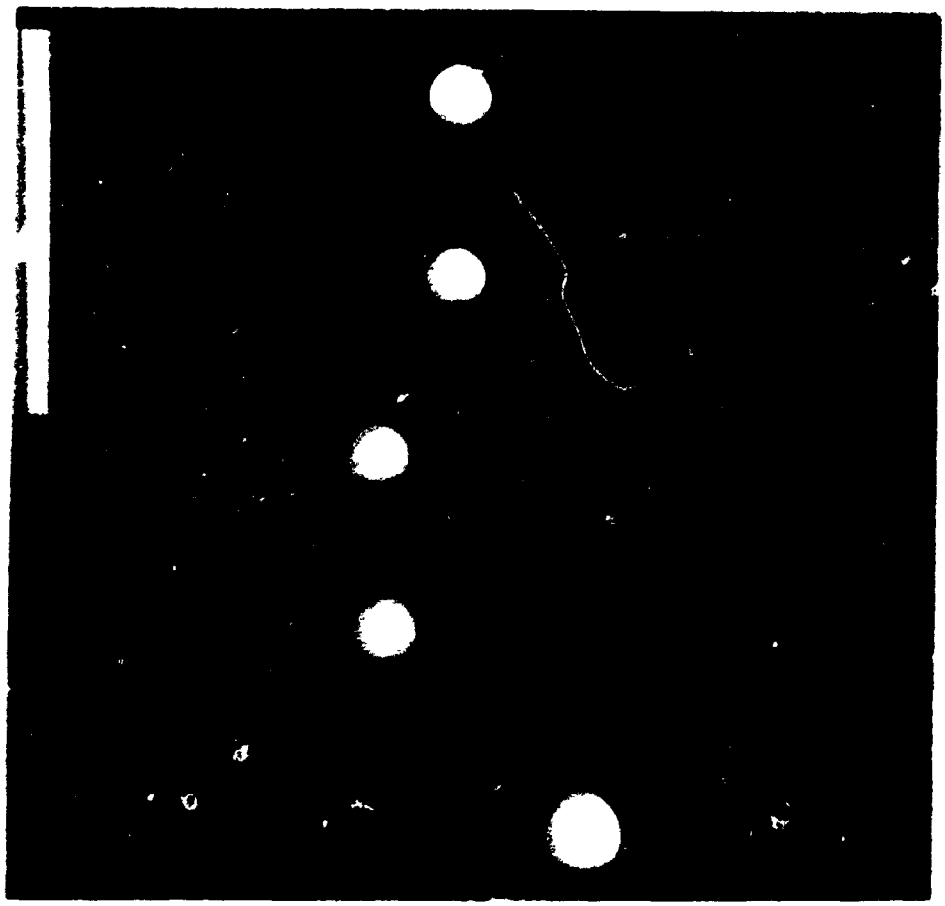

time shorter than the TE and no significant echo occurs. The middle column of 4 tubes as viewed from bottom to top comprised increasing concentrations of egg PC liposomes bearing PC spin label; while the right hand row shows 4 dilutions of egg PC liposomes without contrast agent and the lowest (5th) tube in the right hand column containing water soluble DTPA-Gd^{3+} (dimeglumine or Magnevist^{R}). The presence of liposomes without contrast agent had relatively little effect upon image intensity. Image intensity has been quantitated as a function of TR in Figures 18-20.

The imaging cycle repetition time is a factor that determines signal intensity. The signal level for a specific tissue is proportional to the level of longitudinal magnetization regrowth obtained at the end of each cycle. The level of longitudinal magnetization reached by the end of each cycle is determined by the relationship of TR to the T_1 relaxation time of the tissue. The effect of TR on relative signal strength is as follows:

TR/T_1	Relative Signal Intensity
0.5	39%
1	63%
2	86%
4	98%

(Sprawls, P., 1988). Short TR values are used to obtain T_1-weighted images and to reduce image acquisition time. When the TR value is short in relationship to the tissue T_1 a significant reduction in signal (contrast) intensity is lost. However, as TR is reduced, more excitations can be performed within a given scan time, allowing averaging.

Figure 18

MR image signal dependence on pulse repetition time (TR), for the suspensions of sonicated unilamellar egg PC vesicles described in Figure 17 bearing 25 wt% PE-DTPA. Concentration of Gd^{3+}: 0.31 mM (▲), 0.61 mM (●), 3.1 mM (▼) and 6.1 mM (■).

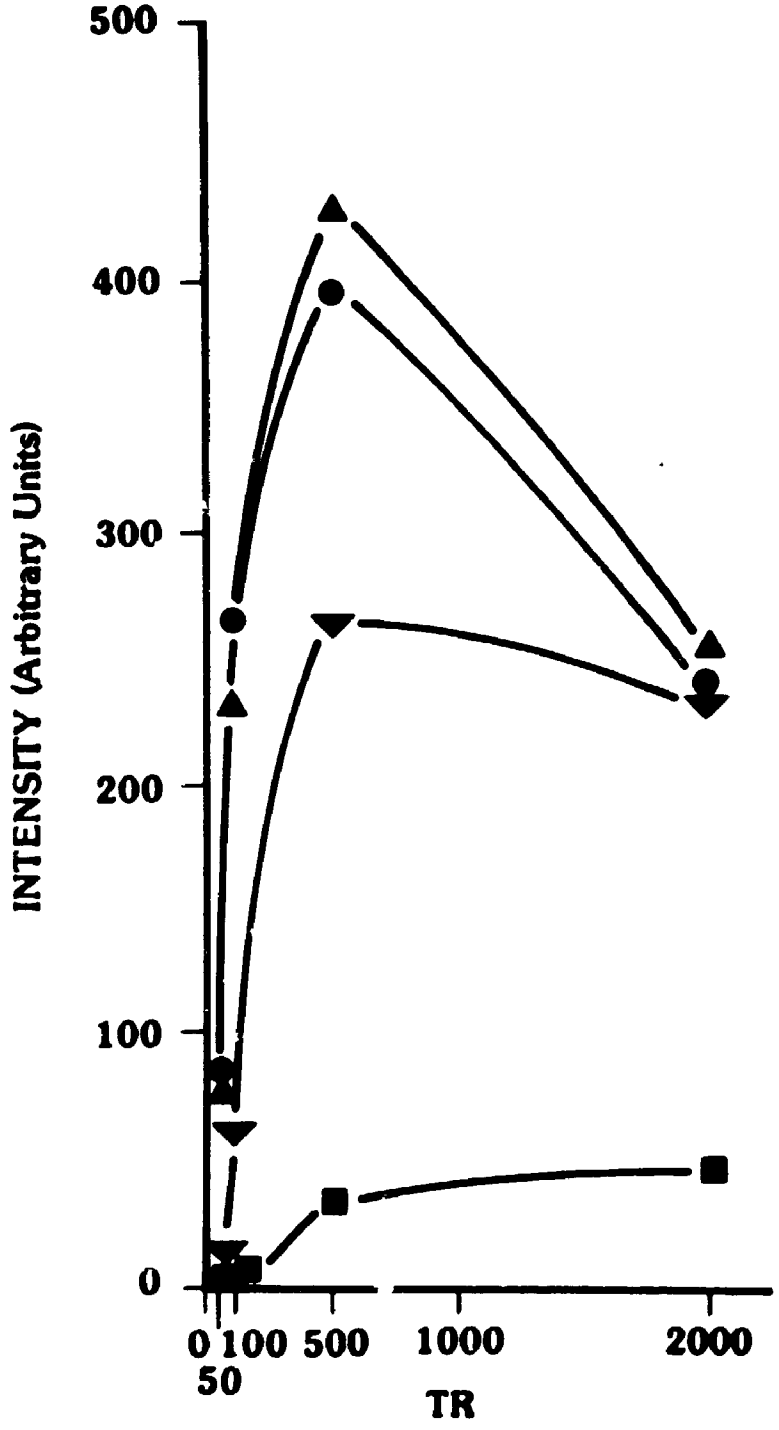
500
400
300
200
100
0
INTENSITY (Arbitrary Units)
0
50
100
500
1000
2000
TR

Figure 19

MR image signal dependence on pulse repetition time (TR), for the suspension of sonicated unilamellar egg PC vesicles described in Figure 17 bearing 50 wt% PC spin label. Concentration of PC spin label: 0.70 mM (■), 1.4 mM (▼), 7.6 mM (●) and 15 mM (▲).

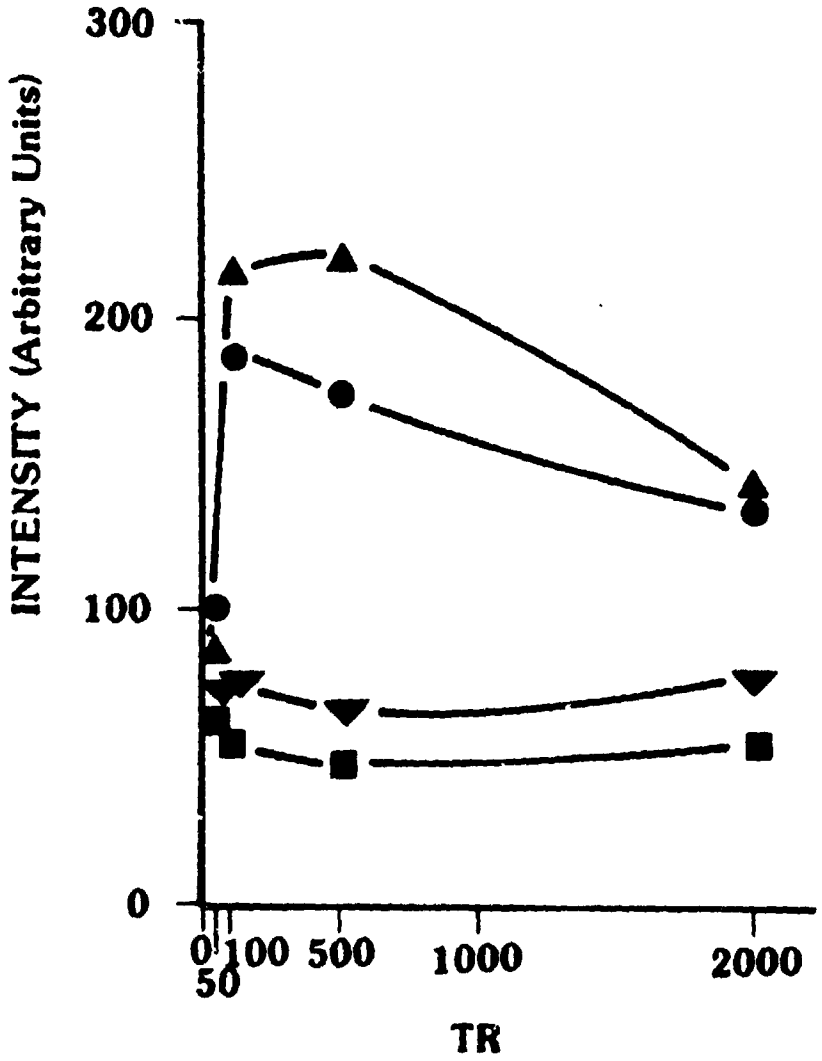
300
200
100
0
INTENSITY (Arbitrary Units)
0
50
100
500
1000
2000
TR

Figure 20

MR image signal dependence on pulse repetition time (TR), for the suspension of sonicated unilamellar egg PC vesicles for controls, as described in Figure 17. Concentration of egg PC: 1.3 mg/ml (■), 2.6 mg/ml (▼), 13.6 mg/ml (●) and 26.6 mg/ml (▲) along with phosphate buffered saline (pH 7.4) (□) and 0.4 M DTPA-Gd^{3+} (Magnevist^{R}) (△).

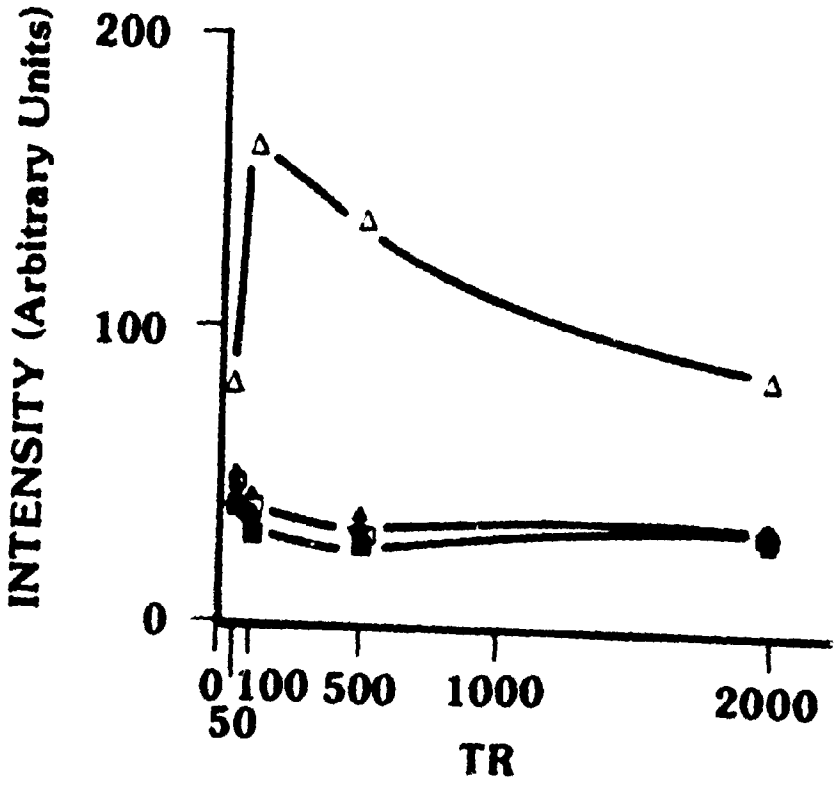
INTENSITY (Arbitrary Units)
200
100
0
0
50
100
500
1000
2000
TR

T_1- and T_2-weighted sequences are very useful for understanding the grey scale of MR imaging. To be able to determine whether two tissues differ with respect to their T_2 relaxation times, it would be desirable to select a sequence that is relatively insensitive to differences in T_1. To achieve insensitivity to differences in T_1, one can select a TR time (the period of time between the beginning of a pulse sequence and the beginning of the succeeding pulse sequnce) (Nixon, J.R., 1987) that is long in comparison to the T_1 of all the tissues. Thus there is enough recovery time between 90° pulses so that full longitudinal magnetization develops in all tissues, regardless of the particular T_1 relaxation time. This sequence should also yield intensity differences between tissues with different T_2 values, so that they are as large as possible. This can be achieved by selecting a TE (the time between the middle of a 90° pulse and the middle of a spin-echo production) (Nixon, J.R., 1987) that is relatively long so that the relative differences in spin-echo intensity between tissues with slow and fast T_2 decay is suitably nigh. Therefore, a T_2-weighted spin echo sequence is one in which the TR is long in relation to the T_1 of the tissues of interest and the TE is also relatively long. In order to minimize the intensity differences that would be caused by T_2 relaxation, it is necessary to make the TE as short as possible. By also selecting a short TR, tissues will be placed in a state of partial saturation, depending on their T_1 relaxation time. Tissues with long T_1 values will fail to remagnetize as much as those with shorter T_1 times and thus their spin-echo signals will be reduced. Therefore, a T_1 weighted spin-echo sequence is one with a relatively short TR and short TE.

It is well known that when imaged, using T_1-weighted pulse sequences such as

those described here, fat deposits show a brightness that is similar to regions whose water protons' relaxation times are shortened by the local presence of contrast agent. A separate aspect of this work involved investigation of the use of "fat suppression" pulse sequences in conjunction with liposomal contrast agents to minimize this problem. This work is the first in which a fat-suppression pulse sequence was employed on a liposomal contrast agent. We have implemented the use of a special spectroscopic technique that was employed for study in orbital imaging (Atlas, S.W. et al., 1987; Brateman, L., 1986). It was initially described for the orbit because of its fat-containing and water containing structures (retrobular fat and globe, muscles, nerves) which made it a suitable anatomic region for spectroscopic imaging. There are many spectroscopic techniques which have been described (Brateman, L., 1986).

One useful technique which provides information and high quality images has been described by Dixon (Dixon, W.T., 1984) and used here. This technique is useful because while providing high-quality images it does not increase scanning time (since the scan time is identical to conventional spin-echo images if the same TR, and matrix size are used). The same TR and TE values are used in the fat suppresion pulse sequence as in the normal sequence without fat suppression. This technique is based upon the difference between the resonant frequencies of the fat protons ($-CH_2-$) and the water protons (H_2O) which is approximately 3.5 ppm. In this method, the timing of the 180° RF pulse is intentionally altered (with reference to the timing of the frequency-encoding gradient pulse) so that there is a separation of the gradient echo from the Hahn echo that would be obtained from the 180° RF pulse. This is different from the situation occurring in conventional spin-echo imaging, where there

is superimposition of the gradient echo with the spin echo. The offset between the echoes using the Dixon technique results in the acquisition of a signal precisely at a time when the signal of fat protons is 180° out of phase to the signal from the water protons. This results in an "out-of-phase" image, as opposed to an image obtained in conventional spin-echo imaging, which is an "in-phase" image (Atlas, S.W. et al., 1988).

This aspect is addressed in Figure 21 which illustrates *in vitro* the effect of fat suppression on the liposome preparations employed by us (compare Fig. 21A, 21B), and a phantom study designed to test the sensitivity of fat suppression to the presence of fat in our system (Fig. 22C, 22D), and relate that information in terms of an absolute value (Fig. 23). The fat suppression spin echo sequence utilized produced images based upon relative differences in T_1. Samples were contained in 10 mm glass tubes supported in rows in plastic racks. The image plane for Figures 21A and 21B was perpendicular to the base of the test tube rack and transected a single row of sample tubes vertically. Figures 21A and 21B represent T_1-weighted images obtained at TR = 500 ms and TE =25 ms without (21A) and with (21B) fat suppression respectively. From left to right the first three tubes each contained 0.5 ml of saline liposome suspensions: egg PC alone, egg PC with PC-spin label, and egg PC with PE-DTPA-Gd^{3+}. The last two tubes contained water soluble DTPA-Gd^{3+} (dimeglumine) and isotonic saline respectively. Note that the image density of the egg PC/saline blank is not obviously different from that of the saline blank without lipid. On the other hand the same egg PC liposomes with PC-spin label or PE-DTPA-Gd^{3+} contrast agent assembled into their membranes markedly altered image intensity, as

Figure 21

"Fat suppression" in conjunction with liposomal contrast agents: *in vitro* analysis using a GE 1.5 T imager. A) and B) illustrate the same row of aqueous samples (in 10 mm glass tubes) imaged without (A) and with (B) fat suppression. Image plane was chosen to transect vertically all 5 sample tubes. Tubes contained: 0.5 ml egg PC liposomes without contrast agent (20 mg total lipid) (1), 0.5 ml egg PC liposomes with 50 wt% PC spin label (22 mM, 20 mg total lipid) (2), 0.5 ml egg PC liposomes with 25 wt% PE-DTPA-Gd^{3+} (5.6 mM, 20 mg total lipid) (3), 0.1 ml non-liposomal DTPA-Gd^{3+} (Magnevist^{R} 0.4 M) (4) and 2.0 ml phosphate buffered 0.15 N saline pH 7.4 (5). All liposomes were sonicated as described in the Methods section, and suspended in phosphate buffered 0.15 N saline at pH 7.4. T_1-weighted images were obtained (TR = 500 ms, TE = 25 ms). Note that samples 3 and 4 had such short relaxation times that they gave no signal under those conditions.

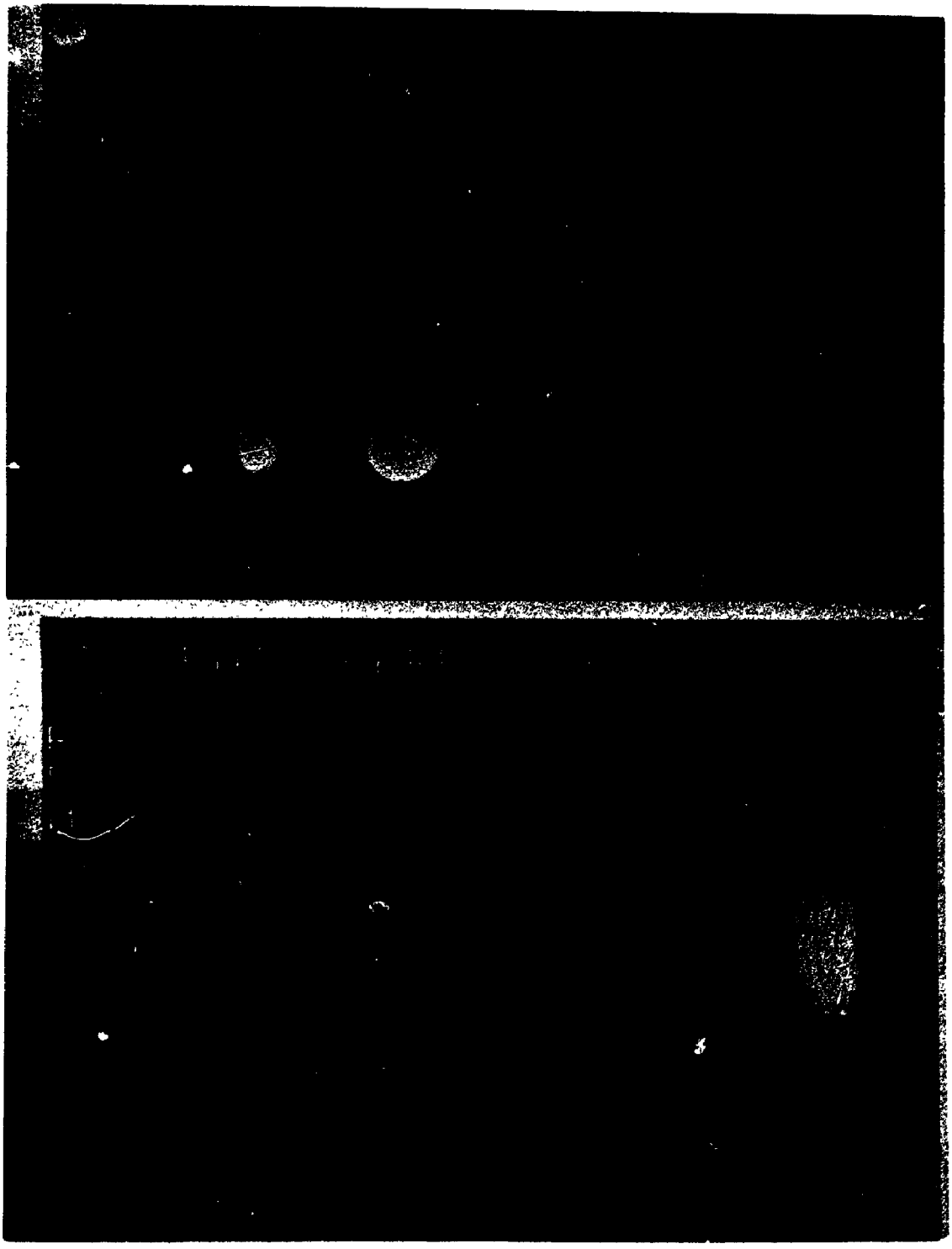

Figure 22

C) and D) represent an experiment to quantitate signal discrimination using fat suppression. Glass tubes of emulsified fat (whole bovine milk) were held in plastic racks. Image plane was parallel to the rack base which transects the sample tubes horizontally. T_1-weighted images were obtained with TR = 500 ms, TE = 25 ms.

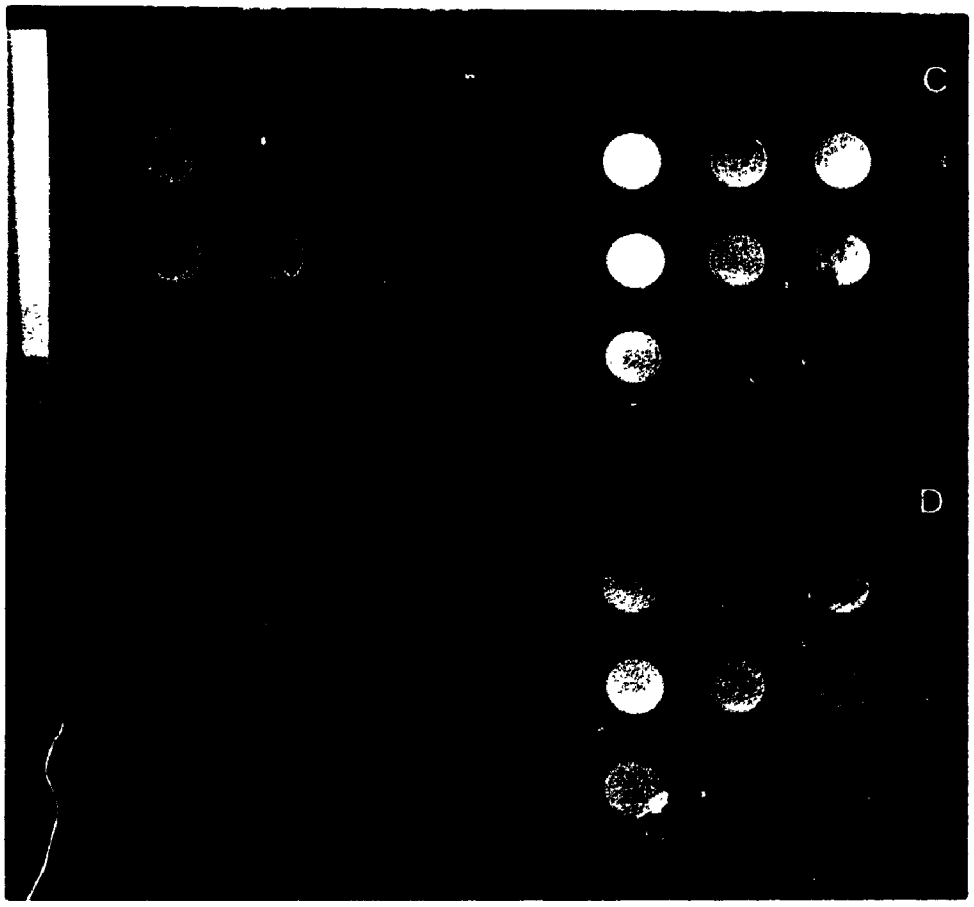
C
D

Figure 23

This plot shows image intensity in arbitrary units for the "normal" pulse sequence (○), pulse sequence with fat suppression (⌓) and pulse sequence with water suppression (□). Note that an absolute sensitivity for detection of fat was approximately 1 g/dl.

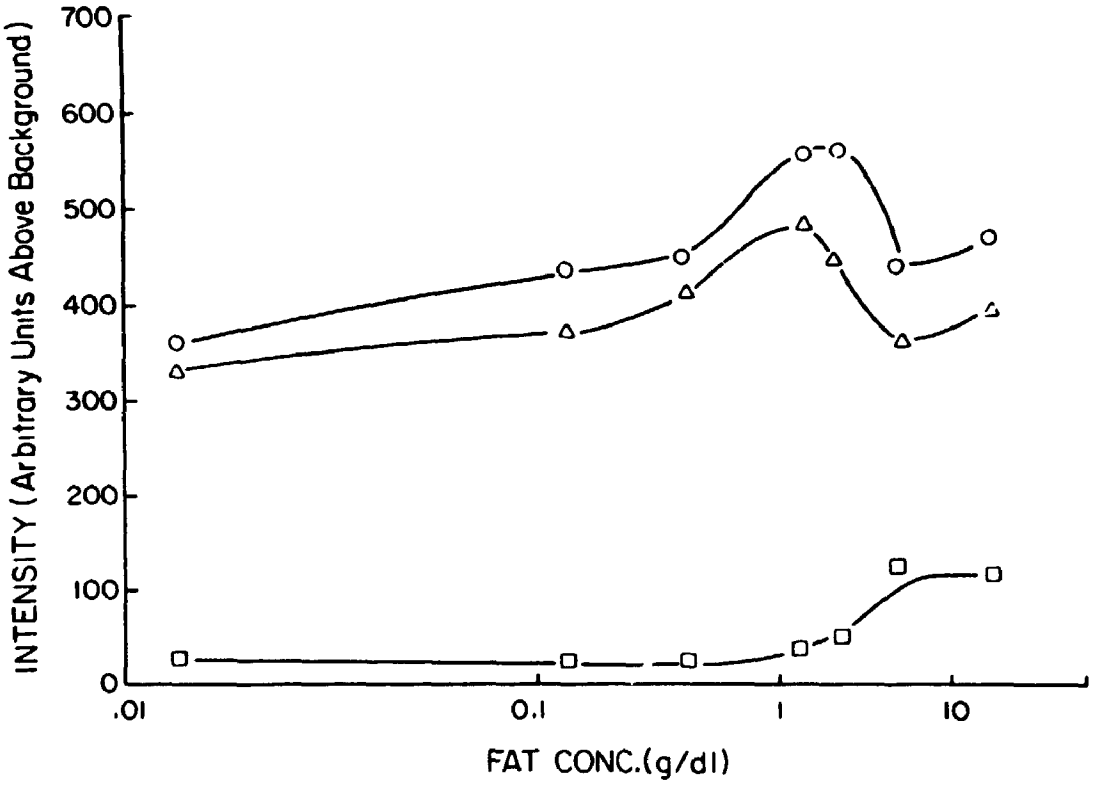
INTENSITY (Arbitrary Units Above Background)
700
600
500
400
300
200
100
0
.01
0.1
1
10
FAT CONC.(g/dl)

did aqueous DTPA-Gd^{3+}. The effect of Gd^{3+}-bearing agents was dramatic: at these concentrations both liposome-bound and aqueous DTPA-Gd^{3+} reduced sample relaxation times so extensively that no signal was obtained and the sample was "invisible" in the image. It will be seen that this latter phenomenon can also occur *in vivo*. Finally, note that while lipid without contrast agent had no visually obvious effect on the MR image of saline, fat suppression affected it differently from the saline blank. In general there was a decrease in image intensity for liposome suspensions when using the fat suppression sequence - as expected given that phospholipid is fat in nature. Figures 22C and 22D illustrate phantom studies for combinations of emulsified fat and water which are quantitated in Figure 23. These data for both water and fat suppression indicate an absolute sensitivity for detection at approximately 1 g fat per dl (Fig. 23).

We subsequently extended our imaging experiments to include liposomal contrast agent studies *in vivo*, examining the contrast agent at intramuscular sites and intravenous targets. Figures 24-27 document the type of result obtained with direct intramuscular injection followed by MR imaging of the region at various time intervals. It also shows the effect of fat suppression sequences, which have not previously been reported with liposomal agents. For this work male Sprague-Dawley rats were sedated via injection in the right thigh muscle with 2 ml/kg Ketamine/Rompun, (10:1) and placed in groups of 3 or 4 in the imager. After obtaining a pre-injection image, rats were removed and injected in the left thigh muscle with 0.5 ml of 0.9% saline containing either liposomes of egg PC alone (20 mg lipid) (Fig. 24), 50 wt% spin label contrast agent (20 mg total lipid, 0.044 mmoles

Figure 24

Intramuscular injection of liposomal egg PC vesicles. Coronal sections are shown of male Sprague-Dawley rats (250 g) sedated with Ketamine/Rompun (2 cc/kg in the right thigh muscle) and injected intramuscularly (left thigh muscle) with sonicated unilamellar egg PC vesicles without contrast agent (20 mg total lipid in 0.5 ml saline). The scans were T_1-weighted with TR = 500 ms, TE = 25 ms. MR image A) is pre-injection scan, B) is a 5 min post-injection scan, C) is a 30 min post-injection scan, D) is a 60 min post-injection scan, E) is a 24 hr post-injection scan, C′) is a 30 min post-injection scan with fat suppression, D′,) is a 60 min post-injection scan with fat suppression, E′) is a 24 hr post-injection scan with fat suppression. Animals shown with heads up and lying on their backs. Arrows indicate sites of contrast.

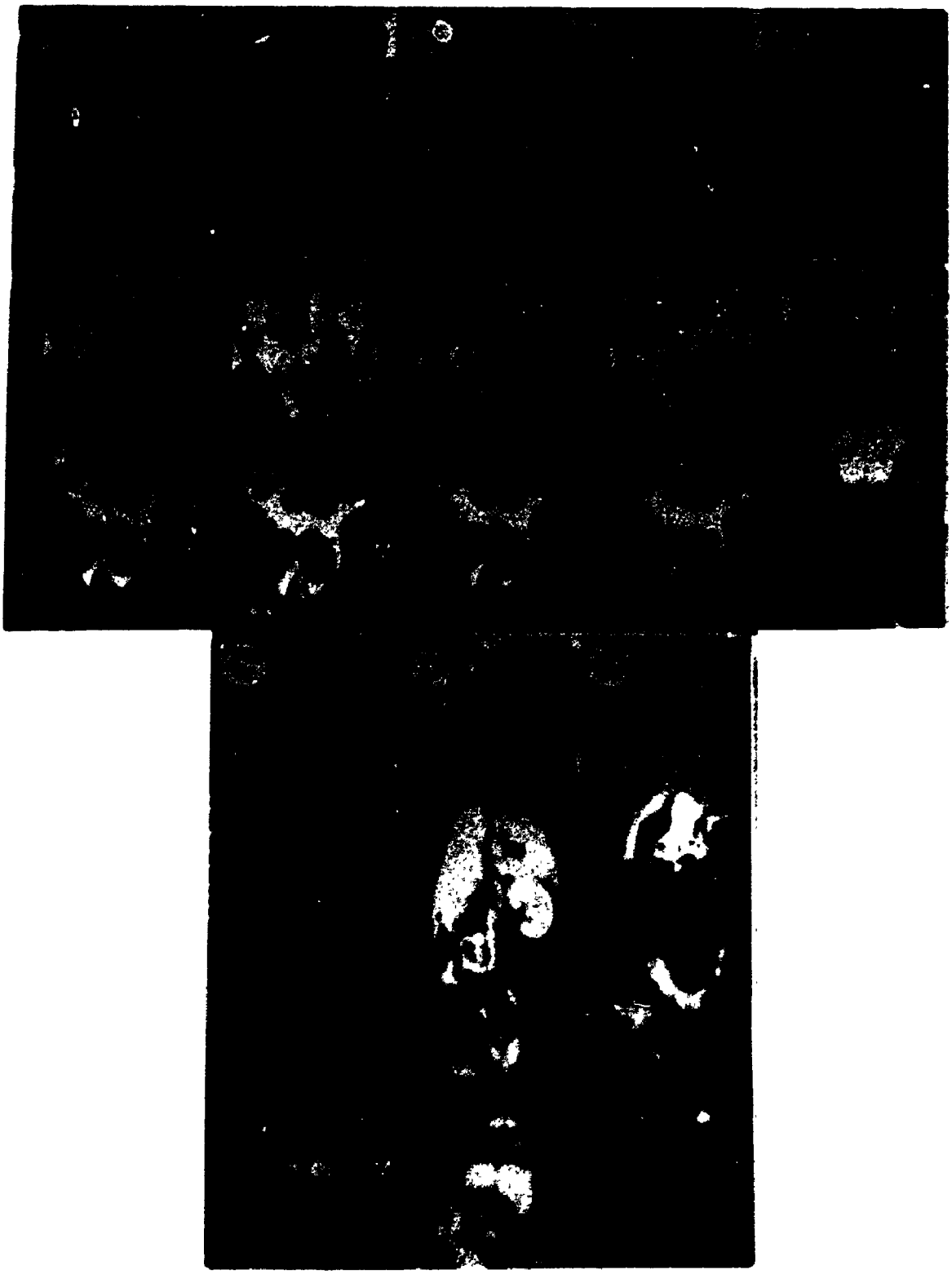

Figure 25

Intramuscular injection of liposomal contrast agents. Coronal sections are shown of male Sprague-Dawley rats (250 g) sedated with Ketamine/Rompun (2 cc/kg in the right thigh muscle) and injected intramuscularly (left thigh muscle) with sonicated unilamellar egg PC vesicles containing 50 wt% PC spin label (20 mg total lipid in 0.5 ml saline, 22 mM spin label). The scans were T_1-weighted with TR = 500 ms, TE = 25 ms. MR image A) is pre-injection scan, B) is a 5 min post-injection scan, C) is a 30 min post-injection scan, D) is a 60 min post-injection scan, E) is a 24 hr post-injection scan, C′) is a 30 min post-injection scan with fat suppression, D′) is a 60 min post-injection scan with fat suppression, E′) is a 24 hr post-injection scan with fat suppression. Animals shown with heads up and lying on their backs. Arrows indicate sites of contrast.


A
C
D
E
G
H
I

Figure 26

Intramuscular injection of liposomal contrast agents. Coronal sections are shown of male Sprague-Dawley rats (250 g) sedated with Ketamine/Rompun (2 cc/kg in the right thigh muscle) and injected intramuscularly (left thigh muscle) with sonicated unilamellar egg PC vesicles containing 25 wt% PE-DTPA-Gd^{3+} (20 mg total lipid in 0.5 ml saline, 5.6 mM Gd^{3+}). The scans were T_1-weighted with TR = 500 ms, TE = 25 ms. MR image A) is pre-injection scan, B) is a 5 min post-injection scan, C) is a 30 min post-injection scan, D) is a 60 min post-injection scan, E) is a 24 hr post-injection scan, C′) is a 30 min post-injection scan with fat suppression, D′) is a 60 min post-injection scan with fat suppression, E′) is a 24 hr post-injection scan with fat suppression. Animals shown with heads up and lying on their backs. Arrows indicate sites of contrast.

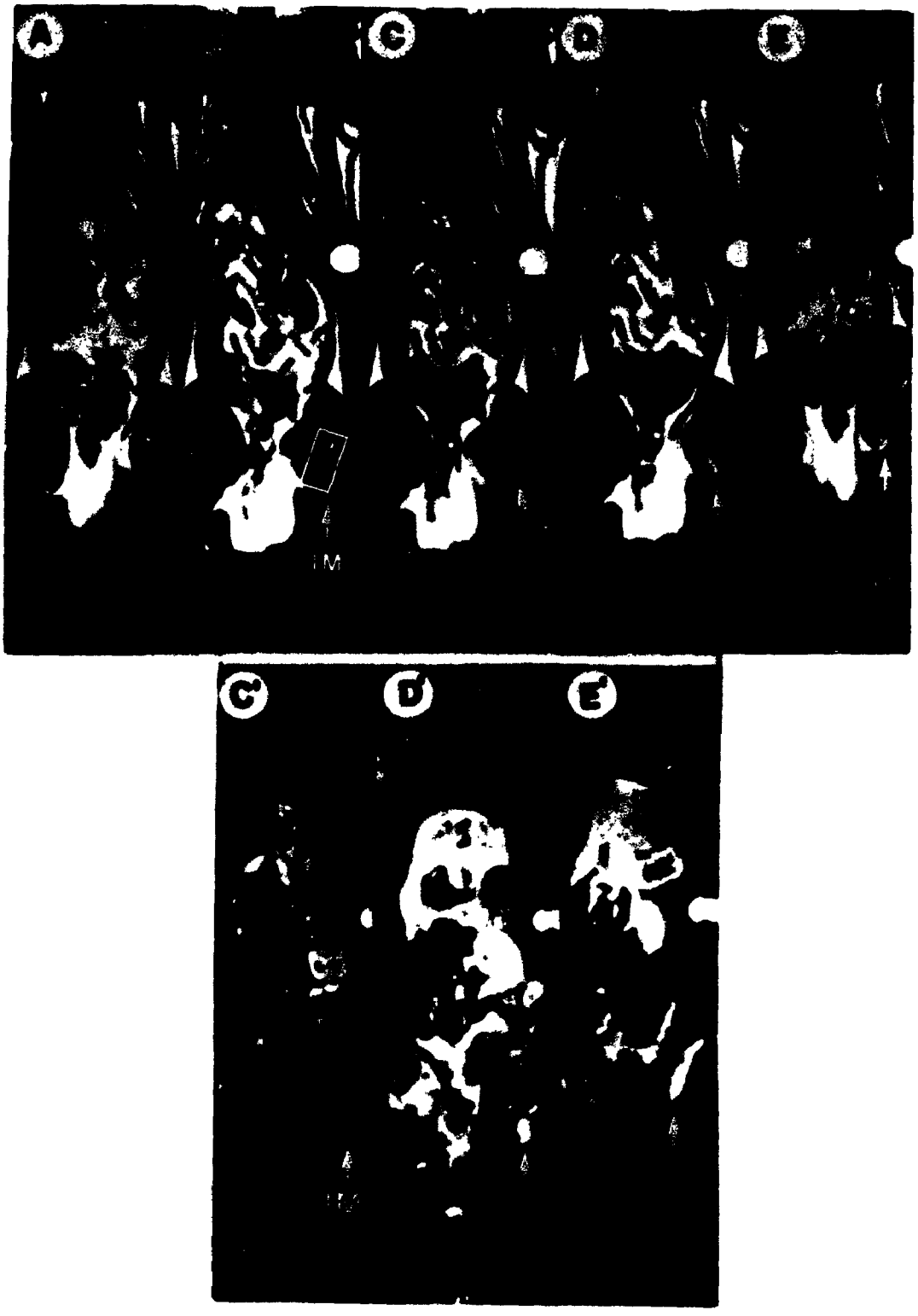
A
B
C
D
IM
E
F

Figure 27

Intramuscular injection of non-liposomal contrast agents. Coronal sections are shown of male Sprague-Dawley rats (250 g) sedated with Ketamine/Rompun (2 cc/kg in the right thigh muscle) and injected intramuscularly (left thigh muscle) with non-liposomal DTPA-Gd^{3+} (water soluble DTPA-Gd^{3+} in 0.1 ml saline, 400 mM). The scans were T_1-weighted with TR = 500 ms, TE = 25 ms. MR image A) is pre-injection scan, B) is a 5 min post-injection scan, C) is a 30 min post-injection scan, D) is a 60 min post-injection scan, E) is a 24 hr post-injection scan, C′) is a 30 min post-injection scan with fat suppression, D′) is a 60 min post-injection scan with fat suppression, E′) is a 24 hr post-injection scan with fat suppression. Animals shown with heads up and lying on their backs. Arrows indicate sites of contrast. K = kidney and B = bladder.

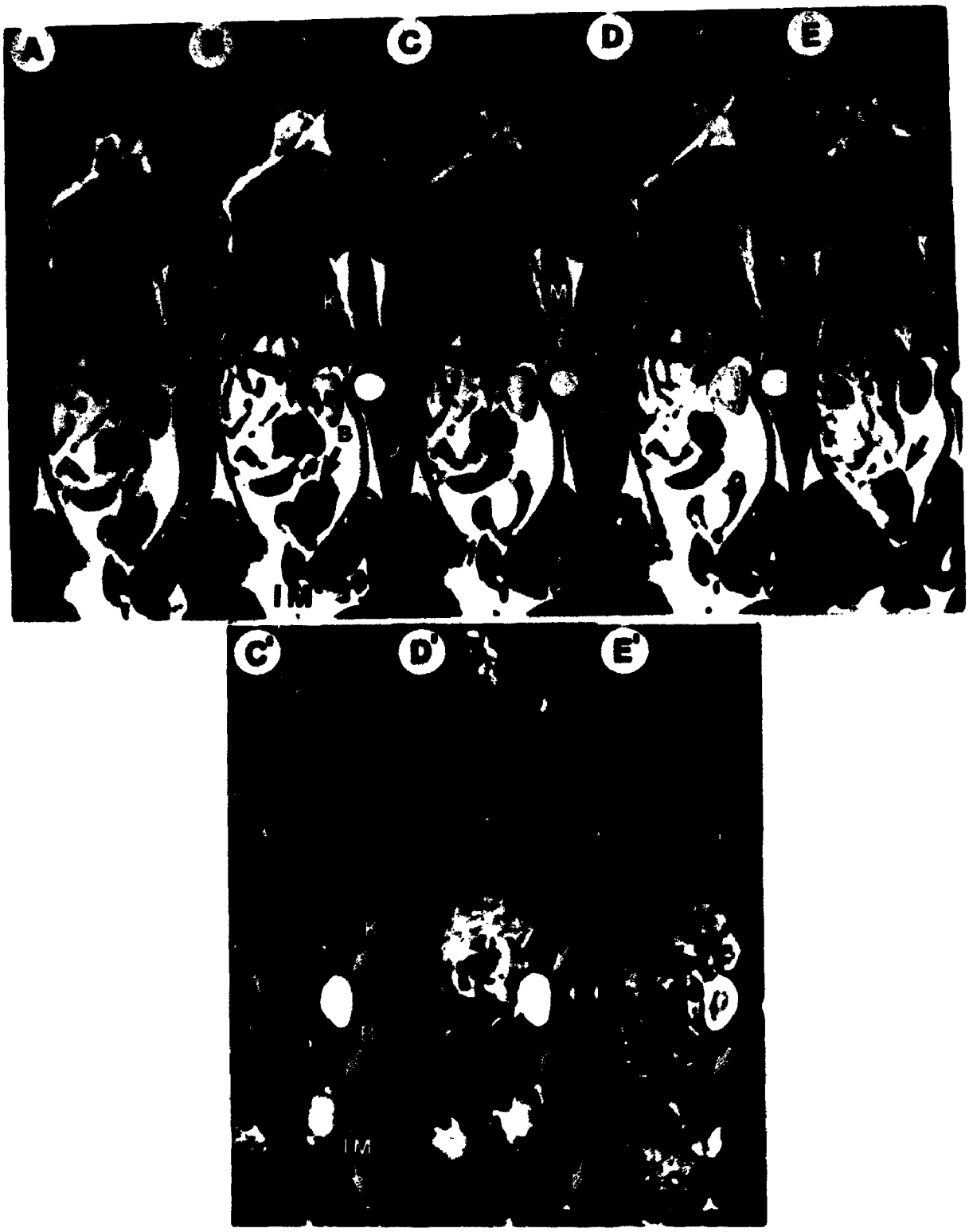
A
C
D
E
C'
D'
E'
IM

spin label per kg) (Fig. 25), liposomes bearing 25 wt % PE-DTPA-Gd^{3+} contrast agent (20 mg total lipid, 0.011 mmoles Gd^{3+} per kg) (Fig. 26), or aqueous DTPA-Gd^{3+} (dimeglumine, 0.16 mmoles per kg) (Fig. 27). Experimental animals were then re-imaged. T_1-weighted pulse sequences were particularly sensitive to the presence of contrast agents in these experiments and are illustrated here. In each case the left hand image is of the animal prior to injection of contrast material. The sequence of images to the right represents time points of 5 min, 30 min, 60 min and 24 hours post contrast injection. The lower 3 images in each group illustrate the effect of fat suppression on the 30 min, 60 min and 24 hour time points respectively. One might hope that fat suppression would optimize the performance of liposomal contrast agents by removing interference from both endogenous fat and liposome phospholipid.

In our hands injection of lipid alone produced little effect on image intensity even at the site of an intramuscular injection (Fig. 24). The same liposomes bearing PC-spin label contrast agent did produce a very significant local enhancement of tissue contrast, which was seen as a bright area that slowly disappeared and was gone by 24 hours (Fig. 25). The liposomal Gd^{3+} contrast agent was more potent and can be seen to have caused a dark focus surrounded by a bright halo (Fig. 26). The dark core is presumably a region in which contrast agent concentration was so high as to shorten the relaxation time well below the TE so that no signal was obtained as described in Figures 17 and 21 (A,B) above. The bright halo represents a region of lesser contrast agent concentration. With time, the region of enhancement was seen to diffuse along fascial planes and the dark core became less noticeable as local

concentration was reduced. Note that the PE-DTPA-Gd^{3+} agent was still evident even after 24 hours and was more potent at all time points than its spin label equivalent. The fact that the liposomes with PE-DTPA-Gd^{3+} remained in the tissue for 24 hours strongly suggests that contrast disappearance in the case of the PC-spin label (Fig. 25) was due to reduction of the nitroxide radical rather than lymphatic uptake of the liposomes. Indeed reduction of the spin labels by tissue enzymes has been predicted in past to present a significant limitation to their use *in vivo* (Brasch, R.C., 1985). Although there was evidence of local tissue redistribution of the liposomal PE-DTPA-Gd^{3+} no uptake by local lymphatics was visualized in the images presented. Contrast along routes of lymphatics was visualized in the images presented. Contrast along routes of lymphatic drainage would be the anticipated finding in an MR instrument with sufficient resolution provided that the contrast agent survives *in vivo* for the time course of uptake (probably some 24 hours) (Poznansky, M.J. and Juliano, R.L., 1984; Gregoriadis, G., 1988).

Non-liposomal, water soluble DTPA-Gd^{3+} (dimeglumine) provided an interesting comparison to the above liposomal samples. For this purpose we injected small quantities of 0.4 M dimeglumine. This non-particulate contrast material diffused rapidly from the intramuscular injection sites to highlight renal cortex followed by collecting system and bladder (Fig. 27). This result was quite different from that obtained with the liposomal agents of Figures 25 and 26. Nevertheless, use of the fat suppression technique did permit imaging of small regions of residual contrast which without fat suppression would have been unremarkable.

Lastly we have considered whether the same agents provide sufficient contrast

for intravenous use, and how the phospholipid spin label compares to the phospholipid chelating agent. As above, Sprague-Dawley rats were sedated with Ketamine/Rompun and scanned prior to the injection of contrast material. In this case, injection of drug was via the left femoral vein. Classically, liposomes of the size described here target to the liver and the spleen (Poznansky, M.J. and Juliano, R.L., 1984; Gregoriadis, G., 1988). We have previously demonstrated that this is in fact the case for the egg PC structures used here by labelling them with $^{111}In^{3+}$, a radiotracer, as described in Chapter 2. Water soluble DTPA-Gd^{3+} on the other hand is rapidly excreted renally. We have experimented with various intravenous injections of liposomal spin label and chelating agent, using for comparison saline or lipid controls and water soluble contrast agents. Figures 28-31 illustrate typical results obtained in this fashion. Data are shown for animals injected with 1 ml of .9% saline suspension of egg PC liposomes without contrast agent (40 mg lipid) (Fig. 28), egg PC liposomes with PC-spin label (total lipid 40 mg, 0.088 mmoles contrast agent per kg) (Fig. 29), egg PC liposomes with PE-DTPA-Gd^{3+} (total lipid 40 mg, 0.022 mmoles contrast agent per kg) (Fig. 30), and 0.2 ml non liposomal DTPA-Gd^{3+} (dimeglumine) (0.32 mmoles per kg) (Fig. 31). In each case a set of 5 T_1-weighted images is provided: from left to right, pre-injection, 30 min post injection, 60 min post injection, 120 min post injection, and 120 min post injection with fat suppression. It will be seen that liposomes without contrast agent had little effect on tissue image density (Fig. 28). The PC-spin label contrast agent highlighted liver tissue (and spleen) significantly, and this enhancement increased over the time period of the experiment. The PE-DTPA-Gd^{3+} liposomal contrast agent (Fig. 30) was extremely effective in rapidly

Figure 28

Intravenous injections of liposomal egg PC vesicles. Coronal sections are shown of male Sprague-Dawley rats (250 g) sedated with Ketamine/Rompun (2 cc/kg in the right thigh muscle) and injected intravenously (left femoral vein) with sonicated unilamellar egg PC vesicles without contrast agent (40 mg total lipid in 1.0 ml saline). The scans were T_1-weighted with TR = 500 ms, TE = 25 ms. MR image A) is a pre-injection scan, B) is a 30 min post-injection scan, C) is a 60 min post-injection scan, D) is a 120 min post-injection scan and D') is a 120 min post-injection scan with fat suppression. Animals shown with heads up and lying on their backs. Arrows indicate site(s) of contrast.

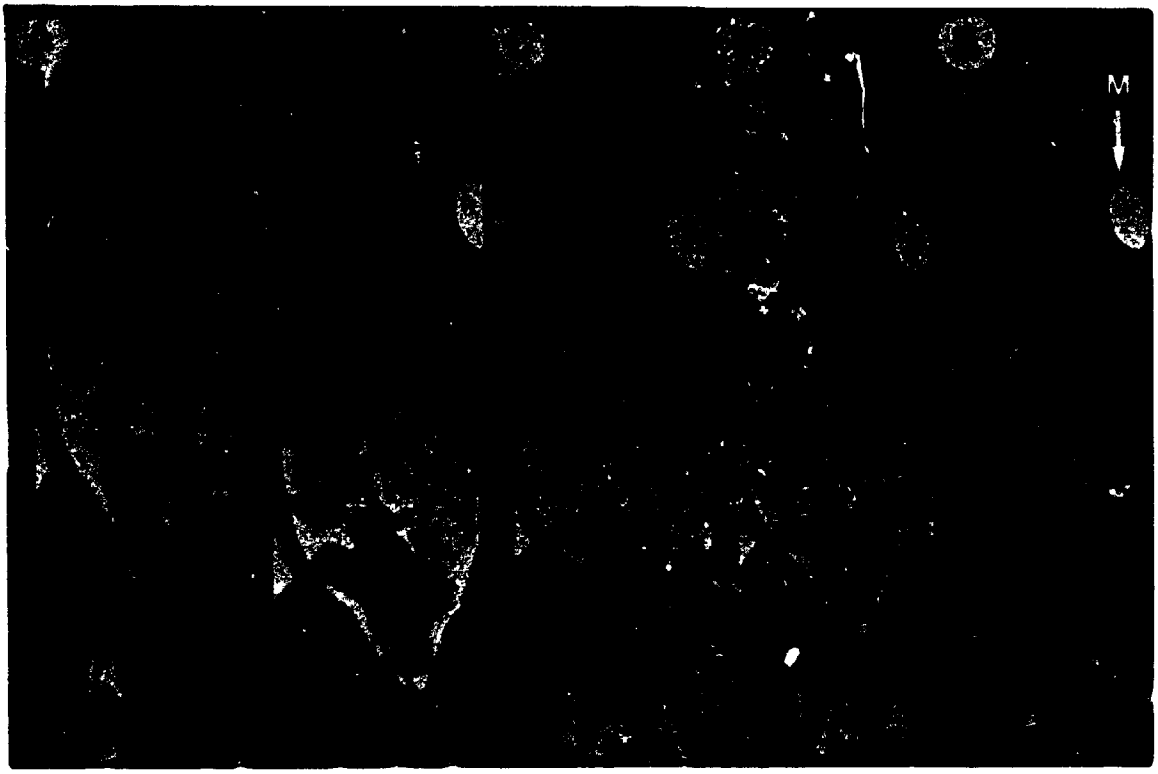
M

Figure 29

Intravenous injections of liposomal contrast agents. Coronal sections are shown of male Sprague-Dawley rats (250 g) sedated with Ketamine/Rompun (2 cc/kg in the right thigh muscle) and injected intravenously (left femoral vein) with sonicated unilamellar egg PC vesicles containing 50 wt% PC spin label (40 mg total lipid in 1.0 ml saline, 22 mM spin label). The scans were T_1-weighted with TR = 500 ms, TE = 25 ms. MR image A) is a pre-injection scan, B) is a 30 min post-injection scan, C) is a 60 min post-injection scan, D) is a 120 min post-injection scan and D') is a 120 min post-injection scan with fat suppression. Animals shown with heads up and lying on their backs. Arrows indicate site(s) of contrast. S = spleen and L = liver.

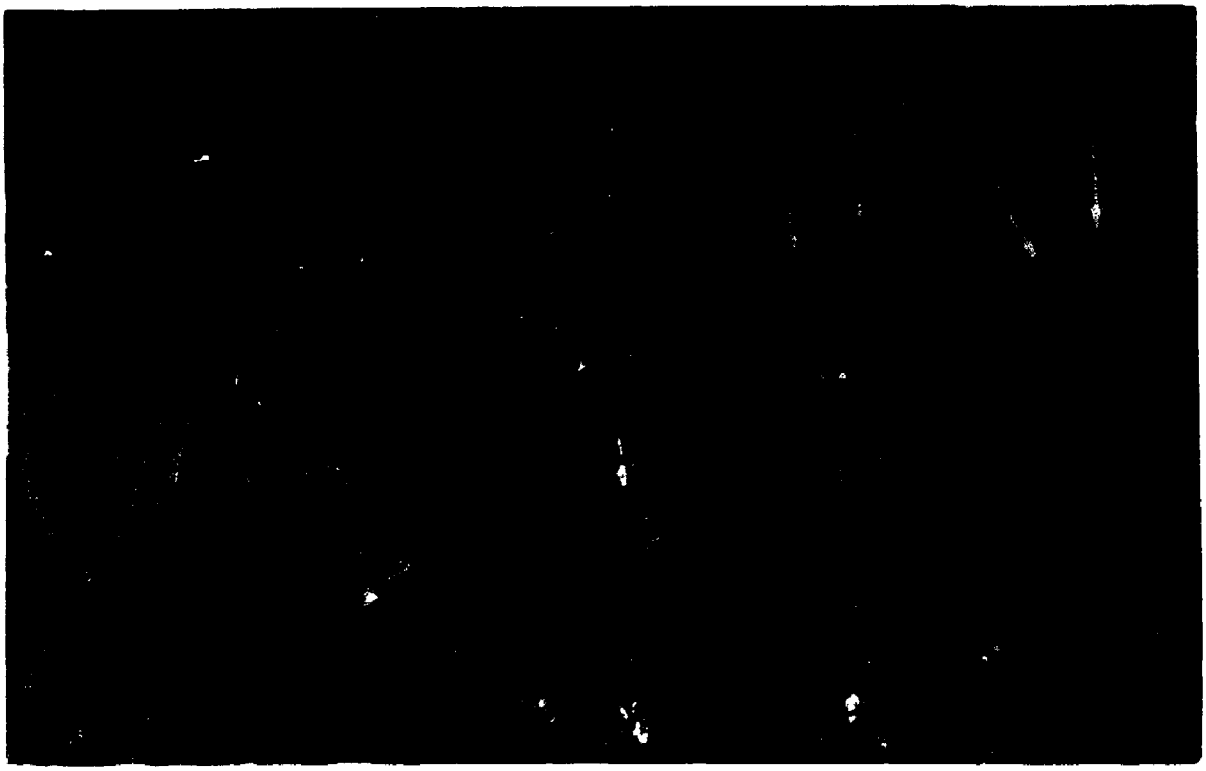

Figure 30

Intravenous injections of liposomal contrast agents. Coronal sections are shown of male Sprague-Dawley rats (250 g) sedated with Ketamine/Rompun (2 cc/kg in the right thigh muscle) and injected intravenously (left femoral vein) with sonicated unilamellar egg PC vesicles containing 25 wt% PE-DTPA-Gd^{3+} (40 mg total lipid in 1.0 ml saline, 5.6 mM Gd^{3+}). The scans were T_1-weighted with TR = 500 ms, TE = 25 ms. MR image A) is a pre-injection scan, B) is a 30 min post-injection scan, C) is a 60 min post-injection scan, D) is a 120 min post-injection scan and D′) is a 120 min post-injection scan with fat suppression. Animals shown with heads up and lying on their backs. Arrows indicate site(s) of contrast. L = liver.

Figure 31

Intravenous injection of liposomal contrast agents. Coronal sections are shown of male Sprague-Dawley rats (250 g) sedated with Ketamine/Rompun (2 cc/kg in the right thigh muscle) and injected intravenously (left femoral vein) with non-liposomal DTPA-Gd^{3+} (water soluble DTPA-Gd^{3+} in 0.2 ml saline, 0.4 M). The scans were T_1-weighted with TR = 500 ms, TE = 25 ms. MR image A) is a pre-injection scan, B) is a 30 min post-injection scan, C) is a 60 min post-injection scan, D) is a 120 min post-injection scan and D') is a 120 min post-injection scan with fat suppression. Animals shown with heads up and lying on their backs. Arrows indicate site(s) of contrast. K = kidney and B = bladder.


K
B

highlighting the tissues to which liposomes are known to target. Thus its *in vitro* efficacy was directly reflected in its *in vivo* performance. Note that water soluble DTPA-Gd^{3+} was, as expected, rapidly cleared renally and highlighted first kidney and then bladder. This renal excretion was not seen with either liposomal agent.

It seems very likely that liposomal contrast agents of the type described here would find clinical utility in certain diagnostic situations involving liver and spleen. Spin label derivatives appear not to be the method of choice because of their lesser potency. They will have the additional drawback of fairly rapid reduction by the body of the nitroxide radical to its non-paramagnetic counterpart.

3.4 Conclusion

Two phospholipids - one bearing a nitroxide free radical covalently bound to its polar headgroup, and the other bearing a similarly-attached chelating agent with bound gadolinium -were compared *in vivo* as liposome-associated contrast agents for MR imaging. In each case the phospholipid contrast agent was incorporated into the membrane of sonicated unilamellar liposomes of natural (egg) phosphatidylcholine having diameters in the 20-70 nm range. Phosphatidylcholine with a (polar headgroup) methyl group replaced by a nitroxide spin label proved to be considerably less effective in highlighting regions of liposome biodistribution than did phosphatidylethanolamine with DTPA-Gd^{3+} attached via one carboxyl group to the lipid headgroup amino function. When injected intramuscularly into rats, the spin label liposomes produced local contrast that persisted for 60 minutes. Under similar conditions the liposomal gadolinium agent provided contrast for over 24 hours and

allowed for visualization of redistribution based upon local tissue structure. Its water-soluble counterpart, non-liposomal gadolinium-DTPA (dimeglumine), was rapidly excreted renally from the same intramuscular sites and provided kidney and bladder contrast within 15 minutes of injection. When delivered intravenously both liposomal agents highlighted animals' livers and spleens within 1-2 hours, although the spin label agent was only marginally effective in providing contrast. In addition we record here the fi-st application of "fat suppression" pulse sequences in conjunction with liposomal contrast agents.

Lipidic, liposome-based paramagnetic species offer non-toxic, convenient and realistic particulate contrast agents for MR imaging; although the spin label derivative showed distinctly inferior potency and shorter lifetime in tissue. The concommitant use of fat suppression was extremely valuable for obtaining optimal image definition of tissues containing liposomal contrast.

CHAPTER 4. A LONG CHAIN SPIN LABEL USED FOR GLYCOSPHINGOLIPID STUDIES: EVIDENCE THAT TRANS-BILAYER FATTY ACID INTERDIGITATION MAY BE A GENERAL PHENOMENON

4.1 Introduction

The concept of the phospholipid bilayer is of two monolayers whose hydrophobic surfaces are in apposition. Thus one tends to envisage a planar region of contact between two flat surfaces composed of fatty acid terminal methyl groups. It has been pointed out however that fatty acids within natural membranes vary widely in chain length so that some may protrude beyond the above-mentioned planar array of methyl termini, while others will fail to reach it.

Much of the current interest in glycosphingolipids has been derived from two factors: 1) their involvement as specific recognition sites for exogenous macrostructures ranging from antibodies to cells, and 2) their possible modulatory role in membrane structure and function. A certain amount of discussion regarding these roles has centred around a peculiar feature of the glycosphingolipids: the common great range of fatty acid chain length. The sphingosine backbone itself is generally 18-carbons long. Given that glycosphingolipids sit in the bilayer membrane in a fashion analogous to phospholipids, one would anticipate that a chain of 15 of these carbons would extend down into the membrane parallel to the fatty acids of the host matrix. Such a length of acyl chain is similar to the most abundant fatty acids of phospholipids (16- and 18-carbons). However it is typical for the glycosphingolipids

to have a high proportion of fatty acids with up to 24 carbons. Hence there is commonly an alkyl chain disparity of 9 carbons in depth of bilayer penetration within a given glycosphingolipid (i.e. between the sphingosine portion and the fatty acid portion). Both the receptor function and membrane structural effects of glycosphingolipids have been suggested to be affected by this feature. Sen-Itiroh Hakomori, who introduced the concept of glycosphingolipid crypticity, has raised the question of the role of glycosphingolipid fatty acid composition, in this regard (Lampio, A. et al., 1986). Carl Alving, in establishing the basis for all current model membrane studies of the effect of fatty acid chain length on glycosphingolipid receptor function, has demonstrated the increased "accessibility" of sugar headgroups to exogenous macrostructures achieved by lengthening glycosphingolipid fatty acids (Alving, C.R. and Richards, R.L., 1977) or shortening host matrix fatty acids (Alving, C.R. and Richards, R.L., 1977; Schichijo, S. and Alving, C.R., 1986). It has however proven difficult to differentiate amongst the possible roles of glycosphingolipid dynamics, lateral distribution, and head group orientation or protrusion in determining receptor function (Balakrishnan, K. et al., 1982; Endo, T., et al., 1982; Thomas, P.D. and Podder, S.K., 1982; Myers, M. et al., 1984; Utsumi, H. et al., 1984; Grant, C.W.M., 1987).

A glycosphingolipid with a very long fatty acid may well "fit" in a characteristic fashion into a bilayer membrane (liquid) crystal lattice comprised of phospholipids with 16-and 18-carbon acyl chains (Grant, C.W.M., 1987). This in turn would be expected to influence variables that affect its structural and receptor roles.

Lesser degrees of disparity in acyl chain length within a given lipid molecule

are also a common feature of membrane phospholipids - especially the combination of a 16- and 18-carbon fatty acid. The effect of such chain length differences within a given pure phosphatidylcholine has been considered via studies of the phase transition behaviour and x-ray appearance of lipid bilayers (Davis, P.J. and Keough, K.M.W., 1985; Huang, C. and Mason, J.T., 1986).

Measurable structural effects are seen to occur, particularly when chain length disparity is a significant fraction of bilayer thickness. "Interdigitation" is a term coined to describe the phenomenon whereby pure phosphatidylcholines with intramolecular fatty acid chain length heterogeneity, when hydrated to form bilayers may insert the methyl ends of long fatty acids from one side across more than half the membrane thickness to protrude amongst the acyl chains of the opposite side of the bilayer (Keough, K.M.W. and Davis, P.J., 1979; Davis, P.J. and Keough, K.M.W. , 1985; Huang, C. and Mason, J.T., 1986).

This concept has been strengthened by studies of bilayers comprised of synthetic mixed-chain phospholipids by the above mentioned authors and for sphingomyelins with fatty acids of selected lengths (Maulik, P.R. et al., 1986; Levin, I.W. et al., 1985). Such a concept is particularly attractive for bilayers made up totally of a population of phospholipids having one shorter and one longer chain. However phospholipid bilayers containing only a small amount of glycosphingolipid present a different situation, in that the host matrix is typically 16- to 18-carbon fatty acids while the odd molecule (the few % GSL) may be vastly different. The very long chain fatty acid then has options that include extending amongst the acyl chains of its companion monolayer or collapsing into a highly localized nucleus of disorder.

Presumably this situation also exists in cell membranes.

In this chapter, we describe the synthesis of a novel 24-carbon fatty acid spin label, and the results of experiments in which it was attached to the sphingosine backbone of lactosyl ceramide, a simple neutral glycosphingolipid, followed by globoside, a complex neutral glycosphingolipid, and finally G_{M1}, a charged ganglioside. Fatty acids bearing covalently attached nitroxide free radicals ("spin labels") have seen wide and successful application in membranes, although having been originally designed for use with phospholipids, nothing has been done previously with long chain species. The long chain fatty acid spin label introduced here provides a realistic method of examining many aspects of chain length disparity in model and cell membranes. By comparison with the behaviour of the conventional 18-carbon fatty acid spin label attached to lactosyl ceramide we have been able to address for the first time the question of "interdigitation" as it applies to glycosphingolipids in a bilayer membrane, and show that the trans-bilayer interdigitation phenomenon of glycosphingolipids bearing the long chain fatty acids may be a general phenomenon.

In this chapter we also address the fate of long chain fatty acids of glycosphingolipids present as minor components in membranes of non-interdigitating phosphatidylcholines. Thus, in this pursuit, we include derivatives of galactosyl ceramide previously synthesized in this lab (the C-18 analogue) (Sharom, F.J. et al., 1976), lactosyl ceramide, globoside (Mehlhorn, I. et al., 1988), and G_{M1}. These were synthesized having either the 18-carbon or 24-carbon fatty acid with the spin label covalently attached to carbon number 16.

The nitroxide radical at C-16 is used to measure the degree of motional

anisotropy (order) for the glycosphingolipid fatty acid in the region of the host phospholipid terminal methyl groups. We have found that the order at C-16 is much greater for a 24-carbon fatty acid than for an 18-carbon fatty acid attached to galactosyl ceramide, lactosyl ceramide, globoside and G_{M1} respectively. This is consistent with interdigitation of the longer chain.

In our work with lactosyl ceramide, the natural fatty acid had been removed by a single step via base hydrolysis. An 18-carbon or 24-carbon fatty acid spin label could then be attached in a one-step addition reaction. However, in the case of globoside and G_{M1} a much more complex synthesis was necessary to arrive at the fatty acid-substituted species, since the hydrolysis step that removes the pre-existing fatty acid may also remove headgroup sugar N-acetyl functions. This latter difficulty in the production of the lyso derivatives from glycosphingolipids bearing N-acetyl groups was recently solved by Neuenhofer et al., who reported the synthesis of lyso G_{M1} and subsequent selective re-N-acetylation of the amino sugars (Neuenhofer, S. et al., 1985). We have been able to use the same approach with globoside, and have reacylated the resultant lyso glycosphingolipids with either the 18-carbon or 24-carbon spin labelled fatty acids.

4.2 Materials and Methods

4.2.1 Source of Materials

L-α-phosphatidylcholine from egg yolks was purchased from Avanti Polar Lipids, Birmingham, AL. L-α-dimyristoyl phosphatidylcholine, L-α-dipalmitoyl phosphatidylcholine, and N-lignoceroyl-dihydrolactocerebroside were from Sigma, St.

Louis, MO. N,N'-dicyclohexylcarbodiimide (DCC), thionyl chloride, cadmium chloride, barium hydroxide, 2-amino-2-methyl-1-propanol, p-toluene-sulfonic acid and m-chloroperbenzoic acid were all from Aldrich, Milwaukee, WI. Cholesterol was from Serdary Research, London, Can. All of the above lipids were pure by the criterion of giving single spots on thin layer chromatography plates (Merck silica gel 60) eluted with 65:25:4 (v/v/v) $CHCl_3/CH_3OH/H_2O$, and developed with 1:2.75 sulfuric acid/ethanol spray. Hexadecanedioic acid was from ICN/K&K, Plainsville, NY. Octyl bromide and ethyl bromide were from Sigma. *Clostridium perfringens* type VI was from Sigma. Silicic acid (Bio-Sil A 200-400 mesh) was from Bio-Rad, Richmond, CA. All solvents were "spectral" or reagent grade.

4.2.2 Isolation of Globoside, G_{M1} and Galactosyl Ceramide

Globoside was isolated from porcine red blood cells according to the method of Hakomori and Siddiqui (Hakomori, S. and Siddiqui, B., 1974), except that the crude glycosphingolipid extract was run on a silicic acid column (Bio-Sil A, 3 x 70 cm eluted with 1 / $CH_3OH/CHCl_3$ (1:9, v/v) and 1.5 / $CH_3OH/CHCl_3$ (1:4, v/v), followed by a gradient of 1:4 - 2:3 (v/v)). The globoside fraction was further purified on a small silicic acid column (Bio-Sil A, 1 x 10 cm) eluting with $CHCl_3/CH_3OH/NH_4OH$ (60:40:4, v/v/v). It ran as a single spot on TLC plates eluted with 55:25:4 (v/v/v), $CHCl_3/CH_3OH/H_2O$.

The ganglioside, G_{M1}, was prepared and purified following the procedure of Felgner et al (Felgner, P.L. et al., 1983) as modified by Thompson et al (Thompson, T.E. et al., 1985). This involved isolation of a fraction consisting of GD_{1a}, GD_{1b} and

GT_{1b} from total beef brain gangliosides (prepared according to Kanfer (Kanfer, J.M., 1969), and treatment with neuraminidase (*Clostridium perfringens* type VI). Galactosyl ceramide was isolated from the organic phase of the above isolation of G_{M1} and purified via silicic acid column in a CH_3OH gradient in $CHCl_3$.

4.2.3 Synthesis of 16-Nitroxy-lignoceric and 16-Nitroxy-stearic Acids

Spin labelled fatty acids employed in this work were prepared following the general method of Hubbell and McConnell (Hubbell, W.L. and McConnell, H.M., 1971). This approach involved deriving long chain keto methyl esters of the formula $CH_3(CH_2)_m\ C(=O)(CH_2)_n\ C(=O)OCH_3$ via reaction of alkylcadmium compounds, $[CH_3(CH_2)_m]_2\ Cd$, with ω-carbalkoxyacyl chlorides, $Cl\ C(=O)CH_2)_n\ C(=O)OCH_3$. The spin label (N-oxyloxazolidine) ring is then produced at the location of the ketone by the method of Keana et al. (Keana, J.W. et al., 1967).

20 g (0.07 mol) of hexadecanedioic acid was dissolved in 64 ml of CH_3OH. HCl gas was bubbled through the solution and allowed to reflux for 2 hr. 240 ml of H_2O was added to the cooled solution and then extracted with 3 x 75 ml of benzene. The organic layer was washed with 250 ml H_2O, 250 ml 5% Na_2CO_3 and finally with 250 ml H_2O. The organic layer was dried with $CaCl_2$ and rotary evaporated to dryness. It formed a dark brown oil, and upon cooling it crystallized.

127 ml of a 1.0 N $Ba(OH)_2$ solution (prepared in anhydrous CH_3OH and titrated with 0.100 N HCl using Bromthymol Blue indicator) was added to the dimethylester. The flask was sealed with a drying tube and allowed to stir overnight at room temperature. The precipitate was filtered on a Buchner funnel and washed

with about 50 ml of CH_3OH. The moist barium salt was put into a 1 *l* separatory funnel and 100 ml of 4 N HCl was added along with 80 ml of diethyl ether. The aqueous layer which contained the $BaCl_2$ was removed and the ether layer was washed with 3 x 100 ml H_2O. The ether was removed and the residue dried under vacuum.

For every mole of the monomethyl ester, 2 moles plus 20% excess of $SOCl_2$ is required to form the acid chloride. Therefore, 19.03 g of $SOCl_2$ was added to the monomethyl ester and allowed to heat to 38°C for 4 hr. The material was then stoppered and placed into a desiccator until the appropriate Grignard was formed.

2.21 g of Mg turnings were placed into a round bottom flask with 112 ml of anhydrous ether. From a dropping funnel 17.53 g of octyl bromide in 43 ml of anhydrous ether was added slowly over a period of about 30 min, and allowed to reflux for 2 hr. Meanwhile, the excess $SOCl_2$ was removed from the acid chloride and it was dissolved in 30 ml of dry benzene. The Grignard reaction was cooled in an ice bath and 8.34 g of anhydrous $CdCl_2$ was added. After 30 min, the ether was distilled off (not to dryness) and to the solid, 113 ml of dry benzene was added. The acid chloride in benzene was added and the whole refluxed for 60 min. The reaction was cooled in an ice bath and 18 ml of H_2O was added, followed by about 60-70 ml of a 0.1 N H_2SO_4 solution. The upper benzene phase was collected and washed with H_2O, filtered through Na_2SO_4 and dried over Na_2SO_4 (50 g) overnight. The benzene was removed and the oil which resulted solidified into a tan coloured solid. Yield was 16 g.

350 g of silica gel (Bio-Sil A, 100-200 mesh) was loaded into a 6.5 x 90 cm

column. The 16 g of the above solid was dissolved in benzene and loaded onto the column. Fractions were collected as follows: 4 x 250 ml benzene, 4 x 250 ml 4% ether/benzene and 4 x 250 ml 6% ether/benzene. Isolated material was 8.5 g.

The 8.5 g (0.027 mol) of the ketone was dissolved in 141 ml of toluene in a 500 ml round bottom flask. To this 27.2 ml of 2-amino-2-methyl-1-propanol and 27.2 mg of p-toluene sulfonic acid monohydrate were added. The mixture was set up in a Dean-Stark apparatus and refluxed for 6 days with continuous H_2O removal. At the end of the 6 days the toluene layer was washed with 6 x 55 ml of $NaHCO_3$ (sat.) and 4 x 55 ml H_2O. The toluene was then dried over Na_2SO_4 and reduced to a clear yellowish viscous liquid. Yield was 6 g.

The above oil was dissolved in 136 ml of diethyl ether in a 500 ml round bottom flask and cooled to 0°C in an ice bath. 6.1 g of m-chloroperbenzoic acid was dissolved in 27 ml of diethyl ether and added to the oil via a dropping funnel over a 2 hr period with stirring. The flask was removed from the ice bath and allowed to sit at room temperature overnight. The ether was then washed with 4 x 55 ml $NaHCO_3$ (sat.) followed by 4 x 55 ml H_2O. The ether was dried over Na_2SO_4 overnight and then rotary evaporated to dryness.

580 g of silica gel (Davisil 62, 60-200 mesh, Desiccant Activated) was loaded in benzene into a column 6.5 x 90 cm. The above oil was dissolved in 70 ml of benzene and the elution profile was as follows: 1 x 1000 ml benzene, 1 x 500 ml 0.5% ether/benzene, 2 x 500 ml 1% ether/benzene, 3 x 500 ml 1.5% ether/benzene and finally 12 x 250 ml 2% ether/benzene. Yield isolated was 2 g.

The above 2 g was dissolved in 20 ml of dioxane. To this 8 ml of 1.0 N NaOH

was added along with 20 ml of H_2O to dissolve the dioxane solution. To this mixture, 30 ml of ether was added to extract apolar compounds. At this point the ether layer was yellow. The aqueous layer was washed with 2 x 30 ml of ether. The ether layer was now clear. To convert the compound from the sodium salt, dilute HCl was added. 30 ml of ethyl acetate was added on top of the aqueous layer to avoid prolonged exposure of the spin label to the HCl. As the pH approached 1, the yellow colour entered the ethyl acetate layer. The aqueous layer was extracted with 140 ml of ethyl acetate and dried over Na_2SO_4. The solvent was removed to yield a viscous yellow oil. Yield was 271 mg.

The resultant spin labelled fatty acids may then be named according to their (m n) values as above, or according to the number of the fatty acid carbon which has the spin label ring. Thus the long and short chain fatty acids, synthesized for this work were the (7,14) and (1,14) spin labels or the 16-nitroxy-lignoceric acid and the 16-nitroxy-stearic acid respectively.

The resultant long chain fatty acid (methyl ester) with ketone at C-16 had the known IR features of keto-fatty acid esters. It was positively identified by ^1H NMR (Varian HA 200) and found to have integrated peak intensities within 3% of those expected from the formula. The corresponding 16-nitroxy-stearic acid was produced using the exact method as above, except that ethyl bromide was used to prepare the appropriate Grignard reagent instead of octyl bromide, and the amounts of reagents were adjusted for the difference in molecular weight.

4.2.4 Production of Lyso-Lactosyl Ceramide

The base hydrolysis step which removes the original fatty acid prior to replacement with a spin labelled fatty acid followed the general procedure of Neuenhofer et al. (Neuenhofer, S. et al., 1985). 25 mg (26 μmol) of lactosyl ceramide was dissolved in 10 ml of 1 N methanolic KOH in a 12 ml culture tube with screw cap (Kimble, Kimax 16 x 100 mm). The solution was briefly deoxygenated under a stream of N_2 gas and the cap firmly screwed on. The tube was stirred in an oil bath of 97°C for 24 hr and the reaction was stopped with 0.75 ml of glacial acetic acid. TLC on Merck silica gel 60 plates eluted with 65:25:4 $CHCl_3/CH_3OH/H_2O$ (and developed with H_2SO_4/CH_3CH_2OH spray) showed that the original spot of R_F=0.64 had largely disappeared, to be replaced by a ninhydrin-positive broad spot, of R_F=0.06 and faster running free fatty acid. The sample was dried under nitrogen, freed of salt by a 3 hr dialysis against water, and the lyso-lactosyl ceramide was isolated using a column containing 1 g silicic acid poured in 5% $CH_3OH/CHCl_3$ and eluted first with 20% $CH_3OH/CHCl_3$ and then with 60% $CH_3OH/CHCl_3$. Lyso-galactosyl ceramide was formed in the same fashion as the lyso-lactosyl ceramide above.

4.2.5 Reacylation of Lyso-Lactosyl Ceramide

In a typical reacylation, 13 mg of lyso-lactosyl ceramide was dissolved with 18-20 mg of spin labelled fatty acid in 0.5 - 1.0 ml of calcium hydride-dried pyridine. To this 20 mg of DCC was added and the solution stirred at 22°C in a sealed container over Drierite. Over a period of 24 - 72 hr a single new spot appeared with R_F

indistinguishable from genuine lactosyl ceramide, while the slow-running lyso-compound (ninhydrin-positive) was correspondingly decreased. The spin labelled lactosyl ceramide was isolated on a silicic acid column (1.2 x 11 cm) eluting with 5, 10 and 20% CH_3OH in $CHCl_3$. Overall yield based on native glycosphingolipid was 26%. For galactosyl ceramide this one step procedure was also employed. However, a more complex procedure was required for the formation of lyso-G_{M1} as described by Neuenhofer, (Neuenhofer, S. et al., 1985) and was equally applicable to the formation of lyso-globoside (Mehlhorn, I.E. et al., 1988). It was readily demonstrated by ^1H NMR that the initial base hydrolysis step removed the N-acetyl function from globoside. Subsequent selective replacement of the N-acetyl group was also demonstrated by ^1H NMR. Lyso-glycosphingolipids reacylated with spin labelled fatty acids ran with R_F values identical to those of the glycosphingolipid starting materials.

4.2.6 Liposome Preparation

Lipid bilayer membranes for these experiments were prepared by dissolving all components at the final desired ratio in 1:1 $CHCl_3/CH_3OH$, and removing the solvent under an N_2 atmosphere. Resultant films were further dried by pumping in vacuum for 3 hr at 22°C. Liposomes were prepared by hydration of dry films with 10 mM phosphate buffered normal saline pH 7.4 containing Ca^{2+} and Mg^{2+}. Free Ca^{2+} and Mg^{2+} concentrations in the samples were .96 mM and .55 mM respectively as determined by chemical analysis. All samples were incubated 10°C above their transition temperatures for 15 min to assure diffusional equilibrium within the bilayer, before being allowed to cool to the temperature of study.

4.2.7 EPR Spectroscopy

EPR spectra of samples were run on a Varian E12 spectrometer equipped with a TM_{110} cavity and variable temperature accessory (Varian Assoc., Palo Alto, CA). For this purpose vesicle suspensions were held in 50 µl Dade^R disposable glass micropipettes sealed at one end and supported in a plastic sleeve that permitted gas flow. Typical EPR parameters are as follows; microwave power = 10 mW, microwave frequency = 9.0 GHz, scan range = 100 gauss, field set = 3200 gauss, time constant = 0.3 sec, scan time = 8 min, modulation amplitude = 1.0 gauss and modulation frequency = 100 KHz.

4.3 Results and Discussion

Figure 32A illustrates the long chain (7,14) spin labelled fatty acid covalently attached to the sphingosine backbone of lactosyl ceramide. The conventional 18-carbon chain species (1,14) is also shown for comparison (Fig. 32B). These labelled glycosphingolipids may be named by reference to the long and short fatty acids as lignoceroyl-16-nitroxy- and stearoyl-16-nitroxy-lactosyl ceramide respectively. The procedure employed for generating them followed a scheme similar to the one which was originally developed by our laboratory to produce the spectral probe labelled (1,14) galactosyl ceramide (Sharom, F.J. and Grant, C.W.M., 1975). As mentioned in section 4.2.3 - 4.2.4 it involved the base hydrolysis of the native fatty acid at the amide junction and replacement via DCC activation of the spin labelled fatty acid. To our knowledge this is the first report of a spin labelled lactosyl ceramide. When looking at Figure 32A, one can see that the methyl end of the fatty acyl chain of the

lignoceroyl species extends a considerable distance beyond that of the sphingosine backbone, while the stearoyl derivative only extends some 3 carbons beyond that of the sphingosine backbone (Fig. 32B). Yet the spin probe itself remains at the same "depth" in both cases and monitors the region very near the methyl terminus of a host bilayer matrix.

The opportunity for this type of comparison has not arisen previously, so we show in Figure 33, EPR spectra of lignoceroyl-16-nitroxy-lactosyl ceramide and stearoyl-16-nitroxy-lactosyl ceramide in a multitude of phospholipid bilayer host matrices. In particular we selected the fluid, natural matrix, egg phosphatidylcholine (composed primarily of 16-carbon and 18-carbon fatty acids); as well as the synthetic matrices, dimyristoyl (14-carbon) and dipalmitoyl (16-carbon) phosphatidylcholines. We also show the effect of cholesterol in the dipalmitoyl matrix. In each of the above cases the concentration of glycosphingolipid was kept low (2 mol %) so as to mimic the situation in cell membranes. Several comments can be made concerning the appearance of these spectra. Firstly, the spectra show no obvious evidence of the phenomenon known as spin-exchange broadening (Devaux, P. et al., 1973). This is a phenomenon whereby spin labels that collide with neighbouring spin labels broaden one another's spectral lines in a very characteristic way (see section 2.3.1 for an extended definition). Spin exchange broadening would certainly occur for instance if the labelled glycosphingolipids were in pure clusters, rigorously phase-separated from the host phospholipid matrix. Indeed spin exchange broadening is readily detectable in homogeneous systems analogous to those described here when the concentration of labelled species is 15 mol%.

Figure 32

Chemical structures of the long chain (7,14) lignoceroyl-16-nitroxy-lactosyl ceramide A) and the short chain (1,14) stearoyl-16-nitroxy-lactosyl ceramide B) respectively. Galactosyl ceramide, globoside and G_{M1} differ in oligosaccharide components, while lactosyl ceramide also lacks the double bond in the ceramide portion thus, being a dihydro derivative. Note that in each case the nitroxide free radical is covalently attached at C-16 of the fatty acid chain. R refers to the sugar headgroup.

A

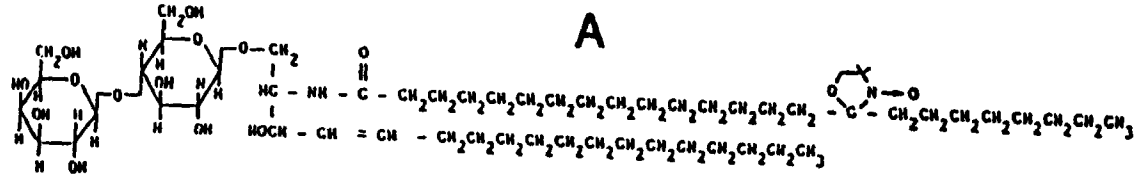

B

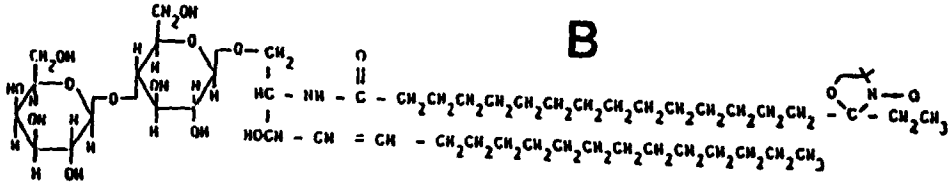

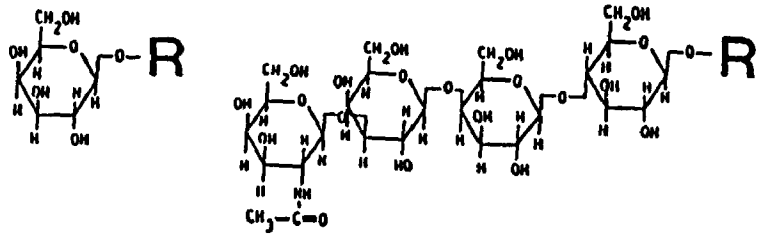

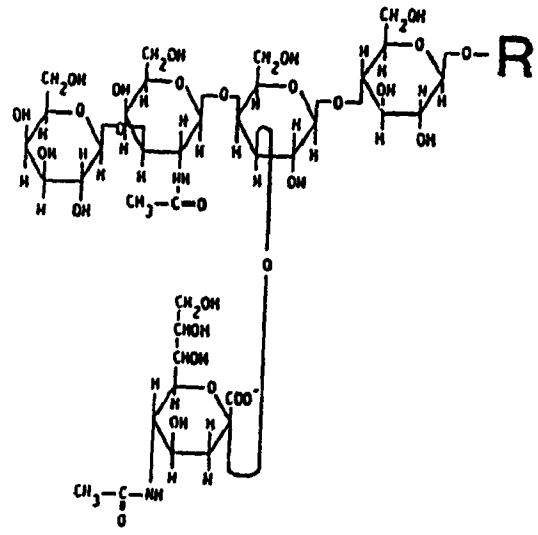

Figure 33

EPR spectra of the long chain (C-24, left hand column) and short chain (C-18, right hand column) spin labelled glycosphingolipids in various phospholipid bilayers. Egg PC, egg phosphatidylcholine; DMPC, dimyristoyl phosphatidylcholine; DPPC, dipalmitoyl phosphatidylcholine; DPPC/CHOL, 2:1 (mol ratio) dipalmitoyl phosphatidylcholine/cholesterol. In each case the glycosphingolipid comprised 2 mol % of the membrane lipid. Samples were prepared by hydrating dried films in 20 mM phosphate buffered saline (pH 7.4) at 50°C, and then allowed to cool slowly to 20°C.

Sample suspensions were held in 50 μl glass capillary tubes sealed at one end. Spectra shown were recorded at 10°C using a Varian E12 spectrometer with variable temperature accessory and TM_{110} cavity. Dotted vertical lines mark the field location of the outer spectral extrema in the most rigid matrix (DPPC). The separation of these peaks is related to spin label correlation time (i.e. inversely related to spin label mobility). The locations of spectral features used for order parameter calculations such as those described in the caption to Table 2 are indicated by short vertical bars for the DPPC samples (outer spectral splitting corresponds to dotted vertical lines; inner spectral splitting is smaller).

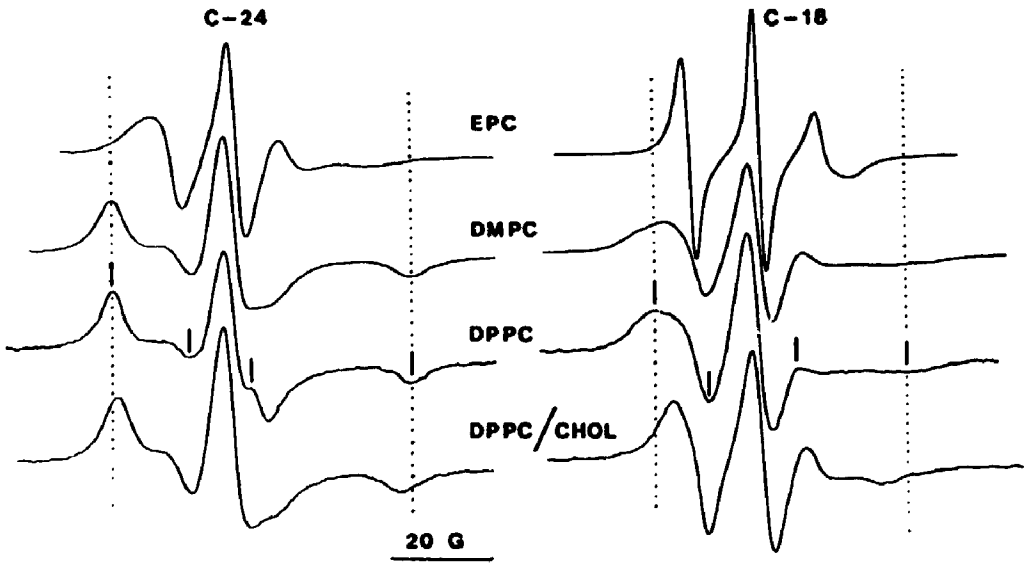
C-24
C-18
EPC
DMPC
DPPC
DPPC/CHOL
20 G

The literature offers some divergent opinions in this area, especially with regard to the question of lateral distribution of glycosphingolipids (Curatolo, W., 1987a; Curatolo, W., 1987b; Thompson, T.E. and Tillack, T.W., 1985; Grant, C.W.M., 1987). Interpretation is complicated by the fact that different techniques have been used in arriving at published conclusions and that fatty acid composition is a significant variable. Here we have controlled for fatty acid composition of the glycosphingolipid in substituting known 18-and 24-carbon fatty acids for the natural ones. At the same time we have covalently attached a probe molecule in a known location that samples glycosphingolipid microenvironment even at extremely low concentrations in any membrane. The spin label probe on the fatty acid chain is sensitive to motion, orientation, and the presence of other nearby spin labels. In addition, within the recently determined limitations of the technique, we have used freeze-etch electron microscopy with modest success to test for distribution differences amongst G_{M1}, globoside and lactosyl ceramide by marking their locations with lectins or antibodies (Mehlhorn, I.E., et al, 1989).

The question of lateral phase separation of glycosphingolipids in membranes is an important one from both a structural and a functional viewpoint (Grant, C.W.M., 1987; Thompson, T.E. and Tillack, T.W., 1985). This phenomenon however is clearly marginally understood at present. Currently it seems to be agreed that, in some model membranes at least, glycosphingolipids tend to phase separate into domains of selective enrichment that coexist in a given bilayer. There is much debate about domain size and composition, the effect of the fatty acid type, and especially about the likelihood of the phenomenon occurring in "natural" lipid mixtures and in

cell membranes. The spin labels described here will lend themselves particularly well in answering certain such questions. Distinguishing between various subtle degrees of phase separation will however require systematic study, perhaps spectral simulation (Mehlhorn, I.E., et al, 1989) and comparison with information on the same systems from other techniques such as immunology and electron microscopy. Secondly, comparisons within each vertical column of spectra in Figure 33 show the relative features expected of the lipid matrices involved. Thus the spectra of glycosphingolipids in the natural mixture, egg phosphatidylcholine (which is not rigid at 10°C) show the 3 relatively narrow lines so characteristic of spin labels tumbling with correlation times in the range of 10^{-9} sec (McCalley, R.C. et al., 1972). The rigid synthetic matrices, dimyristoyl and dipalmitoyl phosphatidylcholine, show spectral features such as the "outer wings" (outer spectral extrema) marked by the dotted lines for the DPPC spectra, that approach those expected of immobile spin labels. The distance between these outer wings may be directly related to label immobility or correlation time, τ_c (McCalley, R.C. et al., 1972).

In accordance with this logic, note that the addition of cholesterol makes the spectral features measurably less rigid in keeping with its known tendency to disorder gel phase phospholipid bilayers (Demel, R.A. and Dekruyff, B., 1976). The nitroxide spin label of course reflects in its EPR spectrum the mobility of that portion of a host molecule to which it is attached. In this case being attached to a fatty acid carbon well down in the membrane, the order parameter gradient of phospholipid (McConnell, H.M. and McFarland, B.G., 1972) and glycosphingolipid (Sharom, F.J. et al., 1976) acyl chains would predict considerable mobility for the label at C-16 in

a fluid host matrix. Thirdly, comparing between columns of spectra in Figure 33, in each pair of spectra representing lignoceroyl-16-nitroxy-lactosyl ceramide vs stearoyl-16-nitroxy-lactosyl ceramide in a given host matrix, the former shows distinct evidence of lower mobility. That is, the spectral appearance (McCalley, R.C. et al., 1972) indicates that the spin label on the long chain fatty acid in the region of the host matrix terminal methyl group (the bilayer's most disordered and fluid region) is considerably less mobile than the label on the short chain fatty acid. Such a result would be anticipated if the temporal oscillations of the C-16 carbon on lignoceroyl lactosyl ceramide were less than those in stearoyl lactosyl ceramide in a given bilayer. However such a result might occur associated with local order, or local disorder, of the fatty acid segment involved.

The design of this pair of spin labelled glycosphingolipids makes it possible to consider a basic question which has until now not been addressed in the literature: the arrangement of the long-chain fatty acid in glycosphingolipids relative to other membrane components. As already described, a closely related question has been addressed for pure phospholipids in which one fatty acid is longer than the other, and the suggestion has been made that the longer chains of each monolayer interdigitate with the shorter chains of the opposing monolayer. In the glycosphingolipid case the chain length discrepancy is considerably greater than that typical of natural phospholipids. Also glycosphingolipids comprise only a small percentage of the lipids in membranes and are thought to be restricted to the outer surface - so it is not obvious that an exceedingly long chain has an opposing slot to interdigitate into. The situation is illustrated diagrammatically in Figure 34: does the "extra" length of alkyl

chain of a glycosphingolipid with 24-carbon fatty acid ball up longitudinally via *trans* → *gauche* isomerization to form a focus of disruption (situation A); or does it interdigitate with chains of the opposing monolayer (situation B). The presumed arrangement of the glycosphingolipid with short (18-carbon) fatty acid is also illustrated (situation C): it is shown fitting with minimal disruption amongst the 16-carbon and 18-carbon fatty acid phospholipids that comprise the bulk of membranes, as we originally determined for galactosyl ceramide (Sharom, F.J. et al., 1976). Since the spin labels of lignoceroyl-16-nitroxy-lactosyl ceramide and stearoyl-16-nitroxy-lactosyl ceramide are localized to the region of "crossover" for acyl chains interdigitating from one monolayer to the other, one may hope to gain some insight into whether situation A or B of Figure 34 is the more common by examining the "order parameters" associated with the spin labelled portions of the acyl chains.

The concept of order parameter, "S", in membranes arose out of early spin label studies in which people asked the question, "what is the degree of alignment of a given length of fatty acid chain perpendicular to the plane of the membrane?" (Hubbell, W.L. and McConnell, H.M., 1971; McConnell, M.H. and McFarland, B.G., 1972; Seelig, J., 1970). Even in fluid membranes, alkyl chains tend to assume extended conformations perpendicular to this plane, and to pack in a hexagonal liquid-crystal lattice. The spin label order parameter, S, has been defined in such a way that it varies between 0 and 1 according to how well the fatty acid segment to which the spin label is attached remains aligned as described above (perfect alignment gives S = 1, while total disorder gives S = 0) (Hubbell, W.L. and McConnell, H.M., 1971; Seelig, J., 1970). It has been pointed out that one should not

Figure 34

Possible arrangements for the spin labelled fatty acid of glycosphingolipids described here in a bilayer membrane of 16- and 18-carbon fatty acid phosphatidylcholine. The headgroup of lactosyl ceramide is denoted by 2 linked hexagons: A, 24-carbon chain folded back upon itself to form a focus of disruption; B, 24-carbon chain extended so as to interdigitate with fatty acids of the opposing monolayer; C, 18-carbon chain in standard configuration. Note that the spin label is localized to a point roughly in the center of the hydrophobic interior.

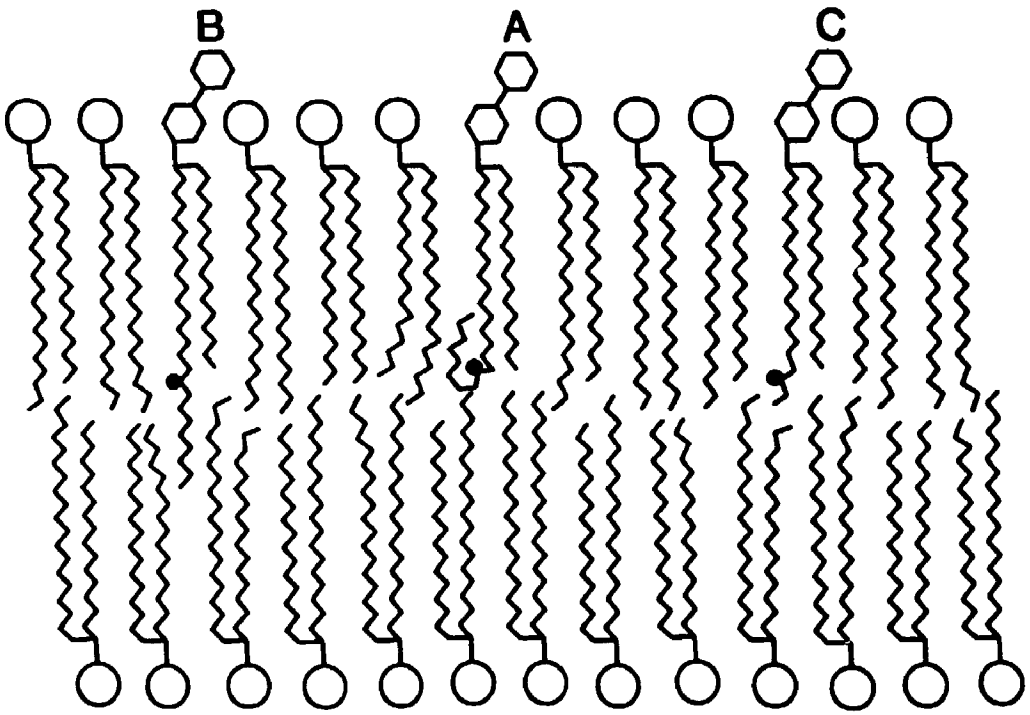
B
A
C

confuse motional rate with degree of alignment, S: a segment of a given fatty acid may exhibit high mobility, while maintaining a high degree of overall alignment perpendicular to the bilayer plane (eg. by pirouetting and wagging about its long axis). By the same token a given segment might be highly immobilized, but with random orientation. In Figure 34, situation A would be expected to predispose toward an especially low order parameter, while situation B would do just the opposite. Note once again that since motional rate is not an obvious component of such considerations, the correlation time data alluded to in the previous paragraph will not help distinguish between these two possibilities.

Order parameter information is present in EPR spectra in that the separation between spectral peaks is related to the orientation of the nitroxide radical relative to the spectrometer magnetic field vector. A general and convenient technique for obtaining such information from sample spectra has been described (Hubbell, W.L. and McConnell, H.M., 1971; Keana, J.W., et al., 1967; Seelig, J., 1970) and comprehensively reviewed (Griffith, O.H. and Jost, P.C., 1976; Marsh, D., 1981) by several groups. The basic approach is to identify a separation, $2T_{\perp}'$, of two particular inner peaks, and subtract this value from the separation, $2T_{||}'$, of two outer peaks (illustrated for DPPC spectra in Figure 33). The ratio of the result to that found for the same spin label in a perfect crystal (order parameter = 1) gives an approximate order parameter, S^{app}. This may then be refined by correcting for polarity of the spin label environment and for slight differences between the measured splitting, $2T_{\perp}'$, and the desired matrix element, $2T_{\perp}$, (see caption to Table 2).

Order parameter calculations for lactosyl ceramide as well as for galactosyl

ceramide, G_{M1} and globoside with 18-carbon and 24-carbon fatty acid spin label in 4 different lipid matrices are tabulated (Table 2). These should be examined with regard to Figure 34 in light of the possible fatty acid arrangements described.

It is clear from Figure 35 that the spectra obtained are sensitive to factors related to dynamics and organizational differences between short and long chain glycosphingolipids. Our hypothesis was that, by placing a spin probe at the point where interdigitation is determined, we could test the effect of the "extra" length of hydrocarbon chain on local order. We examined the phenomenon in membranes with different properties: the highly fluid matrix, egg phosphatidylcholine (egg PC); the rigid matrix, dipalmitoyl phosphatidylcholine (DPPC); the system of intermediate fluidity, 2:1 DPPC/cholesterol; and the short chain matrix, dimyristoyl phosphatidylcholine (DMPC). The ratio of glycosphingolipid to host matrix has been kept low, in the order of 1-2% for all our experiments.

Order parameters were determined by the method summarized in the caption to Table 2. They have been arranged in groups corresponding to the different glycosphingolipid families. Within each family of glycosphingolipids, for example lactosyl ceramide, the order parameter reflects the anticipated relative fluidities of the various host lipids. Thus for both the 24-carbon fatty acid lactosyl ceramide and the 18-carbon fatty acid lactosyl ceramide the order at C-16 is highest in the crystalline DPPC host matrix ($S = 0.81$ and $S = 0.42$ respectively). These values drop, in going to the DPPC/cholesterol matrix which has intermediate fluidity, and are lowest in the natural, highly fluid egg PC ($S = 0.24$ and $S = 0.08$ respectively). However, the striking aspect is that each value of S for the long chain species is some

2 or more times that for its short chain analogue. This is certainly inconsistent with any model that would view the long chains of glycosphingolipid as collapsed at the plane of the host methyl terminii, and argues in favour of interdigitation as follows: situation A, of Figure 34 (long chain fatty acid forming a focus of local disorder) should lead to an S value similar to or less than that of the short chain analogue. Instead, as mentioned, we observed that S values for the long chain spin labelled glycosphingolipid are much greater than those of the short chain analogue in fluid, rigid, and cholesterol-containing matrices. Such a result would be expected if interdigitation were occurring (situation B of Figure 34). A third possibility, which is not shown might also be considered for arrangement of the extra length of the 24-carbon fatty acid: the long chain might bend sharply by 90° at the depth of the surrounding phospholipid terminal methyl groups. The upper portion of the fatty acid could then remain hexagonally packed with surrounding orderly acyl chains, while the extra length might lie in the plane of the membrane, extended amongst the phospholipid methyl terminii. This is a significant possibility because, conceptually at least, if the 90° bend were below the spin label (i.e. at carbon 17 or greater) a higher S value might be predicted for the long chain glycosphingolipid fatty acid, as observed. However the result with the DMPC host matrix seems to rule out such a possibility since the 14-carbon fatty acids in the latter case would dictate that the 90° bend be above the spin label, forcing the nitroxide ring to take on a relatively random arrangement with a low S value, whereas in fact the values of S observed for short and long chains of all 4 glycosphingolipids in DMPC fit into the same pattern as the other host matrices.

Figure 35

Typical comparative features of the short vs the $lo_{1.0}$ chain spin labelled glycosphingolipids; A) N-stearoyl-G_{M1}; B) N-lignoceroyl-G_{M1} at 2 mol % in bilayers of dipalmitoyl phosphatidylcholine. Spectral features used to calculate order parameters are illustrated. Samples were in phosphate buffered isotonic saline containing Ca^{2+} and Mg^{2+}, and were run at 22°C. S values were calculated according to the legend for Table 2.

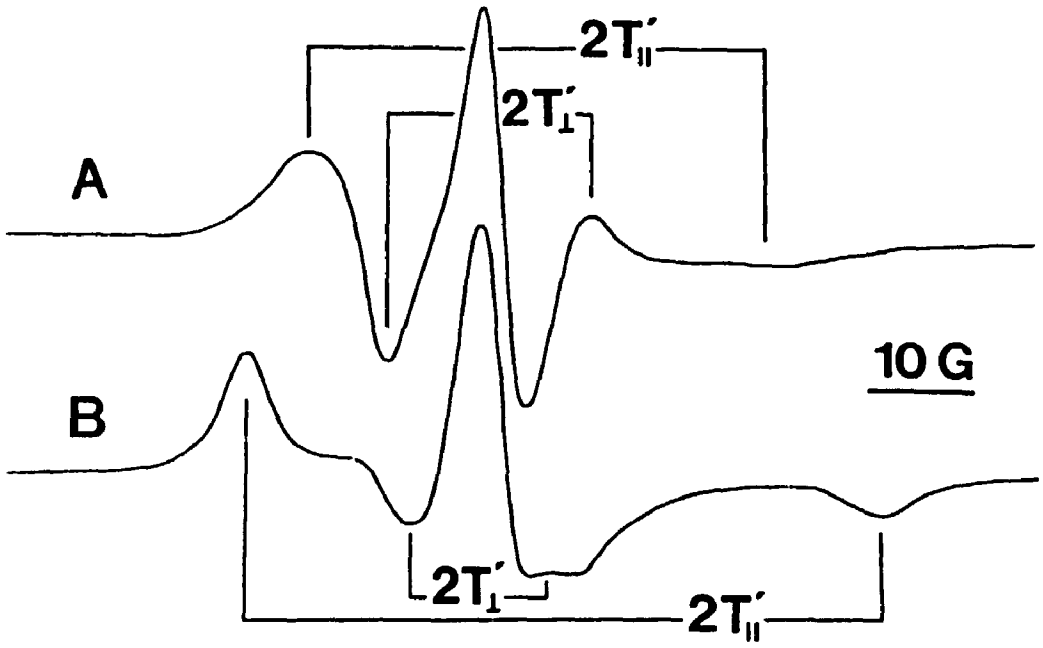
2T∥′
2T⊥′
A
10 G
B
2T⊥′
2T∥′

TABLE 2

Order parameter data for galactosyl ceramide, lactosyl ceramide, globoside, and G_{M1} with spin label at C-16 of the fatty acid chain. Data are given for the long chain and short chain derivatives for comparison. Glycosphingolipid was incorporated at 2 mol% in liposomes of either egg phosphatidylcholine (egg PC), dimyristoyl phosphatidylcholine (DMPC), dipalmitoyl phosphatidylcholine (DPPC), or DPPC/cholesterol (2:1 mol ratio). Sample preparation as in Materials and Methods. Sample buffer was phosphate buffered normal saline pH 7.4 containing 0.96 mM Ca^{2+} and 0.55 mM Mg^{2+}. $T_{\parallel}'$ is ½ the measured outer spectral splitting (as shown for DPPC bilayers in Figure 33), and is an accurate reflection of the desired matrix element, $T_{\parallel}$. $T_{\perp}'$ is ½ the measured inner spectral splitting (also shown as an example for DPPC in Figure 33). A better estimate of the true value of the desired matrix element is $T_{\perp} = T_{\perp}' + 1.4\,(1-S^{app})$ where

$$S^{app} = \frac{T_{\parallel}' - T_{\perp}'}{T_{zz}^{c} - \tfrac{1}{2}(T_{xx}^{c} + T_{yy}^{c})}$$

is a first approximation to the order parameter and $T_{zz}^{c} = 32.9$ gauss, $T_{xx}^{c} = 5.9$ gauss, $T_{yy}^{c} = 5.4$ gauss are parameters from a crystal in which S = 1. A better value for the order parameter is then obtained as

$$S = \frac{T_{\parallel} - T_{\perp}}{T_{zz}^{c} - \tfrac{1}{2}(T_{xx}^{c} + T_{yy}^{c})} \cdot \frac{a_o^{crystal}}{a_o^{bilayer}}$$

where $a_o^{bilayer} = 1/3(T_{\parallel} + 2T_{\perp})$ and $a_o^{crystal} = 1/3(T_{xx}^{c} + T_{yy}^{c} + T_{zz}^{c})$ correct for polarity differences between crystal and bilayer.

S Values shown are averages of 2-4 measurements with a precision of $\pm$ 0.02 - 0.04.

TABLE 2 - Galactosyl Ceramide

Glycosphingolipid Fatty Acid Length (long= 24 carbons short = 18 carbons) and Host Matrix Phospholipid	Temperature (°C)	$T_{\parallel}'$ ($\cong T_{\parallel}$) (gauss)	$T_{\perp}'$ (gauss)	S^{app}	$T_{\perp}$ (gauss)	S
long in Egg PC (fluid)	10	20.7	9.8	.40	10.7	.39
short in Egg PC (fluid)	10	16.4	12.0	.16	13.1	.12
long in Egg PC (very fluid)	22	17.8	11.0	.25	12.0	.22
short in Egg PC (very fluid)	22	15.9	12.6	.12	13.8	.08
long in DMPC (rigid)	22	28.1	8.4	.72	8.8	.69
short in DMPC (rigid)	22	20.0	10.3	.36	11.2	.33
long in DPPC (rigid)	22	28.7	7.6	.78	7.9	.76
short in DPPC (rigid)	22	21.1	9.5	.42	10.3	.42
long in DPPC/CHOL (intermediate fluidity)	22	26.0	8.4	.65	8.9	.64
short in DPPC/CHOL (intermediate fluidity)	22	19.9	10.3	.35	11.2	.34

TABLE 2 - Lactosyl Ceramide

Glycosphingolipid Fatty Acid Length (long= 24 carbons short = 18 carbons) and Host Matrix Phospholipid	Temperature (°C)	$T_{\parallel}'$ (≈$T_{\parallel}$) (gauss)	$T_{\perp}'$ (gauss)	S^{zzz}	$T_{\perp}$ (gauss)	S
long in Egg PC (fluid)	10	21.0	9.7	.41	10.5	.40
short in Egg PC (fluid)	10	16.5	11.9	.17	13.1	.13
long in Egg PC (very fluid)	22	18.0	10.9	.26	11.9	.24
short in Egg PC (very fluid)	22	15.9	12.5	.12	13.8	.08
long in DMPC (rigid)	22	27.7	8.3	.71	8.7	.68
short in DMPC (rigid)	22	19.8	10.4	.34	11.3	.32
long in DPPC (rigid)	22	28.6	6.8	.80	7.1	.81
short in DPPC (rigid)	22	20.8	9.4	.42	10.2	.42
long in DPPC/CHOL (intermediate fluidity)	22	26.2	8.3	.66	8.8	.64
short in DPPC/CHOL (intermediate fluidity)	22	19.7	10.2	.35	11.1	.33

TABLE 2 - Globoside

Glycosphingolipid Fatty Acid Length (long= 24 carbons short = 18 carbons) and Host Matrix Phospholipid	Temperature (°C)	$T_{\parallel}'$ ($\simeq T_{\parallel}$) (gauss)	$T_{\perp}'$ (gauss)	S^{app}	$T_{\perp}$ (gauss)	S
long in Egg PC (fluid)	10	21.3	9.7	.3	10.5	.42
short in Egg PC (fluid)	10	16.5	12.0	.17	13.1	.13
long in Egg PC (very fluid)	22	18.2	10.9	.27	11.9	.24
short in Egg PC (very fluid)	22	16.0	12.5	.13	13.7	.09
long in DMPC (rigid)	22	27.3	8.8	.68	9.2	.64
short in DMPC (rigid)	22	19.5	10.5	.33	11.4	.31
long in DPPC (rigid)	22	29.1	6.1	.84	6.3	.89
short in DPPC (rigid)	22	21.1	9.5	.43	10.3	.42
long in DPPC/CHOL (intermediate fluidity)	22	26.4	8.3	.66	8.8	.65
short in DPPC/CHOL (intermediate fluidity)	22	19.7	10.2	.35	11.1	.33

TABLE 2 - G_{M1}

Glycosphingolipid Fatty Acid Length (long= 24 carbons short = 18 carbons) and Host Matrix Phospholipid	Temperature (°C)	$T_{\parallel}'$ ($\approx T_{\parallel}$) (gauss)	$T_{\perp}'$ (gauss)	S^{app}	$T_{\perp}$ (gauss)	S
long in Egg PC (fluid)	10	21.4	9.8	.43	10.6	.41
short in Egg PC (fluid)	10	16.5	11.9	.17	13.1	.13
long in Egg PC (very fluid)	22	18.3	10.9	.27	11.9	.25
short in Egg PC (very fluid)	22	16.0	12.6	.13	13.8	.08
long in DMPC (rigid)	22	28.0	8.3	.72	8.7	.69
short in DMPC (rigid)	22	19.9	10.3	.35	11.2	.33
long in DPPC (rigid)	22	28.9	6.4	.83	6.6	.86
short in DPPC (rigid)	22	20.9	9.4	.42	10.3	.42
long in DPPC/CHOL (intermediate fludity)	22	26.3	8.2	.66	8.7	.65
short in DPPC/CHOL (intermediate fluidity)	22	19.8	10.3	.35	11.2	.33

It should be noted that the systems studied here are very different from the pure mixed chain bilayers studied by other workers in that only a small percentage of the lipids are capable of interdigitating (i.e. the few percent glycosphingolipid in a host of phospholipid or phospholipid/cholesterol). However the results are consistent with what has been observed by others. For instance Shipley and coworkers have remarked on the striking degree of order conferred upon the region of a sphingomyelin fatty acyl chain that interdigitates (Maulik, P.R. et al., 1986). They suggest that it arises from favourable van der Waals interactions gained by such interdigitation. Boggs and Rangaraji (Boggs, J.M. and Rangaraji, G., 1985) and Boggs and Mason (Boggs, J.M. and Mason, J.T., 1986) have utilized 18-carbon free fatty acids with spin label at the C-16 or C-5 position as probes to make the interesting observation that spectra of the species with spin label at C-16 behave similarly to those of the C-5 spin label (i.e. highly immobile and ordered) when interdigitation of the surrounding homogeneous mixed chain phospholipids occurred. Note however, that in their systems this is thought to be caused by the spin label itself moving physically across the bilayer mid point due to interdigitation of the surrounding phospholipids (decreased bilayer thickness) to assume a new positior. near the bilayer surface on the opposite side of the membrane. In our systems the host phospholipid membrane presumably does not change thickness by having 2% 18-carbon vs 24-carbon fatty acid glycosphingolipid so that the spin label remains at the same position in the membrane. With regard to glycosphingolipid interdigitation, Bunow and Levin recorded Raman spectroscopic evidence that in lamellar structures of pure galactosyl ceramide the long chain fatty acids were extended, consistent with their interdigitating

across the membrane (Bunow, M.R. and Levin, I.W., 1980).

A feature of Table 2 that should be noted in passing is that the order parameters for a given host matrix type (eg. DPPC) and a given spin labelled fatty acid (eg. 18-carbon) are essentially identical amongst all 4 glycosphingolipid families. This may be somewhat surprising, given current views that the nature of the headgroup may exert a strong influence upon glycosphingolipid physical behaviour (Grant, C.W.M., 1987; Thompson, T.E. and Tillack, T.W., 1985; Curatolo, W., 1987a). However, order parameter, especially at the center of the bilayer, is likely not the most sensitive parameter to differences in the glycosphingolipid headgroup. The important question of possible headgroup sugar effects upon glycosphingolipid physical behaviour will require more systematic investigation. To date we have seen no differences amongst the spin labelled families studied in this chapter in terms of spectral features and variation in temperature or concentration.

It seems that long fatty acid spin labels are likely to prove useful in dealing with problems relating to glycosphingolipids. It is known of course that the spin label ring can represent a finite perturbation on the system being probed. However some of the most successful applications of spin labels have been in membrane systems very similar to those described here. In certain cases it has been possible to check EPR order parameter data with non-perturbing NMR probes - and the results have been found to be in basic agreement (Seelig, A. and Seelig, J., 1974; Stockton, G.W. et al., 1976) (see Chapter 5 and 6). Quantitative differences between results from NMR and EPR almost certainly partly reflect the different timescales of the two techniques.

4.4 Conclusion

"Interdigitation" is a term coined to describe the phenomenon whereby pure phosphatidylcholines with intramolecular fatty acid chain length heterogeneity, when hydrated to form bilayers may insert the methyl ends of long fatty acids from one side across more than half of the membrane thickness to protrude amongst the acyl chains of the opposite side of the bilayer. In this chapter we address the fate of long fatty acid chains of glycosphingolipids present as minor components in membranes of non-interdigitating phosphatidylcholines. In this pursuit, derivatives of lactosyl ceramide, galactosyl ceramide, globoside and G_{M1} were synthesized having either 18-carbon or the new 24- carbon fatty acid with a spin label covalently attached at C-16. Labelled glycosphingolipids were incorporated at 1-2 mol% into bilayers of egg PC, DPPC, DPPC/cholesterol and DMPC. In each case the C-16 carbon of the glycosphingolipid long chain fatty acid showed considerably greater "order" and immobility than did the C-16 of the fatty acid which was similar in length to the host matrix phospholipids. We interpret this as strong evidence that the long chain fatty acid interdigitates across the mid point of the bilayer in the systems studied. Clearly this phenomenon did not require that the phospholipid host matrix have mixed chain lengths. Furthermore, it was totally independent of glycosphingolipid family: for a given host matrix and (glycosphingolipid) fatty acid chain length the order parameter values found were the same amongst all 4 glycosphingolipid families tested.

CHAPTER 5. GLYCOSPHINGOLIPID INTERDIGITATION IN PHOSPHOLIPID BILAYERS EXAMINED BY DEUTERIUM NMR AND EPR

5.1 Introduction

The hydrophobic midplane of the cell (bilayer) membrane is frequently presented as a well-defined region at which two planar surfaces comprised of acyl chain methyl termini contact one another. However, it is well known that there is considerable disparity in acyl chain length of membrane lipids: lengths as low as 14 carbons and as high as 24 carbons being widely observed. The concept of "interdigitation" has been put forward to describe (Chapter 4) the phenomenon whereby a chain longer than half the membrane thickness might cross the midplane to protrude amongst acyl chains of the opposing monolayer (Keough, K.M.W. and Davis, P.J., 1979; Davis, P.J. and Keough, K.M.W., 1985; Huang, C. and Mason, J.T., 1986; Mattai, J. et al., 1987; Boggs, J.M. and Mason, J.T., 1986). This concept has been addressed most systematically for bilayer model membranes comprised of single pure phospholipids with one long and one short fatty acid chain (i.e., phosphatidylcholines exhibiting intramolecular fatty acid chain length disparity). Pure sphingomyelins with fatty acids of selected length (Maulik, P.R. et al., 1986; Levin, I.W. et al., 1985) and pure galactosyl glycosphingolipids (Bunow, M.R. and Levin, I.W., 1980; Boggs, J.M. et al., 1988) have also been studied. In these situations the longer chains are seen as matching up stoichiometrically with the shorter chains of the opposing monolayer when chain length differences are not extreme.

Our interest has been to extend this concept to glycosphingolipids in cell membranes. The glycosphingolipid molecule possesses one fatty acid, typically 18-24 carbons in length. The sphingosine portion, which contributes the equivalent of a second acyl chain, extends to a membrane depth of only 13 to 15 carbons. Hence glycosphingolipids may be expected to behave as mixed-chain lipids. However glycosphingolipids are a small fraction of the total lipids in most eucaryote membranes, and are restricted to the outer surface. Furthermore, since the single fatty acid is commonly up to 24 carbons long, acyl chain length mismatch within a given glycosphingolipid is greater than that in surrounding phospholipids - most of which will have 16- or 18-carbon fatty acids. Thus the situation for glycosphingolipids in cell membranes is different from that of the pure single-component systems so far studied (Harwood, J.L., 1989). We have proposed previously (Chapter 4) that glycosphingolipid long chain fatty acids exhibit a type of interdigitation in phospholipid membranes. The proposal was based on the results of our experiments with gal cer, lac cer, globoside and G_{M1} bearing a long chain (24-carbon) spin labelled fatty acid (Grant, C.W.M. et al., 1987; Mehlhorn, I.E. et al., 1988). In these earlier experiments the nitroxide radical was covalently attached at C-16 of the glycosphingolipid fatty acid, and thus could be used to measure its motional anisotropy (order) in the region of the host phospholipid terminal methyl groups. The order at C-16 was much greater for a glycosphingolipid 24-carbon fatty acid than for its 18-carbon analogue, suggesting that interdigitation of the longer chain may be occurring, resulting in 'tethering' of the upper portion. Alternative acyl chain arrangements were less consistent with spectral observations.

However while nitroxide spin label EPR spectroscopy is ideally suited to monitoring membrane structures (McConnell, H.M., 1976; Meirovitch, E. and Freed, J.H., 1984), a significant concern is that the spin label itself may present enough of a spatial perturbation to leave the final conclusion in doubt. In this chapter we describe an extension of our previous experiments (Chapter 4) to the non-perturbing deuterium probe. Deuterium NMR (^{2}H NMR) has developed into a valuable technique in membrane biochemistry. This method, in our hands consists of selectively deuterating, or completely deuterating fatty acids of various lengths, then incorporating it into the system of choice. From the powder spectrum (Fig. 39) a quadrupole splitting can be measured and an order parameter can be directly calculated. This order parameter, while not being a readily visualized concept (unlike in the EPR spectra) is a well-defined physical parameter and very useful for membrane work. The quadrupole coupling can be measured only in multilamellar preparations, since in small vesicles the interactions of interest are completely motionally averaged, resulting in a single line. The signals can be assigned in a straight forward manner and there are no complications from naturally occurring deuterium because its natural abundance is very low (0.01%) and deuterium labelling is very efficient; in excess of 98% for fatty acids. Since ^{2}H NMR relaxation proceeds by only one mechanism (quadrupole relaxation), spin-lattice (T_1) relaxation time measurements provide a good indication of motion in a phospholipid system.

5.2 Materials and Methods

5.2.1 Source of Materials

L-α-Distearoyl and L-α-dimyristoyl phosphatidylcholines were from Avanti Polar Lipids, Birmingham AL. Octadecanoic-d_{35} acid (98.8 atom % D) and deuterium depleted water were from MSD Isotopes, Montreal Canada. Galactosyl ceramide was isolated from the non-polar residue after a Folch extraction (Folch, J. et al., 1957) of lyophilized beef brain grey matter. The material was subjected to column chromatography on silicic acid (Bio-Sil A 200-400 mesh) using a gradient of CH_3OH in $CHCl_3$. Stearic acid selectively dideuterated at carbon 17 was a generous gift from A.P. Tulloch. Stearic acid with nitroxide spin label at carbon 12 of the fatty acid chain was prepared following the general method of Hubbell and McConnell (Hubbell, W.L. and McConnell, H.M. 1971).

5.2.2 Synthesis of Probe Labelled Galactosyl Ceramide

Lyso gal cer (gal cer with natural fatty acid removed) was produced from isolated gal cer by hydrolysis in stirred methanolic KOH at 97°C in a sealed glass culture tube (Neuenhofer, S., et al., 1985) or by hydrolysis in refluxing butanolic KOH (Taketomi, T. and Yamakawa, T., 1963) and was ninhydrin positive. Probe-labelled gal cer was synthesized by coupling of spin-labelled or deuterated fatty acids to lyso gal cer as described previously (Sharom, F.J. and Grant, C.W.M., 1975). Reactions were followed by thin-layer chromatography on Merck silica gel 60 plates eluted with 65:25:4 $CHCl_3/CH_3OH/H_2O$ and developed with ninhydrin and/or sulfuric acid/ethanol spray. Probe-labelled galactosyl ceramides did not stain with ninhydrin and co-

migrated with natural gal cer. Probe-labelled derivatives were stable to overnight treatment with aqueous KOH at 5 mg/ml - conditions which cleave ester bonds readily.

5.2.3 Liposome Preparation

Lipid bilayer membranes for these experiments were prepared by dissolving all components at the final desired ratio (10 mol % glycosphingolipid) in 1:1 $CHCl_3/CH_3OH$, and removing the solvent under a N_2 atmosphere. Resultant films were further dried by pumping in vacuum (rotary pump) for 2 h at 22° C. Liposomes were generated by hydration of such films with deuterium depleted water. Samples were lyophilized three times from 100 µl of deuterium depleted water, after which the hydrated samples were subjected to eight freeze-thaw cycles. Each sample comprised 30-45 mg total lipid in a volume of 150-200 µl. All samples were incubated 10° C above their transition temperatures for 15 min to assure diffusional equilibrium within the bilayer before being allowed to cool to the temperature of study.

5.2.4 EPR Spectroscopy

EPR spectra were run on a Bruker ER 200D-SRC spectrometer equipped with a TM_{110} cavity and variable temperature accessory. For this purpose vesicle suspensions were held in 50 µL Dade^R disposable glass micropipettes sealed at one end.

5.2.5 ^{2}H NMR Spectroscopy

^{2}H NMR spectra were acquired at 30.7 MHz on a 'home-built' spectrometer

operated by a Nicolet 1280 computer. Spectra were recorded using the quadrupolar echo pulse sequence (Davis, J.H. et al., 1976) with full phase cycling (Perly, B., et al., 1985) and quadrature detection. The $\pi/2$ pulse length was 2.2 μs (5 mm solenoid coil) the pulse spacing was 60 μs, and the recycle time was 800 ms. Spectra were not folded about the Larmor frequency. The sample was enclosed in a glass dewar and the temperature was electronically regulated to within $\pm$ 0.5°C.

5.3 Results and Discussion

^{2}H NMR has proven to be one of the most effective spectroscopic techniques available for probing the highly anisotropic membrane structure (Seelig, J. and Browning, J.L., 1978; Smith, I.C.P. and Mantsch, H.H., 1982; Smith, I.C.P. et al., 1977; Seelig, J., 1977; Davis, J.H., 1983). Constraints imposed on molecular fluctuations by the liquid crystal membrane matrix lead to anisotropic motion of the lipid molecules, which is reflected in incomplete averaging of deuterium quadrupolar interactions (Seelig, J., 1977). For glycosphingolipids in membranes (as for phospholipids) motion occurs about the bilayer normal, which projects the average quadrupolar interaction along this axis. For membranes in which the bilayer normal is 90° with respect to the magnetic field direction the residual quadrupolar splitting is given by

$$\Delta\nu_Q = 3/4 \; e^2qQ/h \; S_{CD}$$

where e^2qQ/h is the quadrupolar coupling constant (170 kHz (Seelig, J., 1977)) and S_{CD} is the C-^{2}H bond order parameter (Seelig, J., 1977). For acyl chains, S_{CD} measures the time average of the angular fluctuations of the C - ^{2}H bond with respect

to the director axis resulting from molecular motion and acyl chain conformational isomerization. In the case of paramagnetic spin label anisotropic motion is reflected in a corresponding order parameter for the nitroxide radical (Hubbell, W.L. and McConnell, H.M., 1971; Seelig, J., 1970; Griffith, O.H. and Jost, P.C., 1976; Gaffney, B.J., 1976; Marsh, D., 1981). The structures of the labels used in this study are depicted in Figure 36A for the stearoyl-12-nitroxy-galactosyl ceramide and in Figure 36B for the stearoyl-d_{35}-galactosyl ceramide.

The experimental system utilized in the present study is represented in Figure 37. Gal cer, containing either spin labelled-or ^2H labelled-stearic acid, was examined at a concentration of 10 mol % in bilayers of DSPC (Fig. 37A) or DMPC (Fig. 37B). In the case of DSPC the glycosphingolipid had the same fatty acid chain length as its surrounding host matrix, while in DMPC the glycosphingolipid carried an 'extra' 4 carbons relative to its host matrix. In principle gal cer with perdeuterated fatty acid has the potential to probe its membrane arrangement at all depths. In practice most of the spectral features cannot be assigned unambiguously to individual methylene residues due to peak overlap. Nevertheless, it is well known that in fluid membranes ^2H peaks can typically be resolved for the methyl terminal carbon and for several of the methylene groups immediately proximal to it. In addition, methylene units located in the "plateau" region (C-2 to C-10) may be assigned as a unit. In the case of the spin labelled glycosphingolipid derivative the spectral probe was attached to C-12 of the glycosphingolipid fatty acid so that it monitored the motional alignment ("order") of a region 6 carbons from the methyl terminus of the fatty acid. It was hoped that this choice would minimize steric interference of the nitroxide ring system with the

Figure 36

Chemical structures of the major probe-labelled glycosphingolipids used in this work: stearoyl-12-nitroxy-galactosyl ceramide A) and stearoyl-d_{35}-galactosyl ceramide B).

A

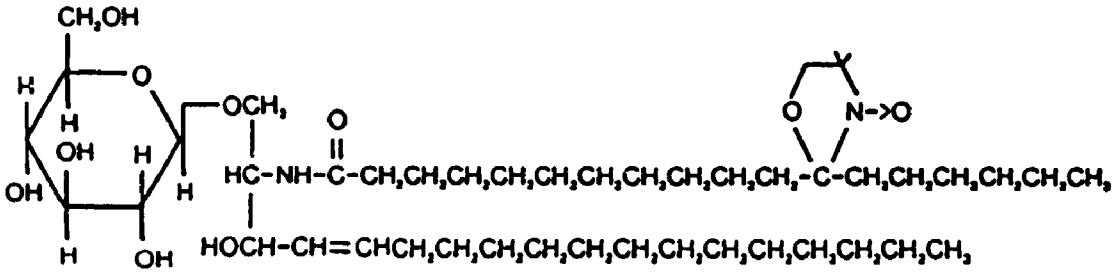

B

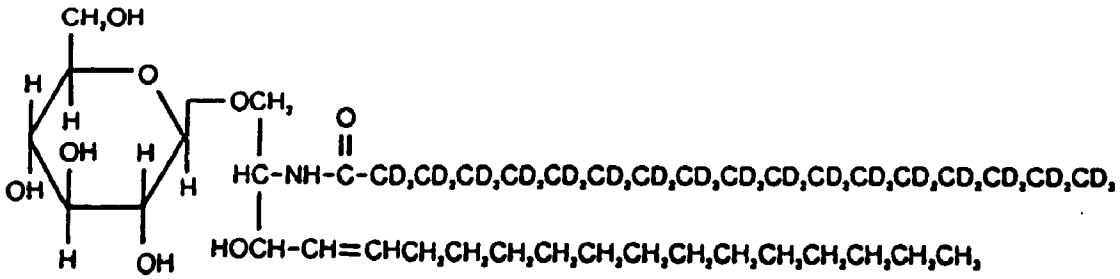

Figure 37

Possible arrangements of galactosy ceramide in fluid phosphatidylcholine bilayer membranes having A) the same chain length (DSPC), or B) 4 carbon shorter chain length (DMPC). Galactosyl ceramide is distinguished from phospholipids by a shaded hexagonal headgroup: in each case the single glycosphingolipid fatty acid is stearic acid (18 carbons). The 3 major possibilities shown for galactosyl ceramide fatty acid organization in the 14-carbon fatty acid DMPC host matrix are (1B from left to right): extended so as to interdigitate with phospholipid fatty acids of the opposing monolayer, bent at 90° into the plane defined by host matrix methyl termini, and collapsed via *trans* → *gauche* isomerization into a focus of disorder.

A

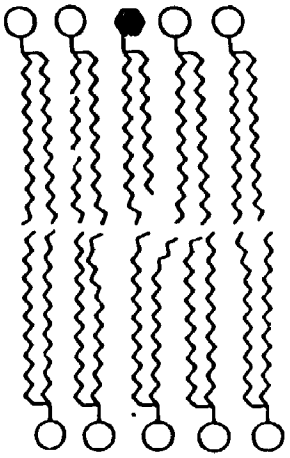

B

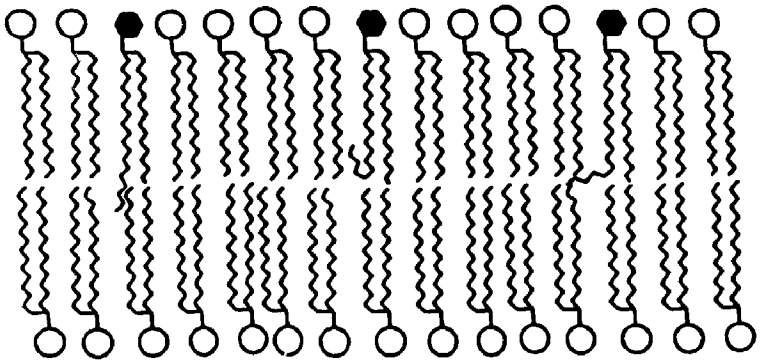

putative interdigitating fatty acid segment. In the EPR experiments, probe-labelled gal cer comprised only one-fifth of the total glycosphingolipid in the sample to avoid excessive spin exchange broadening of spectral features (Devaux, P., et al., 1973).

In examining Figure 37A (glycosphingolipid acyl chain length identical to that of the phospholipid host matrix, DSPC), one might anticipate that gal cer would behave much like surrounding phospholipids with regard to chain organization. However as illustrated diagrammatically in Figure 37B, conceptually at least, the terminal carbons of gal cer in the short chain host matrix, DMPC, have various options. Important conformational possibilities include interdigitation, collapse via *trans-gauche* isomerization into a focus of disorder, and bending into the plane of the bilayer at 90° to the rest of the chains (see Chapter 4). Another option is that the disproportionately long glycosphingolipid fatty acid might result in a tendency for the entire molecule to sit slightly higher in the membrane, leading to greater headgroup protrusion at the surface. Of course this could also occur in association with any of the other major options illustrated. While we have in the past considered protrusion from the bilayer surface to be a less likely explanation for certain aspects of glycosphingolipid fluidity gradient profiles (Sharom, F.J. et al., 1976), it has been proposed by Alving (Alving, C.R. and Richards, R.L., 1977; Alving, C.R. et al., 1980) and more recently by Esmann et al (Esmann, M., et al., 1988) and by Crook et al (Crook, S.J. et al., 1986) as a modifier of glycosphingolipid receptor function.

A separate consideration in experimental design was the difference in phase transition temperatures between short and long chain host matrices: 23° C for DMPC and 54-55° C for DSPC (Hinz, J.D. and Sturtevant, J.M., 1972; Shimshick, E.J. and

McConnell, H.M., 1973; Findlay, E.J. and Barton, P.G., 1978). The characteristic ordered-fluid phase transition of phospholipid bilayers can be readily detected from the partitioning of TEMPO ("spin label") between the aqueous and fluid lipid environments (See Fig. 38 for typical spectra). Well below the phase transition there is no partitioning into the ordered-phase lipid and the spectrum is characteristic of TEMPO alone in water (Fig. 38A). As the temperature is raised, and the lipid fluidizes, TEMPO begins to partition into the lipid phase, as is indicated by the appearance of the additional high-field peak, H, which is characteristic of TEMPO in the lipid phase. A TEMPO parameter, f, can be defined to measure the degree of partitioning:

$$f = H/H+P$$

where H and P are the heights of the lipid and aqueous peaks, and the plots of f vs T°C can be used to detect the phase transitions (Shimshick, E.J. and McConnell, H.M., 1973). To allow for this and to assure similar host matrix fluidities, spectra were compared for samples at comparable reduced temperatures (Rance, M., et al., 1980). In order to permit a direct comparison of the orientational order parameters obtained under a variety of physical conditions and in the presence of a variety of structural substituents, it is necessary to refer to some commonly coinciding states. The gel to liquid-crystalline phase transition is certainly the single greatest effector of orientational order in membrane lipids, and its effects must be accounted for. In order to minimize effects arising from differences in the thermotropic behaviour of various fatty acid structures, it is common practice to normalize the order parameters with respect to the phase transition and refer to some reduced temperature, (T_r),

such that

$$T_r = (T - T_m)/T_m$$

where T_m is the phase transition temperature and T is the temperature of measurement in degrees Kelvin (Seelig, J., and Waespe-Sarcevic, N., 1978). We have considered our experimental results in light of the various molecular possibilities described above. Spectra are illustrated in Figure 39 for the 18-carbon perdeuterated gal cer derivative at comparable reduced temperatures in the host matrix, DSPC (same chain length), and DMPC (shorter chain length). 39A is the spectrum in DSPC at 65° C. It demonstrates the well known increase in methylene group motional disorder with increasing membrane depth. Comparison with known systems permits assignment of the resolved innermost intense spectral doublet as arising from the methyl terminus (C-18) (Smith, I.C.P. and Mantsch, H.H., 1982; Seelig, J., 1977; Davis, J.H., 1983). Moving outward from this point, its neighbouring spectral features are associated with (methylene) deuterium nuclei at C-17, C-16 and C-15 respectively. Measured splittings and calculated order parameters are listed in Table 3. An estimate of $\Delta\nu_Q$ for methylene groups in the plateau region was obtained from the outermost spectral peaks, and these values are also listed. Spectra for deuterated gal cer with 18-carbon fatty acid in the 14-carbon fatty acid DMPC host matrix at 30° C are shown in Figure 39B for comparison. Assignment of the C-17 to C-15 peaks was less trivial in this case since the expectation that $\Delta\nu_Q$ should increase monotonically from methyl terminus to polar headgroup is based upon comparison with systems of homogeneous fatty acid chain length that would not permit interdigitation or its alternative possibilities. The assumption that peak assignment (i.e. relative peak

Figure 38

The characteristic ordered-fluid phase transition of the phospholipid dibehenoyl phosphatidylcholine (DBPC C-22) detected by the partitioning of the TEMPO spin probe between the aqueous and fluid lipid environment. Below the phase transition there is no partitioning of TEMPO into the ordered-phase lipid and the spectrum is characteristic of TEMPO alone in water (A). As the temperature is increased, TEMPO begins to partition into the lipid phase which gives rise to an additional high field peak defined by H (B and C) and represents TEMPO in the lipid phase. A parameter for TEMPO, f can be defined to measure the degree of partitioning, i.e. f=H/H+P. Plotting f as a function of T°C will generate the phase transition temperature plot for the phospholipid. From this plot the Tm can be calculated. The phase transition temperature (T_m) for dibehenoyl phosphatidylcholine is 74°C.

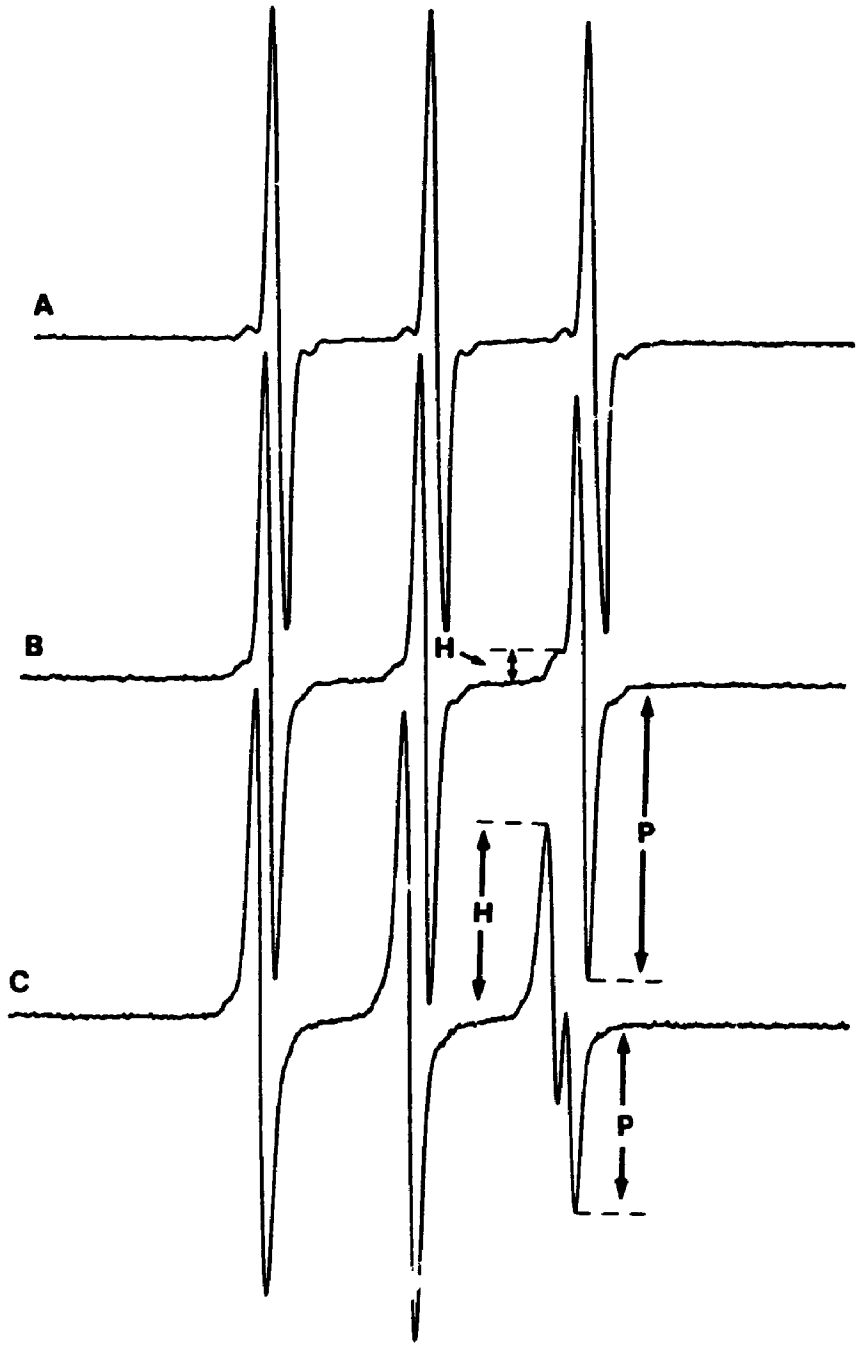
A
B
H
C
H
P
P

Figure 39

^2H NMR spectra at comparable reduced temperatures for stearoyl-d_{35}-galactosyl ceramide in fluid phospholipid bilayers of A) the same acyl chain length and B) 4 carbons shorter acyl chain length. Glycosphingolipid comprised 10 mol % of total lipid in fully hydrated multilamellar vesicles of A) distearoyl phosphatidylcholine at 65° C and B) dimyristoyl phosphatidylcholine at 30° C.

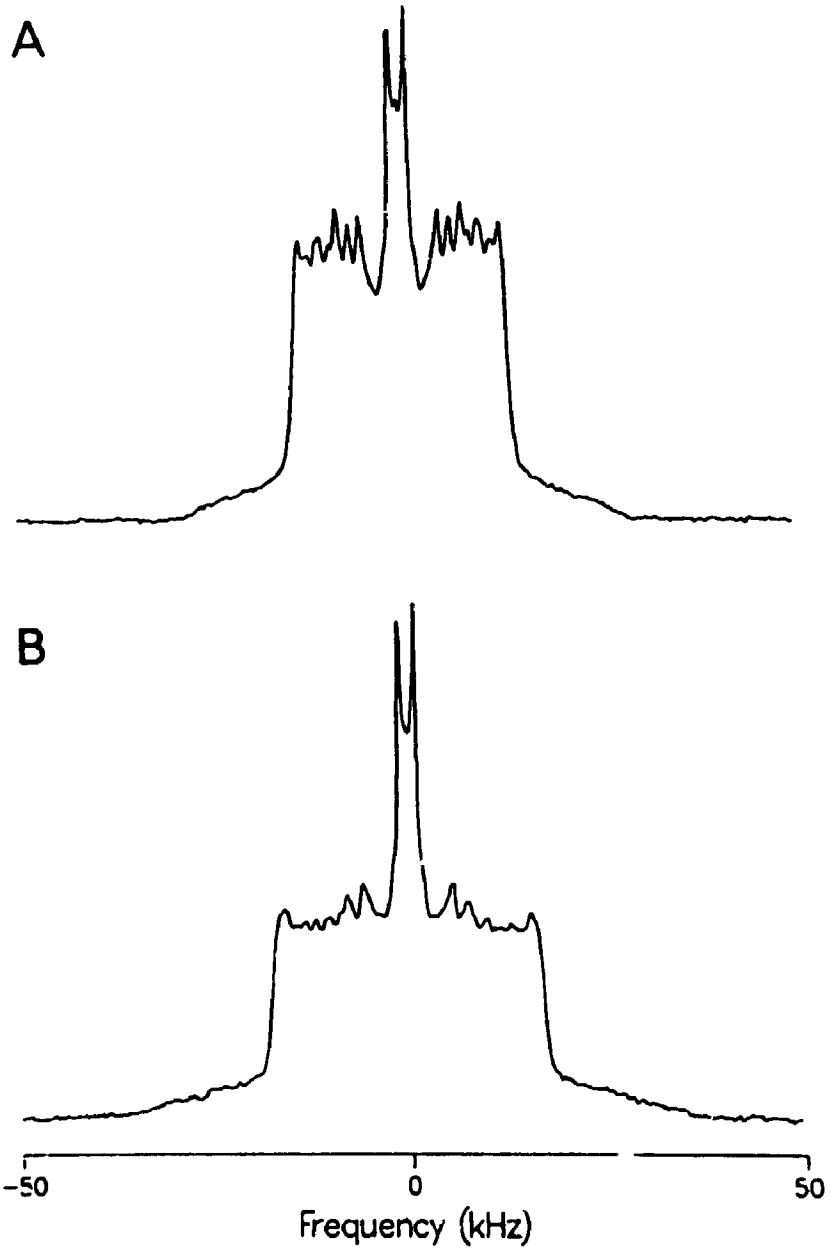
A
B
-50
0
50
Frequency (kHz)

position) remains the same in the shorter chain matrix seems reasonable based on the spectral similarities apparent for gal cer in the DSPC (39A) and DMPC (39B). However it was verified by running the ^2H NMR spectrum of gal cer with 18-carbon saturated fatty acid chain specifically dideuterated at C-17 (see Table 3). Measured values of $\Delta\nu_Q$ for gal cer in the DMPC matrix and calculated order parameters are also recorded in Table 3. At comparable reduced temperatures each assignable carbon of gal cer in the short chain host matrix showed a significantly larger quadrupole splitting (i.e., a higher order parameter) than did its corresponding carbon on the same glycosphingolipid in DSPC. This effect was most marked at methylene groups not in close proximity to the terminal methyl: thus $\Delta\nu_Q$ for the terminal (deutero)methyl group was 8 % higher in the short vs long chain matrix, 16 % higher for the C-17 - deutrons, 23 % for the C-16 - deutrons, and 28 % for C-15 and the plateau region. The basic result is reminiscent of previously published results obtained by EPR spectroscopy using glycosphingolipids with spin label at C-16 of the fatty acid chain (Grant, C.W.M. et al., 1987b; Mehlhorn, I.E., et al., 1988). In earlier spin label experiments glycosphingolipid fatty acids that were longer than those of their host phospholipid bilayer matrix were found to exhibit higher order at C_{16} than did glycosphingolipid fatty acids having similar length to those of their host membrane. This was felt to be consistent with interdigitation of the extra long fatty acid (Grant, C.W.M. et al., 1987b; Mehlhorn, I.E., et al., 1988). Similarly the present results could be explained readily by assuming that the 18-carbon gal cer fatty acid remains aligned with the 14-carbon fatty acids of fluid phase DMPC and is thus 'tethered' by interdigitation of its methyl terminus.

TABLE 3

^2H NMR order parameter data corresponding to Figure 39 for stearoyl-d_{35}-galactosyl ceramide in fluid phospholipid bilayers of the same fatty acid chain length (DSPC) and shorter fatty acid chain length (DMPC). Glycosphingolipid concentration was 10 mol % of membrane lipid. $\Delta\upsilon_Q$ refers to the measured spectral quadrupolar splitting. S_{CD} is the calculated order parameter. "Carbon Number" refers to location of spectral probe on the glycosphingolipid fatty acid chain (carboxyl carbon as 1); the plateau region covers C-2 - C-10. Samples were run at comparable reduced temperatures: 65° C for the DSPC host matrix vs 30° C for DMPC. A sample specifically dideuterated at C-17 was used to verify peak assignment. Errors in measurement of $\Delta\upsilon_Q$ were on the order of $\pm$ 0.5 kHz, giving rise to errors in the calculated S_{CD} for methylene positions ranging from 1.4 - 4 %.

TABLE 3

	gal cer/DMPC/30°C		gal cer/DSPC/65°C	
Carbon Number	$\Delta\upsilon_Q$(kHz)	S_{CD}	$\Delta\upsilon_Q$(kHz)	S_{CD}
C-18	2.8	.022	2.6	.020
C-17	12.3 (11.7*)	.096 (.092*)	10.7	.08
C-16	16.7	.13	13.6	.11
C-15	21.3	.17	16.6	.13
Plateau Region	34.8	.27	27.3	.21

* Values found for gal cer specifically dideuterated at C-17.

Order parameter profiles estimated from the ^2H NMR data (Fig. 40) are qualitatively very similar for the two lipid systems: there is no break or deviation such as might be expected if the 18-carbon glycosphingolipid acyl chain assumed a very different conformation in the region of its contact with the midpoint of the 14-carbon phospholipid acyl chain host matrix. Interestingly, order parameters for methylene groups near the polar headgroup (ones represented in the spectral plateau region and plotted on the upper portions of the curves in Fig. 40) are particularly affected in the short chain matrix. Even when warmed 42° C above host matrix T_m (i.e. at 65° C) S_{CD} for the plateau region of gal cer in DMPC was .20 (spectrum not shown) which is similar to the value of .21 seen for the same glycosphingolipid only 10° C above host matrix T_m in DSPC at 65° C. A possible effect of interdigitation would be to reduce fluctuations of the lipid molecule as a whole, leading to a uniform increase in the entire S_{CD} profile. Inspection of Figure 40 and Table 3 however reveals that, as already noted, the effect was least dramatic at the (deutero)methyl terminus. This might be rationalized as follows. Although interdigitation might be expected to 'tether' the whole chain, thus reducing molecular fluctuation, it might be expected to lead to some degree of local disruption (disordering of chain packing at the point of interdigitation).

Although cell membranes are generally considered to be of intermediate fluidity, we have examined the same system in the gel state. The gel phase spectra of [$^2H_{35}$] gal cer in DMPC and DSPC proved to be significantly different from one another at comparable reduced temperatures (Fig. 41). Unfortunately interpretation of these spectra is complicated because line shape is particularly sensitive to both

Figure 40

Order parameter profiles derived from the ^2H NMR spectra shown in Figure 39 for stearoyl-d_{35}-galactosyl ceramide in a fluid phospholipid matrix of the same chain length (18-carbon DSPC) (▲); and shorter chain length (14-carbon DMPC) (●). Samples were compared at similar reduced temperatures (65°C for DSPC and 30°C for DMPC). Error bars, where absent, are smaller than the symbols. Error boxes indicated for the plateau region approximate the actual spread of $\Delta\upsilon_Q$ values of C-2 - C-10.

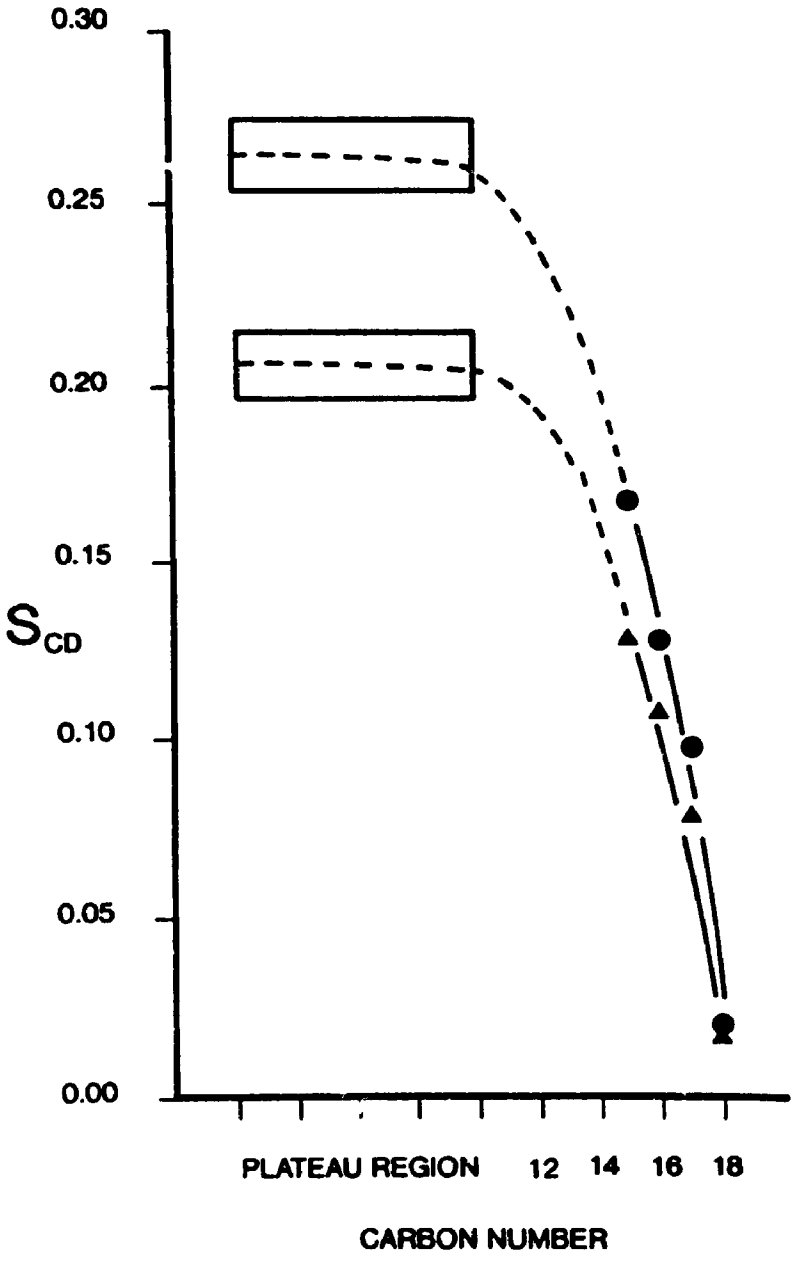
0.30
0.25
0.20
0.15
S_{CD}
0.10
0.05
0.00
PLATEAU REGION
12
14
16
18
CARBON NUMBER

Figure 41

^2H NMR spectra at comparable reduced temperatures for stearoyl-d_{35}-galactosyl ceramide in gel phase phospholipid bilayers of A), C) the same acyl chain length and B), D) 4 carbons shorter acyl chain length. Glycosphingolipid comprised 10 mol % of total lipid in fully hydrated multilamellar vesicles of distearoyl phosphatidylcholine at 52° C and 45° C (A and C respectively), and dimyristoyl phosphatidylcholine at 19° C and 8.5° C (B and D respectively).

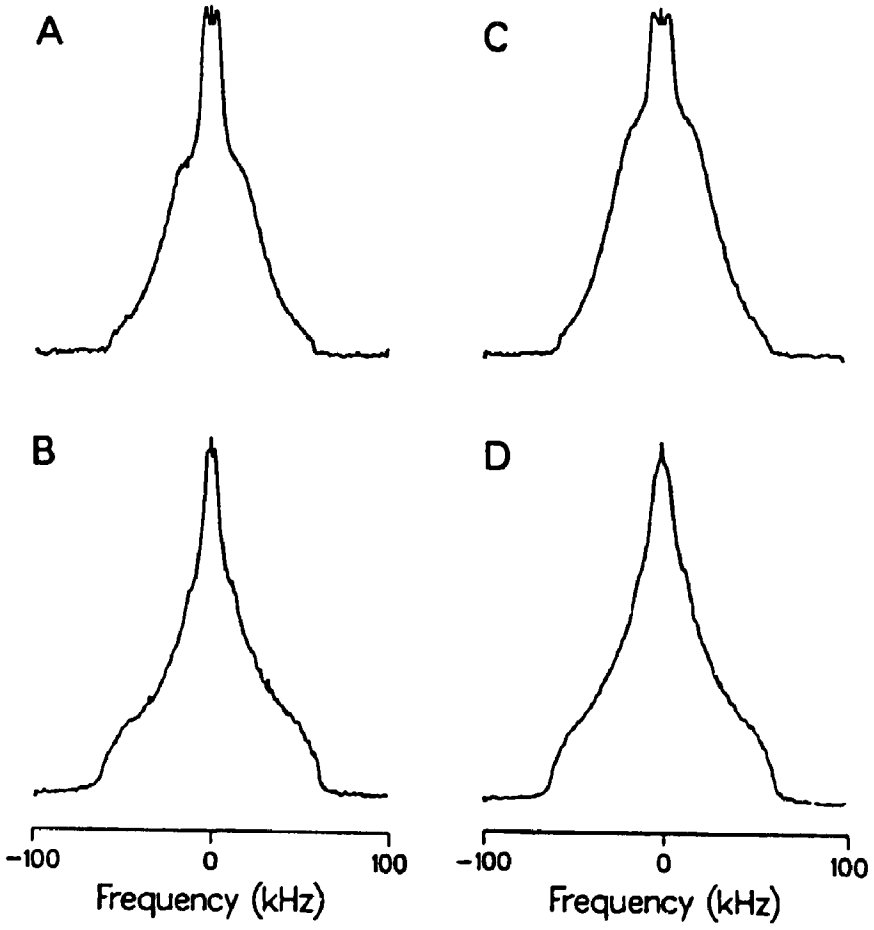
A
C
B
D
-100
0
100
Frequency (kHz)
-100
0
100
Frequency (kHz)

ordering and dynamic effects in the gel phase; and dynamics may differ at similar reduced temperatures. Nevertheless several observations may be made. The spectra differ in two regards: i) in the intensity at $\pm$ 63 kHz, and ii) in the central region where methyl group contributions dominate. The use of orientational order parameters to describe the mean orientation of flexible molecules can be much more involved. Different segments (methylene groups) will have different mean orientations and may undergo different degrees of reorientation depending upon their position in the molecule. Using isotopic labelling it may be possible to measure the complete order parameter tensor for each rigid part of a flexible molecule, for example by measuring the ^1H-^1H dipolar splittings and the ^2H quadrupolar splittings for a methylene group (Higgs, T.P. and MacKay, A.L., 1977). When trying to use these measurements to determine the details of the molecular motion it is necessary to distinguish between molecular reorientation and conformational changes. How successfully these motions can be separated in the analysis depends on their relative timescales and on whether, for example, a conformational change leads to a significant reorientation of the molecule as a whole (Burnell, E.E. and deLange, C.A., 1980). In liquid crystals with long aliphatic chains the interaction between these two classes of motion seems to play a significant role. Thus, for example, when soap molecules are in their all-trans conformation and are simply reorienting about their long axis, which for this conformation is perpendicular to the C-^2H band vectors, the equation to calculate the residual quadrupolar splitting predicts a quadrupolar splitting of 63 KHz. The ^2H NMR spectrum of gal cer in DSPC at 45°C (Fig. 41C) bears a striking resemblance to that of [$^2H_{62}$] DPPC at 20°C (Davis, J.H., 1979). It is

very broad, indicating a distribution of quadrupolar splittings, and suggesting that most of the glycosphingolipid molecules are still rotating rapidly about their long axes on the NMR timescale (Davis, J.H., 1979). For [$^2H_{35}$] gal cer in the shorter chain host matrix, DMPC, there is an increase in intensity at $\pm$ 63 kHz (Fig. 41B,D). Since 126 kHz is the maximum possible splitting for a deuterated methylene group, an increase in intensity at $\pm$ 63 kHz suggests a decrease in rotation rate about the gal cer long axis. Thus for the DMPC matrix in the gel phase, glycosphingolipid molecular motion was reduced relative to that in DSPC - perhaps reflecting a consequence of interdigitation. Note however that the slight reduction in spectral splitting in the central region in the rigid DMPC matrix suggests that the terminal methyl group of gal cer is more disordered than it is in the 18-carbon fatty acid DSPC host matrix. Thus the gel phase results, although considerably more difficult to interpret, is also consistent with a model in which interdigitation may occur, leading to disruption of chain packing near the acyl chain terminus.

In previous spin label studies (Grant, C.W.M., et al., 1987b; Mehlhorn, I.E. et al., 1988) the host phospholipid chain length was kept constant while the acyl chain length of the glycosphingolipids was varied (either C-18 or C-24). In the present study the opposite approach was taken: EPR spectra of gal cer having 18-carbon spin labelled fatty acid were compared in DMPC vs DSPC (Fig. 42). The order parameter, S, for the carbon to which the spin label ring is attached (C-12 in this case) was calculated from the inner and outer peak separations as described previously (see Chapter 4) (Seelig, J., 1970; Griffith, O.H. and Jost, P.C., 1976; Gaffney, B.J., 1976; Marsh, D., 1981). Table 4 lists measured spectral values and derived spin label order

Figure 42

EPR spectra of spin labelled galactosyl ceramide in fluid phospholipid membranes similar to those in Figure 33. Stearoyl-12-nitroxy-galactosyl ceramide comprised 2 mol % of the membrane lipid while unlabelled stearoyl-galactosyl ceramide comprised 8 mol %, with phospholipid making up the remainder. A) distearoyl phosphatidylcholine host matrix (same chain length) at 65° C, B) dimyristoyl phosphatidylcholine (4-carbon shorter chain length) at 30° C. Spectral features used to calculate order parameters are illustrated.

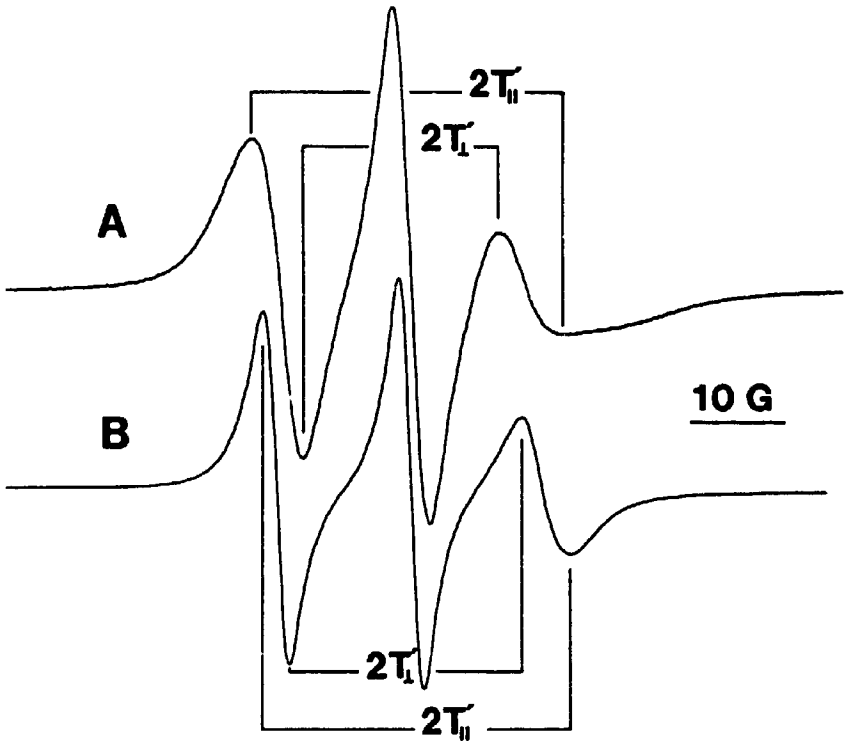
2T∥
2T⊥
A
B
10 G
2T⊥
2T∥

TABLE 4

Spin label EPR order parameter data for stearoyl-12-nitroxy-galactosyl ceramide in phospholipid bilayers of the same fatty acid chain length (DSPC) and shorter chain length (DMPC). Glycosphingolipid concentration was 10 mol % (2 mol % spin labelled) of the membrane lipid. "Host Matrix" refers to the phosphatidylcholine component. $T_{\parallel}'$ is half the measured outer spectral splitting (as illustrated in Figure 42) and accurately reflects the matrix element, $T_{\parallel}$. $T_{\perp}'$ is half the measured inner spectral splitting, and $T_{\perp}$ is a corrected value that more accurately approximates the true matrix element. The error involved in estimating the centres of outer and inner spectral peaks ranged from 0.1 gauss to 0.3 gauss, giving rise to a standard error of some $\pm$ .02 - $\pm$ .04 in calculated order parameter.

TABLE 4

HOST MATRIX	TEMPERATURE (° C)	$T_{\parallel}'(\simeq T_{\parallel})$ (gauss)	$T_{\perp}'$ (gauss)	$T_{\perp}$ (gauss)	S(± .02 - .04)
DMPC	9	29.1	8.9	9.2	.68
DMPC	19	27.4	8.8	9.3	.64
DMPC	30	16.5	10.5	11.6	.20
DMPC	65	16.2	12.5	13.7	.10
DSPC	45	18.0	9.7	10.7	.30
DSPC	52	17.3	11.0	12.0	.21
DSPC	65	16.4	12.2	13.4	.11

parameters at various temperatures. It should be borne in mind however that at temperatures below T_m of the host matrix it is not clear that the order parameter is meaningful since motional rates are severely restricted.

EPR- and NMR-derived order parameters cannot be quantitatively compared since the techniques are sensitive to very different motional timescales (Meirovitch, E. and Freed, J.H., 1984). The overall observation via EPR is, however, the same as that via NMR: at equivalent reduced temperatures order at a given glycosphingolipid fatty acid carbon is markedly higher in a situation that would permit interdigitation. Thus the value of S for C-12 in DMPC at 30° C was .20 while that for C-12 in DSPC at a comparable reduced temperature (65° C) was .11. Note that even at 65° C the value of S in DMPC was .10 which is very close to the DSPC value at the same temperature, and that in the gel phase the value calculated for S (although not a true motional reflection in these cases) was consistent with much greater immobility in the short chain matrix. We did not investigate the possibility that the gel phase systems may well be expected to exhibit metastability with regard to interdigitation (Mattai, J., et al., 1987; Levin, I.W. et al., 1985; Boggs, J.M. et al., 1988).

5.4 Conclusions

The present study demonstrates that it is possible to follow deuterated glycosphingolipids by ^2H NMR at concentrations in the membrane that mimic those found naturally. Of the various possible models for organization of the neutral glycosphingolipid, gal cer, within a fluid membrane, the ^2H NMR results are clearly consistent with partial acyl chain interdigitation when the glycosphingolipid fatty acid

chain is longer than those of its surrounding phospholipids. In such systems acyl chain motions are more restricted than when phospholipid and glycosphingolipid chain lengths are the same. This effect appeared to be transmitted all the way up to the carboxyl portion of the chain, which would be consistent with interdigitation. The ^{2}H NMR results are consistent with spin label results on the same system, and with previous conclusions drawn from studies of four glycosphingolipids having 18-carbon vs 24-carbon spin labelled fatty acids (Grant, C.W.M. et al., 1987b; Mehlhorn, I.E. et al., 1988). The present results suggest that if interdigitation is occurring, the 'extra' segment of glycosphingolipid fatty acid may lead to some disruption of local acyl chain packing in the opposing monolayer. Although our data have been interpreted to favour interdigitation, they do not rule out the possibility of coexistent protrusion of a long-chain glycosphingolipid from the membrane surface. On the other hand, if the glycosphingolipid is indeed tethered by interdigitation, an alternative explanation of the improved receptor function sometimes seen for long chain simple glycosphingolipids (Alving, C.R. and Richards, R.L., 1977; Alving, C.R. et al., 1980; Crook, S.J. et al., 1986; Mehlhorn, I.E. et al, 1988) may be advanced: that the effect may result from altered headgroup dynamics and orientation.

CHAPTER 6. EFFECTS OF FATTY ACID ALPHA-HYDROXYLATION ON A GLYCOSPHINGOLIPID IN PHOSPHATIDYLCHOLINE BILAYERS

6.1 Introduction

Subtle details of GSL physical behaviour and arrangement in membranes have been demonstrated to be involved with both their structural and receptor roles (Curatolo, W., 1987a; Curatolo, W., 1987b; Thompson, T.E. and Tillack, T.W., 1985; Grant, C.W.M., 1987). Moreover glycosphingolipids have features that set them distinctly apart from phospholipids and have the potential to influence their physical behaviour and arrangement: donor H-bonding groups in the carbohydrate headgroup and sphingosine backbone, a disproportionately long (single) fatty acid, and often α-hydroxylation of the fatty acid. This chapter deals with the latter feature, which has been the subject of considerable speculation with regard to its possible influence on glycosphingolipids in cell membranes.

Ki et al noted that nerve conduction velocity in Caudata species having no α-hydroxy fatty acids in their myelin cerebrosides was significantly reduced (Ki, P.F. et al., 1982). Gahmburg and Hakomori have suggested that α-hydroxylation of the fatty acid could potentially affect the phenotypic expression (i.e. receptor function) of a given glycosphingolipid to control its crypticity (Kannagi, R., et al., 1982; Lampio, A., et al., 1986). The basis of effects such as these and other phenomena associated with α-hydroxylation are unknown. However Bunow and Levin have pointed out that pure α-hydroxy galactosyl ceramide from beef brain forms a more disordered gel phase

than does the pure non-hydroxy fraction, and suggest that this may be due to a spatially perturbing effect of the α-hydroxyl group (Bunow, M.R. and Levin, I.W. 1980). Reduction of both the transition temperature and enthalpy of the gel-to-liquid crystalline phase transition of pure gal cer by the presence of an α-hydroxyl group (Curatolo, W. and Jungalwala, F.B., 1985; Maggio, B., et al., 1985) has been related to its causing disruption of the tight acyl chain packing characteristic of a gel phase (Curatolo, W. and Jungalwala, F.B., 1985). The presence of the α-hydroxyl group was also observed to raise the kinetic energy barrier to reaching a stable gel state (Curatolo, W. and Jungalwala, F.B., 1985). Boggs et al have examined pure sulfated gal cer (cerebroside sulfate), and noted that, in this system also, hydroxylation of the fatty acid inhibited certain organizational changes necessary to give rise to the most stable, ordered phase (Boggs, J.M., et al., 1988). Interestingly they recorded a higher phase transition temperature and enthalpy for the gel-to-liquid crystalline transition of the α-hydroxylated material than the non-hydroxylated. However in this case there was the added influence of repulsive effects from the charged sulfate group; and the authors suggested that the α-hydroxyl function might contribute to a hydrogen-bonding network, overcoming this repulsion. Johnston and Chapman found DSC evidence of greater miscibility of α-hydroxy cerebrosides with phospholipids and considered this to be the result of reduced glycosphingolipid-glycosphingolipid attractive forces when dispersed in a phospholipid/membrane (Johnston, D.S. and Chapman, D., 1988).

In this chapter we have addressed by ^{2}H NMR the effect of fatty acid hydroxylation on glycosphingolipid arrangement, at low concentration in a

phospholipid bilayer membrane. A pair of probe-labelled galactosyl ceramides was synthesized for this purpose, having perdeuterated 18-carbon fatty acids that were identical but for the presence in one case of a hydroxyl group at the α-position. These were assembled into lipid bilayers composed of the (shorter) 14-carbon fatty acid phosphatidylcholine, DMPC, since in general glycosphingolipids have longer fatty acids than do their accompanying membrane phospholipids. The orientational ordering of the glycosphingolipid stearic acid residue and its corresponding hydroxy analogue were compared in liquid crystalline and gel state bilayers. The presence of the spectroscopic probe on gal cer itself made it possible to focus selectively on phenomena related to the glycosphingolipid even at the low concentrations reflective of natural membranes.

6.2 Materials and Methods

6.2.1 Source of Materials

Same as in section 5.2.1.

6.2.2 Synthesis of Probe Labelled Glycosphingolipids

Same as in section 5.2.2.

6.2.3 Synthesis of α-Hydroxy-Stearoyl-d_{34} Acid

Preparation of α-hydroxy perdeuterated stearic acid was via an α-bromo intermediate. The α-bromo intermediate was generated by subjecting octadecanoic-d_{35} acid (MSD Isotopes Ltd) to the Hell-Volhard-Zelinsky reaction (Hickinbottom, W.J.,

1948). Briefly, to 1 g of the fatty acid and 50 mg of red phosphorus, in a 25 ml round bottom flask, 500 µl of bromine was added at 62 µl/hr over 8 hr with gentle warming. The reaction mixture was heated to 45°C overnight. After aspiration of excess bromine and hydrolysis with 25 ml H_2O, the solid residue was filtered off, washed with water and extracted into 30 ml of ether. Conversion to the α-hydroxy derivative (Sweet, R.S. and Ester, F.L., 1956) involved refluxing this α-bromo derivative for 96 hours with 1.2 g of KOH (21 mmol) in 6.25 ml of 95% ethanol. Ethanol was removed and the dry residue dissolved by heating to 80°C with 20 ml H_2O. This was acidified with H_2SO_4, cooled to room temperature, and extracted with 30 ml diethyl ether. The ether residue was chromatographed on a column of silicic acid eluted with 1% CH_3OH in $CHCl_3$. The yield was 33% based on octadecanoic-d_{35} acid (perdeutero-stearic acid) starting material. R_F was 0.22 on Merck silica gel 60 plates eluted with hexane/diethyl ether/formic acid (70/30/1). Product was identified by ^2H NMR in $CHCl_3$ and via CI mass spectroscopy (molecular ion M/e peak 334). Gal cer bearing perdeutero-stearic acid co-chromatographed with the faster-running spot of natural gal cer from beef brain (the non-hydroxy fraction), while gal cer bearing perdeutero α-hydroxy stearic acid co-chromatographed with the slower spot of natural gal cer (the hydroxy fraction) using the TLC system described above. Both were stable to overnight treatment with aqueous KOH at 5 mg/ml - conditions which rapidly cleave ester bonds.

6.2.4 Liposome Preparation

Same as in section 5.2.3.

6.2.5 ^{2}H NMR Spectroscopy

Same as in section 5.2.5, except with the following addition; The 90° oriented sample ("depaked") spectra were calculated from the powder spectra.

6.2.6 ^{31}P NMR Spectroscopy

^{31}P NMR spectra were acquired at 121.5 MHz on a Bruker MSL-300 spectrometer. The spectra were recorded using a Hahn echo pulse sequence (Rance, M. and Byrd, R.A., 1983) with Waltz decoupling (gated on during acquisition). The $\pi/2$ pulse length was 4.0 μs (10 mm solenoid coil), the pulse spacing was 60 μs, and the recycle time was 7.5 s. Molecular modeling of glycosphingolipids was performed on an AST Premium 386 computer using PCMODEL version 3.0 (employing default parameters) from Serena Software, Bloomington, IN.

6.3 Results and Discussion

Temperature-dependent ^{2}H NMR spectra of gal cer at 10 mol % in DMPC liposomes are shown in Figure 43. The left column represents gal cer with perdeuterated stearic acid and the right column the α-hydroxy derivative. Initially we will focus our attention on the 30°C spectra, at which temperature the glycosphingolipid molecules are clearly in a liquid crystalline environment. The observation of liquid crystalline spectra at temperatures well below the known phase transition temperatures of the glycosphingolipid (70 and 83°C for α-hydroxy- and non-hydroxy-gal cer, respectively) (Curatolo, W. and Jungalwala, F.B., 1985; Johnston, D.S. and Chapman, D., 1988) argues that the labelled gal cer was dispersed in the

Figure 43

^2H NMR spectra of stearoyl-d_{35}-galactosyl ceramide (left column) and the corresponding α-hydroxy-stearoyl-d_{34}-galactosyl ceramide (right column) in unsonicated bilayers of dimyristoyl phosphatidylcholine. In each case the glycosphingolipid comprised 10 mol % of the membrane lipid. Spectra are shown for temperatures above the main transition temperature of 23°C A), below the main transition temperature B) and below the pre-transition temperature of 15°C in C).

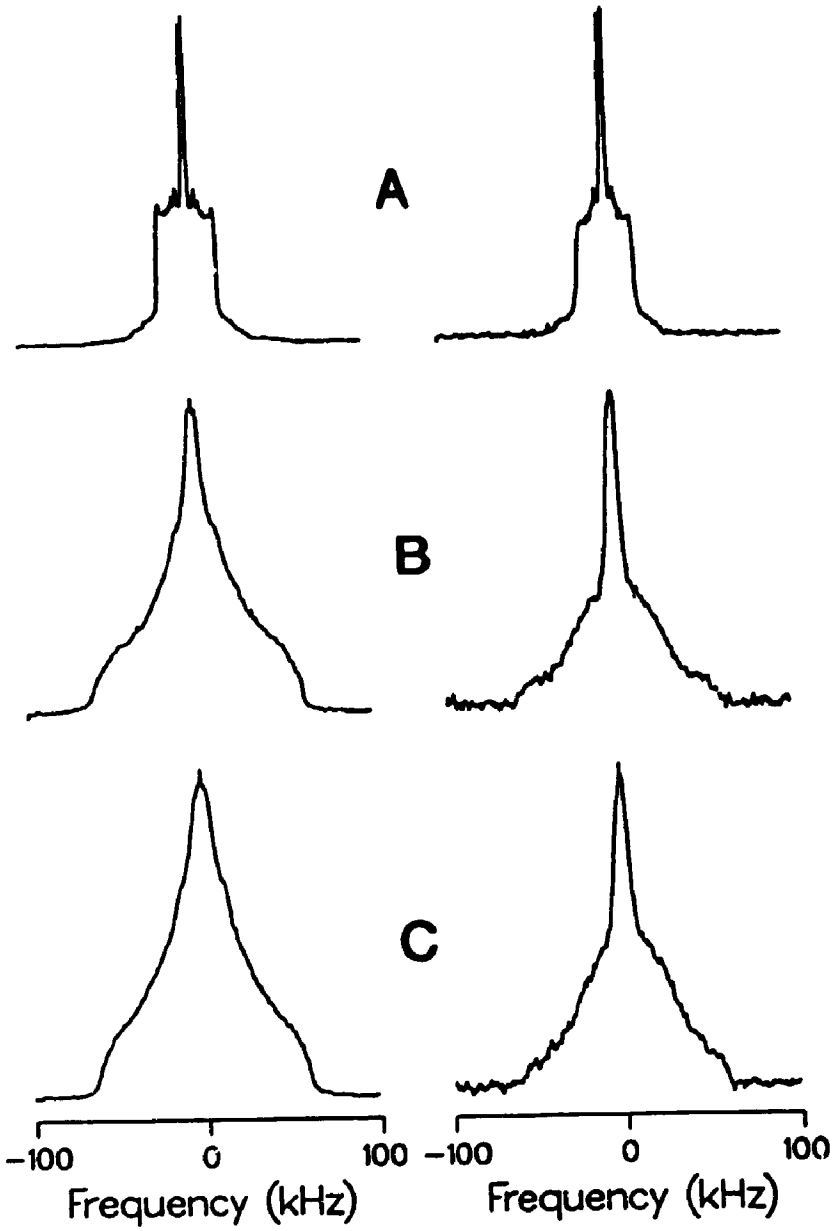
A
B
C
-100
0
100
Frequency (kHz)
-100
0
100
Frequency (kHz)

host matrix. ^{31}P NMR spectra of these samples at the same temperature (not shown) display the characteristic axially symmetric liquid crystalline lineshape with a $\Delta\delta$ value of approx. 40 ppm (Seelig, J., 1978). The ^{2}H spectrum for the non-hydroxy gal cer in DMPC (top left) is typical of that seen for labelled phospholipids (Davis, J.H., 1983); note that the characteristic plateau in order parameter as a function of chain position is clearly observed in the powder spectrum, and (more clearly) in the calculated 90°-oriented sample (depaked) spectrum (Fig. 44 bottom). Based on the quadrupolar splittings observed for the $C^{2}H_2$ units in the "plateau region" (app. 34 kHz), a value for S_{CD} of 0.27 is calculated, which is slightly higher than that obtained for DPPC (Davis, J.H., 1979) or DMPC (Oldfield, E., et al., 1978) in the liquid crystalline phase (app. 0.22-0.25). Such results (see Table 5 and Fig. 45) are in accord with those of Skarjune and Oldfield (Oldfield, E., et al., 1978) who concluded that the hydrocarbon chain organization of pure N-palmitoyl galactosyl ceramide at 90°C is basically similar to that of pure DMPC at the same reduced temperature. They also reflect Sharom's previous observation of higher order parameters for glycosphingolipid fatty acids than phospholipid fatty acids in a given phospholipid host matrix (Sharom, F.J. et al., 1976).

The spectrum of α-hydroxy gal cer at 30°C (Fig. 43 top right) reveals distinct differences from the corresponding non-hydroxy analogue at the same temperature. Inspection of the spectrum reveals a decrease in intensity in the "plateau region" and a loss of resolution of the splittings near the central methyl peaks. The depaked spectrum (Fig. 44 top) reveals a slight reduction in $\Delta\nu_Q$ for peaks attributable to a "plateau region" to app. 32 kHz, corresponding to a value of 0.25 for S_{CD}. Similar

Figure 44

Depaked ^2H NMR spectra obtained at 30°C for the α-hydroxy-stearoyl-d_{34}-galactosyl ceramide in DMPC A) and for stearoyl-d_{35}-galactosyl ceramide in DMPC B).

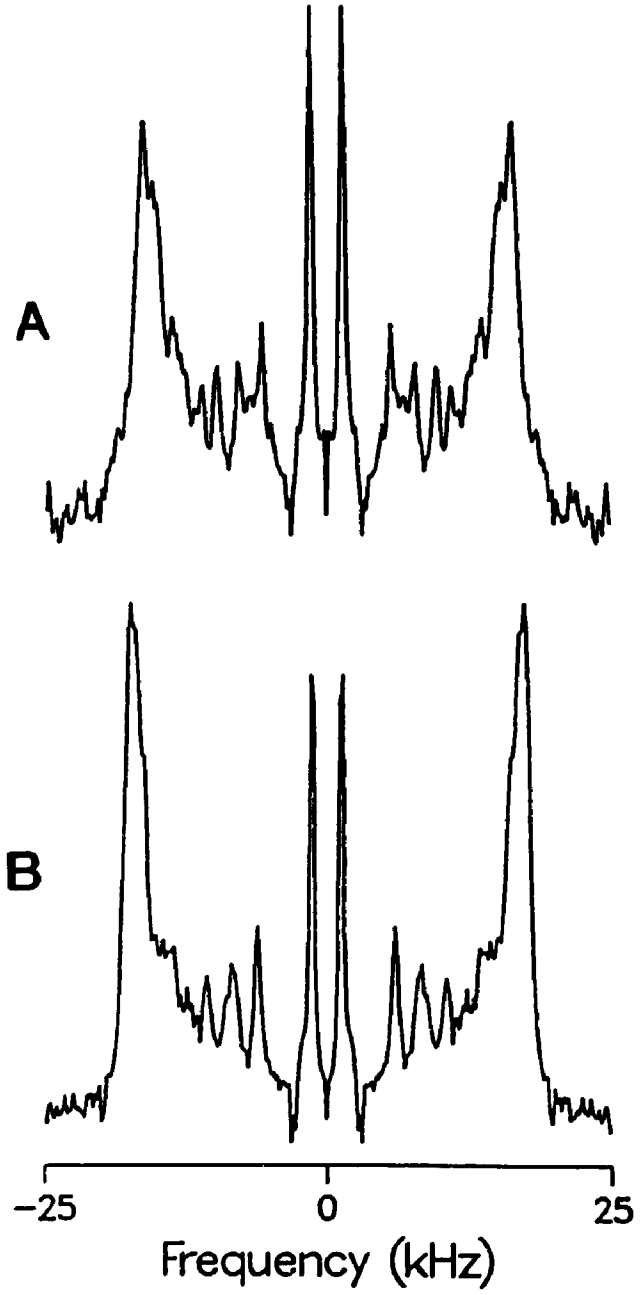
A
B
−25
0
25
Frequency (kHz)

TABLE 5

^2H NMR order parameter data corresponding to Figure 43 for stearoyl-d_{35}-galactosyl ceramide and α-hydroxy-stearoyl-d_{34}-galactosyl ceramide in fluid phospholipid bilayers of dimyristoyl phosphatidylcholine at 30°C. The glycosphingolipid concentration was 10 mol % of membrane lipid. $\Delta\upsilon_Q$ refers to the measured spectral quadrupolar splittings, S_{CD} is the calculated order parameter. "Carbon Number" refers to the location of the spectral probe on the glycosphingolipid fatty acid chain. The plateau region covers C-2 - C-10. A sample specifically dideuterated at C-17 was used to check peak assignment.

TABLE 5

Carbon Number	α-hydroxy-gal cer		gal cer	
	$\Delta\upsilon_Q$ (kHz)*	S_{CD}	$\Delta\upsilon_Q$ (kHz)	S_{CD}
C-18	3.3	0.029	2.8	0.022
C-17	11.5	0.090	12.5	0.098
C-16	15.8	0.124	16.8	0.132
C-15	19.5	0.153	21.3	0.167
Plateau Region	32.8	0.257	34.8	0.273

* Values obtained from depaked spectra

reductions are observed in the three resolved peaks which represent C^2H_2 units near the end of the chain. The ratio of the quadrupolar splittings of non-hydroxy to α-hydroxy gal cer for the plateau and interior methylene group resonances show little variation (1.078 ± 0.015), which implies a relatively uniform reduction in molecular order throughout the length of the α-hydroxy fatty acyl chain (see Fig. 45). Interestingly, the opposite is observed for the terminal methyl splittings, which are slightly greater for the α-hydroxy gal cer (3.2 kHz compared to 2.8 kHz for the non-hydroxy gal cer splittings measured from the powder spectra). A reduction in $\Delta\nu_Q$ for the C^2H_2 groups is supported by first moment (M_1) analysis. The first moments of the powder spectra are directly proportional to the mean quadrupolar splitting of the perdeuterated chain (Davis, J.H., 1983). M_1 values of 7.63×10^4 and 6.06×10^4 were obtained for the non-hydroxy and α-hydroxy gal cer at 30°C, respectively, demonstrating a reduced mean $\Delta\nu_Q$ (and therefore mean S_{CD}) of the latter lipid. As well, the parameter Δ_2, which is proportional to the width of the distribution of quadrupolar splittings (Davis, J.H., 1979), is slightly smaller for the α-hydroxy gal cer.

We now turn our attention to the gel phase spectra of gal cer in DMPC (Fig. 43). Spectra were acquired at 8.5°C (below the 15°C DMPC pretransition) and 19°C (between the DMPC pretransition and the 23°C gel-to-liquid crystalline transition). The spectra of non-hydroxy gal cer (left column, center and bottom) are very broad with substantial intensity in the region of ± 63 kHz, indicating that some of the glycosphingolipid molecules are no longer rotating rapidly about their long molecular axes (Davis, J.H., 1979). The gel phase spectra of α-hydroxy gal cer (right center and bottom) differ. The shoulders reach baseline at ± 61 kHz, suggesting that if the axial

Figure 45

Order parameter profiles for the deuterated fatty acid of the α-hydroxy-stearoyl-d_{34}-galactosyl ceramide (●) and stearoyl-d_{35}-galactosyl ceramide (▲) in multilamellar dispersions of DMPC at 30°C. In each case the deuterated glycosphingolipid comprised 10 mol % of the lipid.

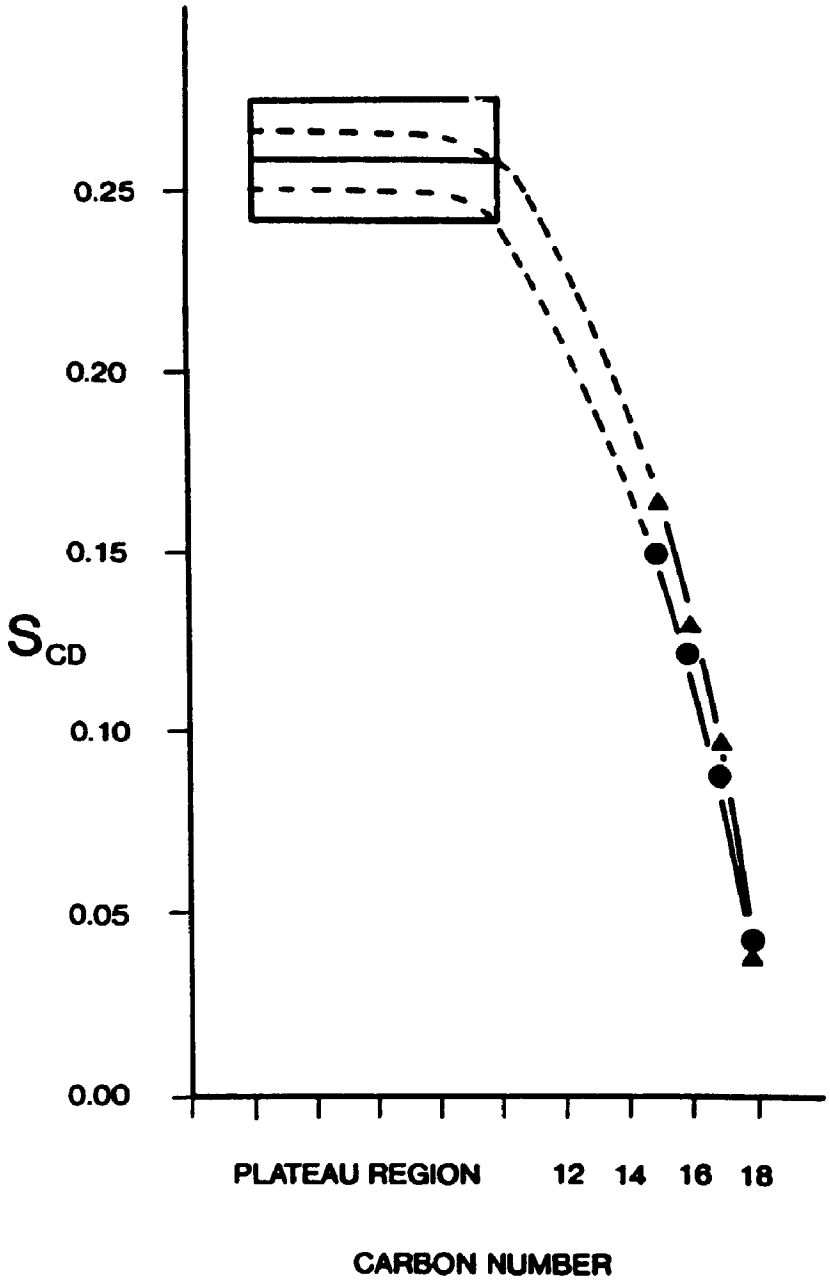
0.25
0.20
0.15
S_{CD}
0.10
0.05
0.00
PLATEAU REGION
12
14
16
18
CARBON NUMBER

rate is as slow as for the non-hydroxy analogue there is a slight increase in gauche population which is supported by the liquid crystalline phase results. As well, there is a sizeable increase of spectral intensity in the center of the spectrum, which may indicate increased chain motion or disordering. M_1 values of 1.21×10^5 and 1.07×10^5 were obtained for the α-hydroxy gal cer at 8.6 and 19°C, respectively, compared to 1.42×10^5 obtained for the non-hydroxy gal cer at both temperatures. These reduced M_1 values indicate a reduction in the mean quadrupolar splitting of the α-hydroxy gal cer. However, Δ_2 is increased for the α-hydroxy gal cer, implying a broader distribution of splittings. This could be obtained if the central region of the chain were relatively more disordered than the plateau region (Davis, J.H., 1979).

The question of lateral distribution of glycosphingolipids in bilayer membranes is one that has engendered considerable discussion (Curatolo, W., 1987a; Curatolo, W., 1987b; Thompson, T.E. and Tillack, T.W., 1985; Grant, C.W.M., 1987). It is complicated by the fact that, when the glycosphingolipid concentration exceeds some 20% of the bilayer, separation of a non-liposomal glycosphingolipid rich phase can occur in some cases. At the concentrations utilized here it is expected that gal cer will be dispersed in the liquid crystalline DMPC matrix, but perhaps will be somewhat phase separated in the gel phase (Skarjune, R. and Oldfield, E., 1982; Ruocco, M.J. et al., 1983; Mehlhorn, I.E. et al., 1989). The above spectral findings indicate that insertion of a hydroxyl group at the α-position of the gal cer fatty acid results in some reduction of glycosphingolipid molecular order in a fluid phospholipid membrane. In the gel phase the result is an increase in motion and/or decrease in order. A reasonable explanation of these observations would seem to be that fatty acyl chains

carrying the bulkier and more polar α-hydroxy group have greater area requirements in the membrane. This could reduce the ability of the α-hydroxy gal cer to pack as tightly into the lipid matrix as its non-hydroxy analogue, thereby leading to a decrease in chain order. Such an explanation is in keeping with molecular modeling of gal cer (Fig. 46). It is also consistent with previous studies of pure gal cer in that the presence of an α-hydroxy group in the fatty acid was seen to lower the phase transition temperature. Thus 18:0-non-hydroxy gal cer and 18:0-α-hydroxy gal cer exhibit T_m at 83 and 70°C, respectively (Curatolo, W. and Jungalwala, F.B., 1985), and in addition the enthalpy of the transition was reduced. By Raman spectroscopy, non-hydroxy gal cer was observed to form a more ordered gel phase than its α-hydroxy counterpart (Bunow, M.R. and Levin, I.W., 1980; Bunow, M.R., 1979). Thus, in general, α-hydroxylation appears to destabilize lipid packing. An interesting exception was observed in pure lamellar systems of sulfated gal cer: in this case Boggs et al (Boggs, J.M., et al., 1988) invoked greater intermolecular H-bonding of α-hydroxy fatty acid sulfatide to explain the higher phase transition temperature of this species relative to its non-hydroxy form. However in this case there appears to have been the additional repulsive effect of the charged sulfate group.

A network of intermolecular H-bonds involving the polar headgroup, the sphingosine hydroxyl, and the fatty acyl α-hydroxy group is thought to play a role in the physical properties of glycosphingolipid bilayers, as well as certain aspects of glycosphingolipid function (for a review, see Curatolo, W., 1987a; Curatolo, W., 1987b). It is possible that some of the effects seen upon addition of an α-hydroxy group are a result of its intermolecular H-bonding role. However it is clear that in

Figure 46

Stereoscopic structures of galactosyl ceramide A) and its α-hydroxy-galactosyl ceramide B) counterpart, as derived by molecular modeling. The α-hydroxy group is indicated by an arrow. In each case the fatty acid was 18 carbons in length (Stearic acid).

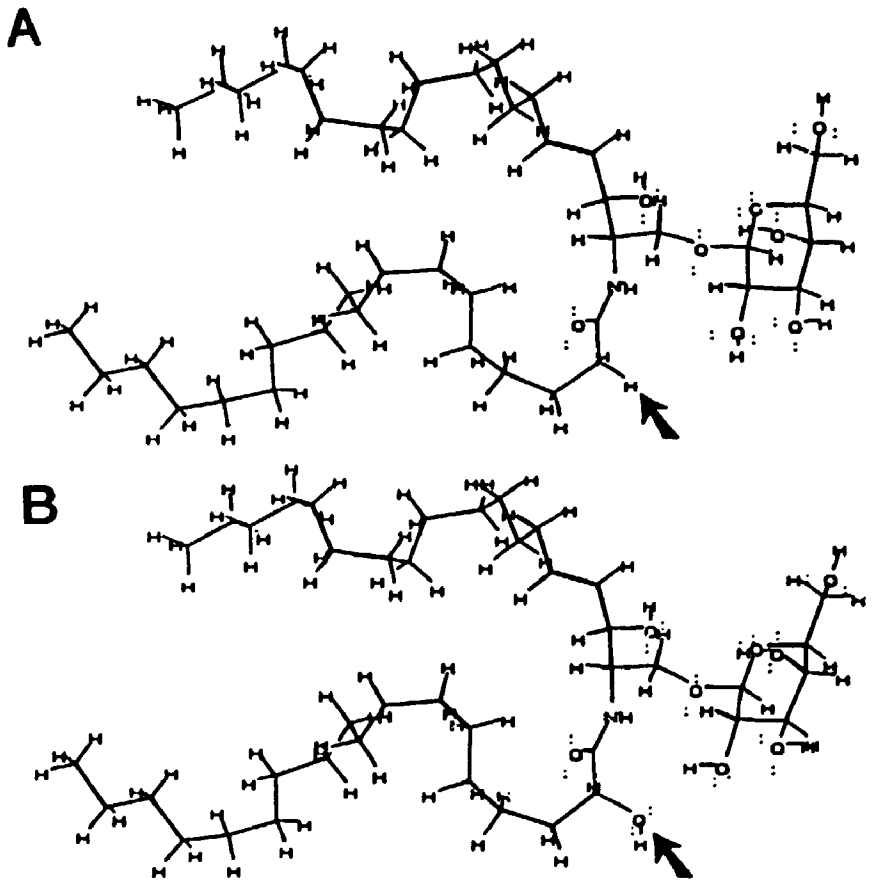
A
B

this case of a glycosphingolipid dispersed at low concentration in a fluid phospholipid matrix, H-bonding was not the controlling factor since it would lead to membrane stabilization.

6.4 Conclusion

The role of glycosphingolipid fatty acid α-hydroxylation as a mediator of lipid organization in cell membranes was considered by ^{2}H NMR. Phospholipid bilayers containing only 10 mol % galactosyl ceramide were examined in an attempt to reproduce intermolecular glycosphingolipid/phospholipid interactions such as those presumed to occur in cell membranes. For these experiments galactosyl ceramides were prepared in which the natural fatty acids were replaced with an 18-carbon hydroxylated or non-hydroxylated derivative that had been perdeuterated. α-hydroxy-stearoyl-d_{34}-galactosyl ceramide and stearoyl-d_{35}-galactosyl ceramide were studied in the 14-carbon fatty acid phospholipid host matrix, dimyristoyl phosphatidylcholine. α-hydroxylation was found to exert a moderate disordering effect on the glycosphingolipid in fluid membranes at all positions along the acyl chain except the terminal methyl group. The relative magnitude of the disordering effect was similar at each chain position, although it caused a noticeable broadening of the range of order parameters associated with the plateau region. Spectral results for the gel phase host phospholipid membrane were more difficult to interpret, but indicated that the presence of the α-hydroxyl group led to greater glycosphingolipid motional freedom and/or conformational disorder.

SUMMARY

Phospholipid molecules when arranged in bilayers undergo anisotropic motion as a result of side-to-side wobbling of the lipid chains as well as fast rotations about their long molecular axis. Therefore glycosphingolipids present as minor components of these bilayers with spin labels attached to their fatty acyl chains will monitor this motion and give rise to EPR spectra which reflect this anisotropy. In our hands stable nitroxide radicals have been covalently attached to carbon 16 of the acyl chains of varying lengths. They have been used to measure the degree of motional anisotropy for the glycosphingolipid fatty acid in a variety of host phospholipid matrices. When the motions are fast with a τ_c greater than 10^{-9}sec, the EPR spectra reveal two characteristic hyperfine splittings, $2T_{\perp}'$ (two particular inner peaks) and $2T_{\parallel}''$ (two particular outer peaks). These two parameters increase as the reporter group is positioned further down into the lipid bilayer and as the fluidity of the system decreases.

It is these two parameters, which describe the anisotropy of the spin label motion. With this in mind, a definition of the spin label order parameter "S" can be arrived at which is effectively $T_{\parallel}' - T_{\perp}'$ normalized relative to the maximum possible anisotropy for the rigidly-oriented, no-motion of a perfect crystal. Thus when S = 1, perfect order is present and conversely when S = 0, one has total disorder. This value may then be refined once again by correcting for the polarity of the spin label environment and for the slight differences between the measured splittings $2T_{\perp}'$ and the desired matrix element $2T_{\perp}$.

It is clear to us that the spectra obtained (with the spin labelled

glycosphingolipids in various phospholipid host matricies) are sensitive to factors related to dynamics and organizational differences between short and long chain glycosphingolipids. Our hypothesis was, that by placing a spin probe at the point where interdigitation is determined, we could test the effect of the "extra" length of hydrocarbon chain on local order. In all the systems studied, the order parameter was higher by a factor of 2 for the long acyl chains as compared to the short acyl chains and the order parameter was highest for the more rigid phospholipid matrix and decreased as the fluidity of the phospholipids increased.

The order parameter is a tensorial property which is dependent on the time-averaged orientation as well as the motion of the segment under study. In the deuterium NMR case, the magnitude of the quadrupole splittings is directly proportional to the order parameter S_{CD}. Therefore, one can look at the C-D bond in a fatty acyl chain and assign a segmental order parameter Smol which is numerically twice the value of S_{CD}. The segmental direction is given as the normal to the plane spanned by the two C-D bonds of the methylene units. Thus with this definition, the orientation of the individual chain segments will coincide with the long molecular axis, when the acyl chain is in its extended all-trans conformation. Just like in the spin label system, when Smol = 1 there is complete order and when Smol = 0 there is complete disorder. We have synthesized gal cer with an 18-carbon fatty acid which has had all of its hydrogens replaced by deuterons. This glycosphingolipid was assembled into lipid bilayers of phospholipids with the same chain length (DSPC) or 4 carbons shorter (DMPC). Thus we were comparing a system in which the scenario necessary for glycosphingolipid interdigitation existed (DMPC), with one in which it

did not (DSPC). In the above systems the fluidity of the two host matrices was made equivalent by running the ^2H NMR spectra at the same reduced temperatures.

The order parameter profiles obtained from the ^2H NMR data are qualitatively very similar for the short chain host matrix (DMPC) and the long chain matrix (DSPC). There is no break or deviation as might be expected if the glycosphingolipid's 18-carbon fatty acid assumed a very different conformation in the region of the 14-carbon host matrix methyl termini. Interestingly motional order for the methylene groups near the polar headgroup was strikingly increased in the matrix that supported interdigitation. This might be rationalized by proposing that an effect of interdigitation is to reduce conformational structures throughout the length of the molecule involved, via "tethering" of the fatty acid chain near its methyl terminus. A similar higher order parameter profile was produced when comparing gal cer having an 18-carbon fatty acid (deuterated) containing an α-hydroxy group in an interdigitating matrix (DMPC) to a non-interdigitating matrix (DSPC) when both were run at a similar reduced temperature.

As part of a research program involving liposomal drug delivery, we experienced a need for markers that remained stable when liposome-associated in the body and could be localized by non-invasive techniques such as MRI. Liposomes can be prepared with considerable versatility in properties such as size, charge and fluidity. In the past, the two basic approaches used by researchers in associating drugs with liposomes involved either entrapment of membrane-impermeant drugs within the aqueous interior of the liposome or "dissolution" of lipophilic drugs in the bilayer itself. We avoid using water-soluble agents, which require entrapment, for two major

reasons: i) loading of liposomes with water soluble species is generally inefficient, and requires special techniques; ii) within the body, liposomes rapidly leak their aqueous contents. It was this latter point which we avoided by employing contrast agents which are based upon natural phospholipid backbones and can incorporate with 100% efficiency into the liposome bilayer with minimal manipulations.

The first of these phospholipid based contrast agents we developed was a spin labelled phosphatidylcholine followed by a more potent (metal chelator-Gd^{3+}) contrast agent, phosphatidylethanolamine-diethylenetriaminepentaacetic acid. Both of these species incorporate into natural phospholipid bilayers with minimal perturbations as revealed by freeze-fracture electron microscopy. Both of these species proved to be very good relaxers of free water for *in vitro* analysis using T_1 and T_2 relaxation times as parameters.

The final test of their success was to determine if their *in vitro* efficacy could be translated to *in vivo* diagnostic imaging. This was accomplished by way of intravenous (and intramuscular) injections into male Sprague-Dawley rats of liposomes bearing the contrast agents. It was determined that both contrast agents were successful in this, but it was the phosphatidylethanolamine-diethylenetriaminepentaacetic acid chelating agent which proved to be much superior in terms of amount of contrast generated and the length of contrast enhancement.

FUTURE WORK

Studies on PC/cholesterol mixtures can be studied with various techniques such as calorimetry, EPR and ^2H NMR. Cholesterol is known to eliminate the sharp gel-liquid-crystalline phase transition of pure phospholipids. At temperatures above the phase transition of pure lipids, cholesterol has an ordering effect, while at temperatures below this, cholesterol causes more disorder. Cholesterol has an effect on the extent of *trans-gauche* isomerization of the methylene units of acyl chains. This causes close packing of the acyl chains hence decreases flexibility. We have begun to introduce cholesterol into samples of various host phospholipid matrices bearing deuterium labelled glycosphingolipids. Glycosphingolipids such as stearoyl-d_{35}-gal cer in DMPC and DSPC as well as α-hydroxy-stearoyl-d_{34}-gal cer in DMPC and DSPC have been studied in a preliminary fashion. Order parameter data will soon be available for these systems so that they can be compared to the systems already studied systems without cholesterol.

At present we have also synthesized lignoceroyl-d_{47}-gal cer. This glycosphingolipid will be studied in various phospholipid matrices such as DSPC (18 carbons) and DBPC (22 carbons) to determine its possible interdigitation and order parameter profile.

Another area of interest lies in the use of ^2H NMR to study the question of whether alterations to the glycosphingolipid sugars are reflected in changes within the membrane. Although such changes have been convincingly demonstrated in pure hydrated glycosphingolipids, the situation is not as clear for systems in which the glycosphingolipid is the minor component, as is the case in many biological

membranes. Gal cer, glc cer and lac cer, have been synthesized with a stearoyl acyl chain having deuterons on the C-2 position. These deuterons are in close association with the sugar headgroups, yet they are buried at the membrane surface. With this type of system it will be possible to address the effects of small changes (ie. the epimerization of the 4-OH group in glucose vs galactose) and large changes (mono vs disaccharide) in headgroup structure on membrane properties.

Experimental Allergic Encephalomyelitis is an experimentally induced auto immune disease which is similar to Multiple Sclerosis. This disease can be induced via intradermal injections of central nervous system tissue which contains the key factor, the antigenic myelin basic protein. This disease causes the breakdown of the blood brain barrier, and it is thought that this is the mode of entry of macrophages from the reticuloendothelial system. We are presently undergoing studies using the chelating contrast agent PE-DTPA-Gd^{3+} mixed with egg phosphatidylcholine to make liposomes in hope that they will be taken up by the macrophages. We wish to load these macrophages with contrast agent, induce the disease in experimental guinea pigs and image the animals to see if contrast can be achieved in the brain. This preliminary study has so far provided promising information and images.

In the future, further work is necessary to determine exactly where the chelating contrast agent PE-DTPA-Gd^{3+} ends up after macrophages digest the liposomes. Possible studies to determine its fate would employ larger animals such as pigs in an attempt to map out its location. We would like to be able to state with confidence, the entire route this novel contrast agent had from the moment of injection to its final clearance from the body.

ADAMS, D.H., JOYCE, G., RICHARDSON, V.J., RYMAN, B.E. and WIDNIEWSKI, H.M.J. (1977) Liposome toxicity in the mouse central nervous system. *J. Neurol. Sci.* 31, 173-179.

ALLEN, T.M., RYAN, J.L. and PAPAHADJOPOULOS, D. (1985) Gangliosides reduce leakage of aqueous-space markers from liposomes in the presence of human plasma. *Biochim. Biophys. Acta* 818, 205-210.

ALVING, C.R. and RICHARDS, R.L. (1977) Immune reactivities of antibodies against glycolipids. I. Properties of anti-galactocerebroside antibodies purified by a novel technique of affinity binding to liposomes. *Immunochemistry* 14, 373-381.

ALVING, C.R., URBAN, K.A. and RICHARDS, R.L. (1980) Influence of temperature on complement-dependent immune damage to liposomes. *Biochim. Biophys. Acta* 600, 117-125.

ANDREWS, S.B., HOFFMAN, R.M. and BORISON, A. (1975) Variations of size and distribution in suspensions of sonicated phospholipid bilayers. *Biochem. Biophys. Res. Commun.* 65, 913-919.

ATLAS, S.W., BILANIAK, L.T. and ZIMMERMAN, R.A. (198[illegible] n *Magnetic Resonance Image* (Stark, D.D. and Brandley, W.G. Jr., ed.), 26, pp. 570-613, C.V. MosbyCompany, Toronto.

ATLAS, S.W., GROSSMAN, R.I. and AXEL, L. (1987) Orbital lesions: Proton spectroscopic phase-dependent contrast MR imaging. *Radiology* 64, 510-514.

BACIC, G., NIESMAN, M.R., BENNETT, H.F., MAGIN, R.L. and SWARTZ, H.M. (1988) Modulation of water proton relaxation rates by liposomes containing paramagnetic materials. *Mag. Res. Med.* 6, 445-458.

BALAKRISHNAN, K., MEHDI, S.W. and McCONNELL, H.M. (1982) Availability of dinitrophenylated lipid haptens for specific antibody depends on the physical properties of host bilayer membranes. *J. Biol. Chem.* 257, 6434-6439.

BARRATT, G.M., TUZEL, N.S. and RYMAN, B.E. (1984) In *Liposome Technology*, Vol. II, (Gregoriadis, G., ed), pp. 93-106, CRC Press, Boca Raton, Florida.

BERQUIST, T.H. (1987) Magnetic resonance of the musculoskeletal system. (Ehman, R.L. and Richardon, M.L. ed.), pp. 1-64, Raven Press, New York, New York.

BLOOM, M., DAVIS, J.H. and MacKAY, A.I. (1981) Direct determination of the oriented sample NMR-spectrum from the powder spectrum for systems with local axial symmetry. *Chem. Phys. Lett.* 80, 198-202.

BOGGS, J.M., KOSHY, K.M. and RANGARAJ, G. (1988) Interdigitated lipid bilayers of long acyl chain species of cerebroside sulfate: A fatty acid spin label study. *Biochim. Biophys. Acta* 938, 373-385.

BOGGS, J.M. and MASON, J.T. (1986) Calorimetric and fatty acid spin label study of subgel and interdigitated gel phases formed by asymmetric phosphatidylcholines. *Biochim. Biophys. Acta* 863, 231-242.

BOGGS, J.M. and RANGARAJ, G. (1985) Phase transitions and fatty acid spin label behaviour in interdigitated lipid phases induced by glycerol and polymyxin. *Biochim. Biophys. Acta* 816, 221-233.

BRASCH, R.C. (1985) Inherent contrast in MR imaging and the potential for contrast enhancement. *West J. Med.* 142, 847-853.

BRASCH, R.C., LONDON, D.A. and WESBEY, G.E. (1983) Nuclear magnetic resonance study of paramagnetic contrast agents for enhancement of renal structures in experimental animals. *Radiology* 147, 773-779.

BRATEMAN, L. (1986) Chemical shift imaging: A review. *American J. of Roentgenology* 146, 971-980.

BUNOCORE, E., HUBNER, G., KABALKA, T., HUANG, L., MOSS, T. and NORLEY, N. (1985) Targeted MR contrast agents for liver and spleen: gadolinium labeled liposomes. *Radiology* 157(P), 313.

BUNOW, M.R. (1979) Two gel states of cerebrosides: calorimetric and Raman spectroscopic evidence. *Biochim. Biophys. Acta* 574, 542-546.

BUNOW, M.R. and LEVIN, I.W. (1980) Molecular conformations of cerebrosides in bilayers determined by Raman spectroscopy. *Biophys. J.* 32, 1007-1021.

BURNELL, E.E. and DeLANGE, C.A. (1980) Effects on interactions between molecular motions and reorientation of NMR of anisotropic liquids. *J. Magn. Res.* 39, 461-480.

CARIDE, V.J. and SOSTMAN, H.D. (1984) In *Liposome Technology.* Vol. II (Gregoriadis, G., ed.), pp. 107-124, CRC Press, Boca Raton, Florida.

CARIDE, V.J., SOSTMAN, H.D., WINCHELL, R.J. and GORE, J.C. (1984) Relaxation enhancement using liposomes carrying paramagnetic species. *Mag. Res. Imaging* 2, 107-112.

CHAN, H.C., MAGIN, R.L., THOMPKINS, W.A.F., MORSE, P.D. and SCHWARTZ, M.M. (1985) ESR study of the interaction between macrophages and liposomes containing spin labels as NMR contrast agents.

Soc. Mag. Reson. Med. "Book of Abstracts" 1, 846-847.

CROOK, S.J., BOGGS, J.M., VISTNES, A.I. and KOSHY, K.M. (1986) Factors affecting surface expression of glycolipids: Influence of lipid environment and ceramide composition on antibody recognition of cerebroside sulfate in liposomes. *Biochemistry* 25, 7488-7494.

CURATOLO, W. (1987a) The physical properties of glycolipids. *Biochim. Biophys. Acta* 906, 111-136.

CURATOLO, W. (1987b) Glycolipid function. *Biochim. Biophys. Acta* 906, 137-160.

CURATOLO, W. and JUNGALWALA, F.D. (1985) Phase behaviour of galactocerebrosides from bovine brain. *Biochemistry* 24, 6608-6613.

DAVIS, J.H. (1979) Deuterium magnetic resonance study of the gel and liquid crystalline phases of dipalmitoyl phosphatidylcholine. *Biophys. J.* 27, 339-358.

DAVIS, J.H. (1983) The description of membrane lipid conformation, order and dynamics by ^2H NMR. *Biochim. Biophys. Acta* 737, 117-171.

DAVIS, J.H., JEFFREY, K.R., BLOOM, M., VALIC, M.I. and HIGGS, T.P. (1976) Quadrupolar echo deuteron magnetic resonance spectroscopy in ordered hydrocarbon chains. *Chem. Phys. Lett.* 42, 390-394.

DAVIS, P.J. and KEOUGH, K.M.W. (1985) Chain arrangements in the gel state and transition temperatures of phosphatidylcholines. *Biophys. J.* 48, 915-918.

DEMEL, R.A. and DeKRUYFF, B. (1976) The function of sterols in membranes. *Biochim. Biophys. Acta* 457, 109-131.

DEVAUX, P.D., SCANDELLA, C.J. and McCONNELL, H.M. (1973) Spin-spin interactions between spin-labelled phospholipids incorporated into membranes. *J. Mag. Reson.* 9, 474-475.

DIXON, W.T. (1984) Simple proton spectroscopic imaging. *Radiology* 153, 189-194.

ENDO, T., MOJIMA, S. and INOUE, K. (1982) Intermolecular interaction between glycolipids and glycophorin on liposomal membranes. *J. Biochem.* 92, 1883-1890.

ESMANN, M., MARSH, D., SCHWARZMANN, G. and SANDHOFF, K. (1988) Ganglioside-protein interactions: Spin-label electron spin resonance studies with (Na^+, K^+)ATPase membranes. *Biochemistry* 27, 2398-2403.

FELGNER, P.L., THOMPSON, T.E., BARENHOLZ, Y. and LICHTENBERG, D.

(1983) Kinetics of transfer of gangliosides from their micelles to dipalmitoyl phosphatidylcholine vesicles. *Biochemistry* 22, 1670-1674.

FINDLAY, E.J. and BARTON, P.G. (1978) Phase behaviour of synthetic phosphatidylglycerols and binary mixtures with phosphatidylcholines in the presence and absence of calcium ions. *Biochemistry* 17, 2400-2405.

FOLCH, J., LEES, M. and SLOANE-STANLEY, G.A. (1957) A simple method for isolation and purification of total lipids from animal tissues. *J. Biol. Chem.* 226, 497-509.

GAFFNEY, B.J. (1976) Lipid spin labels in biological membranes. In *Spin Labeling; Theory and Applications.* (Berliner, L.J. ed.), pp. 567-571, Academic Press, New York.

GRANT, C.W.M. (1987) Fundamentals of physico-chemistry of glycolipids in membranes. In *Gangliosides and Modulation of Neuronal Functions*, Vol. H7, (Rahmann, H. ed.), pp. 119-138, NATO ASI Series Cell Biology, Springer-Verlag, Berlin.

GRANT, C.W.M., BARBER, K.R., FLORIO, E. and KARLIK, S.J. (1987a) A phospholipid spin label used as a liposome associated MRI contrast agent. *Mag. Res. in Medicine*, 5, 371-376.

GRANT, C.W.M., KARLIK, S.J. and FLORIO, E. (1989) A liposomal MRI contrast agent: Phosphatidylethanolamine-DTPA. *Mag. Res. in Medicine* 11, 236-243.

GRANT, C.W.M., MEHLHORN, I.E., FLORIO, E. and BARBER, K.R. (1987b).A long chain spin label for glycosphingolipid studies: Transbilayer fatty acid interdigitation of lactosyl ceramide. *Biochim. Biophys. Acta* 902, 169-177.

GREGORIADIS, G. (1988) In *Liposomes as Drug Carriers - Recent Trends in Progress*, (Gregoriadis, G. ed.), pp. 3-18, Wiley, Chichester, England.

GRIFFETH, L.K., ROSEN, G.M., RAUCKMAN, E.J. and DRAYER, B.P. (1984) Pharmacokinetics of nitroxide NMR contrast agents. *Invest. Radiology* 19, 553-562.

GRIFFITH, O.H. and JOST, P.C. (1976) Lipid spin labels in biological membranes. In *Spin Labelling; Theory and Applications.* (Berliner, L.J. ed.), pp. 453-523, Academic Press, New York.

HAKOMORI, S. and SIDDIQUI, B. (1974) Isolation and characterization of glycosphingolipids from animal cells and their membranes. *Method Enzymol.* 32, 345-367.

HARWOOD, J.L. (1989) Trans-bilayer lipid interaction. *TIBS* 14, 2-4.

HICKINBOTTOM, W.J. (1948) Reactions of organic compounds. (Longman's, Green & Co., 2nd ed.), pp. 239, New York.

HIGGS, T.P. and MacKAY, A.L. (1977) Determination of the complete order parameter tensor for a lipid methylene group from ^{1}H and ^{2}H NMR spin labels. *Chem. Phys. Lipids* 20, 105-114.

HINZ, H.J. and STURTEVANT, J.M. (1972) Calorimetric studies of dilute aqueo us suspensions of bilayers formed from synthetic L-α-lecithins. *J. Biol. Chem.* 247, 6071-6075.

HNATOWICK, D.J., FRIEDMAN, B., CLANCY, C. and NOVAK, M. (1981) Labeling of preformed liposomes with Ga-67 and Tc-99m by chelation. *J. Nuc. Med.* 22, 810-814.

HUANG, C. and MASON, J.T. (1986) Structure and properties of mixed-chain phospholipid assemblies. *Biochim. Biophys. Acta* 864, 423-470.

HUBBELL, W.L. and McCONNELL, H.M. (1971) Molecular motions in spin-labeled phospholipids and membranes. *J. Am. Chem. Soc.* 93, 314-326.

JOHNSON, G.A., GLOVER, G.H., KARIS, J.P., SHIMAKAWA, A. and HERFKENS, R.S. (1986) Ultra high-resolution MR imaging with gradient refocused three-dimentional spin-warp sequences. *Radiology* 161P, 254.

JOHNSTON, D.S. and CHAPMAN, D. (1988) A calorimetric study of the thermotropic behaviour of mixtures of brain cerebrosides with other brain lipids. *Biochim. Biophys. Acta* 939, 603-614.

KABALKA, G.W., BUONOCORE, E.D., HUBNER, K., DAVIS, M. and HUANG, L. (1988) Gadolinium-labeled liposomes containing paramagnetic amphipathic-agents: targeted MRI contrast agents for the liver. *Mag. Res. Med.* 8, 89-95.

KABALKA, G.W., BUONOCORE, E.D., HUBNER, K., MOSS, T., NORLEY, N. and HUANG, L. (1987) Gadolinium-labeled liposomes: Targeted MRI contrast agents for the liver and spleen. *Radiology* 163, 255-258.

KANFER, J.N. (1969) Preparation of gangliosides. *Methods Enzymol.* 14, 660-664.

KANNAGI, R., NUDELMAN, E. and HAKOMORI, S. (1982) Possible role of ceramide in defining structure and function of membrane glycolipids. *Proc. Natl. Acad. Sci. USA* 79, 3470-3474.

KEANA, J.W., KENAN, S.B. and BEETHAM, D. (1967) A new versatile ketone spin label. *J. Am. Chem. Soc.* 89, 3055-3056.

KEOUGH, K.M.W. and DAVIS, P.J. (1979) Gel to liquid-crystalline phase transitions in water dispersions of saturated mixed-acid phosphatidylcholines. *Biochemistry* 18, 1453-1459.

KHATO, J., DelCAMPO, A.A. and SIEBER, S.M. (1983) Carrier activity of sonicated small liposomes containing melphalan to regional lymph nodes of rats. *Pharmacology* 26, 230-240.

KI, P.F., KISHIMOTO, Y., LATTMAN, E.E., STANLEY, E.F. and GRIFFIN, J.W. (1985) Structure and function of urodelemyelin lacking alpha-hydroxy fatty acid containing galactosphingolipids: slow nerve conduction and unusual myelin thickness. *Brain Research* 345, 19-24.

KOENIG, S.H. and BROWN, R.D. III (1984) Determination of proton relaxation rates in tissue. *Mag. Res. Med.* 1, 437-449.

KOENIG, S.H. and BROWN, R.D. III (1987) In *Mag. Res. Annual*, (Kressell, H.Y. ed.), pp. 263-286, Raven Press, New York.

KOENIG, S.H., BROWN, R.D. III, KURLAND, R. and OHKI, S. (1988) Relaxivity and binding of Mn^{2+} ions in solutions of phosphatidylserine vesicles. *Mag. Res. Med.* 7, 133-142.

KORNBERG, R.D. and McCONNELL, H.M. (1971) Inside-outside transitions of phospholipids in vesicle membranes. *Biochemistry* 10, 1111-1120.

KRESSEL, H.Y. (1985) In *Magnetic Resonance Annual*, (Kressel, H.Y. ed.), pp. 231-266, Raven Press, New York.

KRESSEL, H.Y. (1987) In *Magnetic Resonance Annual* (Kressel, H.Y. ed.), pp. 263-286, Raven Press, New York.

KUMAR, A., WELTI, D. and ERNST, R.R. (1975) NMR fourier zeugmatography. *J. Magn. Res.* 18, 69-83.

LAMPIO, A., RAUVALA, H. and GAHMBERG, C.G. (1986) Exposure of major neutral glycolipids in red cells to galactose oxidase. Effect of Neuraminidase. *Eur. J. Biochem.* 157, 611-616.

LEVIN, I.W., THOMPSON, T.E., BARENHOLZ, Y. and HUANG, C. (1985) Two types of hydrocarbon chain interdigitation in sphingomyelin bilayers. *Biochemistry* 24, 6282-6286.

MAGGIO, B., ARIGA, T., STURTEVANT, J.M. and YU, R.K. (1985) Thermotropic behaviour of binary mixtures of dipalmitoyl phosphatidylcholine and glycosphingolipids in aqueous dispersions. *Biochim. Biophys. Acta* 818, 1-12.

MARSH, D. (1981) Electron spin resonance: Spin labels. In *Mol. Biol. Biochem. Biophys.* Vol. 31, Membrane Spectroscopy, (Grell, E. ed.), pp. 51-142, Springer-Verlag, New York.

MATTAI, J., SPRIPADA, P.K. and SHIPLEY, G.G. (1987) Mixed-chain phosphatidylcholine bilayers: structure and properties. *Biochemistry* 26, 3287-3297.

MAULIK, P.R., ATKINSON, D. and SHIPLEY, G.G. (1986) X-ray scattering of vesicles of N-acyl sphingomyelins. Determination of bilayer thickness. *Biophys. J.* 50, 1071-1077.

MAUK, M.R., GAMBLE, R.R. and BALDDESCHWIELER, J.D. (1980) Targeting of lipid vesicles: Specificity of carbohydrate receptor analogues for leukocytes in mice. *Proc. Nat. Acad. Sci. USA* 77, 4430-4434.

MAYHEW, E. (1983) In *Liposomes* (Ostro, M.J. ed.), pp. 289-341 Marcel Dekker, New York.

McCALLEY, R.C., SHIMSHICK, E.J. and McCONNELL, H.M. (1972) The effect of slow rotational motion on paramagnetic resonance spectra. *Chem. Phys. Lett.* 13, 115-119.

McCONNELL, H.M. (1976) In *Spin Labelling; Theory and Applications* (Berlinger, L.J. ed.), pp. 525-560, Academic Press, New York.

McCONNELL, H.M. and McFARLAND, B.G. (1972) The flexibility gradient in biological membranes. *Ann. N.Y. Acad. Sci.* 195, 207-217.

MEIROVITCH, E. and FREED, J.H. (1984) Analysis of slow-motional electron spin resonance spectra in smectic phases in terms of molecular configuration, intermolecular interactions and dynamics. *J. Phys. Chem.* 88, 4995-5004.

MEHLHORN, I.E., BARBER, K.R. and GRANT, C.W.M. (1988) Globoside with spin-labelled fatty acid: bilayer lateral distribution and immune recognition. *Biochim. Biophys. Acta* 943, 389-404.

MEHLHORN, I.E., BARBER, K.R., FLORIO, E. and GRANT, C.W.M. (1989) A comparison of physical behaviour amongst four glycosphingolipid families. *Biochim. Biophys. Acta* 986, 281-289.

MEHLHORN, I.E., FLORIO, E., BARBER, K.R., LORDO, C. and GRANT, C.W.M. (1988) Evidence that trans-bilayer interdigitation of glycosphingolipid long chain fatty acids may be a general phenomenon. *Biochim. Biophys. Acta* 939, 151-159.

MORRIS, P.G. (1986) In *Nuc. Mag. Res. Imaging in Med. and Biol.* (Morris, P.G. ed.), Chapter 6, pp. 256-289, Oxford Science Publications, New York.

MYERS, M., WORTMAN, C. AND FREIRE, E. (1984) Modulation of neuraminidase activity by the physical state of phospholipid bilayers containing gangliosides GD_{1a} and GT_{1b}. *Biochemistry* 23, 1442-1448.

NEUENHOFER, S., SCHWARZMANN, G., EGGE, H. and SANDHOFF, K. (1985) Synthesis of lysogangliosides. *Biochemistry*, 24, 525-532.

NIXON, J.R. (1987) In *Magnetic Resonance of the Musculoskeletal System* (Berquist, T.H. ed.), pp. 1-21, Raven Press, New York.

OLDFIELD, E., MEADOWS, M., RICE, D. and JACOBS, R. (1978) Spectroscopic studies of specifically deuterium labelled membrane systems. Nuclear magnetic resonance investigation of the effects of cholesterol in model systems. *Biochemistry*, 17, 2727-2740.

OLSON, F., MAYHEW, E., MASLOW, D., RUSTUM, Y. and SZOKA, F. (1982) Characterization, toxicity and therapeutic efficacy of adriamycin encapsulated in liposomes. *Eur. J. Cancer Clin. Oncol.* 18, 167-176.

PERLY, B., SMITH, I.C.P. and JARRELL, H.C. (1985) Effects of the replacement of a double bond by a cyclopropane ring in phosphatidylethanolamine. A ^2H NMR study of phase transitions and molecular organization. *Biochemistry* 24, 1055-1063.

POZNANSKY, M.J. and JULIANO, R.L. (1984) Biological approaches to the controlled delivery of drugs: A critical review. *Pharm. Rev.* 36, 277-336.

RANCE, M. and BYRD, R.A. (1983) Obtaining high-fidelity spin-1/2 powder spectra in anisotropic media: Phase cycled Hahn echo spectroscopy. *J. Magn. Reson.* 52, 221-240.

RANCE, M., JEFFREY, K.R., TULLOCH, A.P., BUTLER, K.W. and SMITH, I.C.P. (1980) Orientational order of unsaturated lipids in the membrane of *acholeplasma laidlawii* as observed by ^2H-NMR. *Biochim. Biophys. Acta* 600, 245-262.

RUNGE, V.M. SCHOERNER, W., NIENDORF, H.P., LANIADO, M., KOEHLER, D., CLAUSSEN, C., FELIX, R. and JAMES, JR., A.E. (1985) Initial clinical

evaluation of gadolinium-DTPA for contrast enhanced magnetic resonance imaging. *Mag. Res. Imaging* 3, 17-35.

RUOCCO, M.J., SHIPLEY, G.G. and OLDFIELD, E. (1983) Galactocerebroside-phospholipid interaction in bilayer-membranes. *Biophys. J.* 43, 91-101.

SCHERPHOF, G.L., DAMEN, J. and WILSCHUT, J. (1984) In *Liposome Technology* Vol. III (Gregoriadis, G. ed.), pp. 205-224, CRC Press, Boca Raton, Florida.

SCHICHIJO, S. and ALVING, C.R. (1986) Inhibitory effects of gangliosides on immune reactions of antibodies to neutral glycolipids in liposomes. *Biochim. Biophys. Acta* 858, 118-124.

SEELIG, A. and SEELIG, J. (1974) The dynamic structure of fatty acyl chains in a phospholipid bilayer measured by deuterium magnetic resonance. *Biochemistry* 13, 4839-4845.

SEELIG, J. (1970) Spin label studies of oriented smectic liquid crystals. (A model system for bilayer membranes). *J. Am. Chem. Soc.* 92, 3881-3887.

SEELIG, J. (1977) Deuterium magnetic resonance: Theory and application to lipid membranes. *Quart. Rev. Biophys.* 10, 353-418.

SEELIG, J. (1978) ^{31}P nuclear magnetic resonance and the headgroup structure of phospholipids in membranes. *Biochim. Biophys. Acta.* 515, 105-140.

SEELIG, J. and BROWNING, J.L. (1978) General features of phospholipid conformation in membranes. *FEBS Lett.* 92, 41-44.

SEELIG, J. and WAESPE-SARCEVIC, N. (1978) Molecular order in cis and trans unsaturated phospholipid bilayers. *Biochemistry* 17, 3310-3315.

SELTZER, S.E. (1989) The role of liposomes in diagnostic imaging. *Radiology* 171, 19-21.

SELTZER, S.E., DAVIS, M.A., ADAMS, D.F., SHULKIN, P.M., LANDIS, W.J. and HAVRON, A. (1984) Liposomes carrying diatrizoate: Characterization of biophysical properties and imaging applications. *Invest. Radiol.* 19, 142-151.

SHAROM, F.J., BARRATT, D.G., THEDE, A.E. and GRANT, C.W.M. (1976) Glycolipids in model membranes spin label and freeze-etch studies. *Biochim. Biophys. Acta* 455, 485-492.

SHAROM, F.J. and GRANT, C.W.M. (1975) A glycosphingolipid spin label: Ca^{2+} effects on sphingolipid distribution in bilayers containing phosphatidylserine.

Biochem. Biophys. Res. Commun. 67, 1501-1506.

SHIMSHICK, E.J. and McCONNELL, H.M. (1973) Lateral phase separations in phospholipid membranes. *Biochemistry* 12, 2351-2360.

SIMON, J.H. and SZUMOWSKI, J. (1989) Chemical shift imaging with paramagnetic contrast material enhancement for improved lesion depiction. *Radiology* 171, 539-543.

SKARJUNE, R. and OLDFIELD, E. (1982) Physical studies of cell surface and cell membrane structures: Deuterium nuclear magnetic resonance studies of N-palmitoylglucosylceramide (cerebrosides) head group structure. *Biochemistry* 21, 3154-3160.

SMITH, I.C.P. and MANTSCH, H.H. (1982) New methods and Applications. In *^2H NMR Spectroscopy*, (Levy, G.C. ed.), Chapter 6, pp. 97-117, Amer. Chem. Soc., Washington, D.C.

SMITH, I.C.P., STOCKTON, G.W., TULLOCH, A.P., POLNASZEK, C.F. and JOHNSON, K.G. (1977) Deuterium NMR and spin label ESR as probes of membrane organization. *J. Coll. Int. Sci.* 58, 439-451.

SPRAWLS, P. (1988) In *Magnetic Resonance Image* (Stark, D.D. and Brandley, W.G. Jr., ed.), Chapter 2, pp. 24-35, C.V. Mosby Company, Toronto.

STOCKTON, G.W., POLNASZEK, C.F., TULLOCH, A.P., HASEN, F. and SMITH, I.C.P. (1976) Molecular motion and order in single-bilayer vesicles and multilamellar dispersions of egg lecithin and lecithin-cholesterol mixtures. A deuterium nuclear magnetic resonance study of specifically labeled lipids. *Biochemistry* 15, 954-966.

SWEET, R.S. and ESTER, F.L. (1956) 2-Hexadecenoic acid and related compounds. *J. Org. Chem.* 51, 1426-1429.

SZOKA, F.C., MILLHOLLAND, D. and BARZA, M. (1987) Effect of lipid composition and liposome size on toxicity and *in vitro* fungicidal activity of liposome-intercalated amphotericin B. *Antimicro. Agents Chemother.* 31, 421-429.

SZOKA, F.C. and PAPAHADJOPOULOS, D. (1980) Comparative properties and methods of preparation of lipid vesicles (liposomes). *Ann. Rev. Biophys. Bioeng.* 9, 467-508.

SZUMOWSKI, J. and PLEWES, D.B. (1987) Separation of lipid and water MR imaging signals by chopper averaging in the time domains. *Radiology* 165, 247-250.

TAKETOMI, T. and YAMAKAMA, T. (1963) Immunochemical studies of lipids. *J. Biochem.* 54, 444-451.

THOMAS, P.D. and PODDER, S.K. (1982) Reactivity of glycoconjugates in membranes. I. Determination of transbilayer distribution of gangliosides in lipid vesicles by chemical methods. *Biochim. Biophys. Acta* 688, 453-459.

THOMPSON, T.E., ALLIETTA, M., BROWN, R.E., JOHNSON, M.L. and TILLACK, T.W. (1985) Organization of ganglioside G_{M1} in phosphatidylcholine bilayers. *Biochim. Biophys. Acta* 817, 229-237.

THOMPSON, T.E. and TILLACK, T.W. (1985) Organization of glycosphingolipids in bilayers and plasma membranes of mammalian cells. *Ann. Rev. Biophys. Biochem.* 14, 361-386.

TURSKI, P., KALINKE, T., STROTHER, L., PERMAN, W., SCOTT, G. and KORNGATH, S. (1988) Magnetic resonance imaging of rabbit brain after intracarotid injection of large multivesicular liposomes containing paramagnetic metals and DTPA. *Mag. Res. Med.* 7, 184-196.

UTSUMI, H., SUZUKI, T., INOUE, K. and NOJIMA, S. (1984) Haptenic activity of galactosyl ceramide and its topographical distribution on liposomal membranes. Effects of temperature and phospholipid composition. *J. Biochem.* 96, 97-105.

WEINSTEIN, J.N. and LESERMAN, L.D. (1984) Liposomes as drug carriers in cancer chemotherapy. *Pharmac. Ther.* 24, 207-233.

WELCH, M.J. and WELCH, T.J. (1975) In *Radiopharmaceuticals* (Subramanian, G., Rhodes, B.A., Cooper, J.F. and Sudd, V.J. ed.), Vol. 8, Soc. Nuc. Med. Inc., New York.